USGS
science for a changing world

Geologic and Geophysical Maps of the Santa Maria and Part of the Point Conception 30'×60' Quadrangles, California

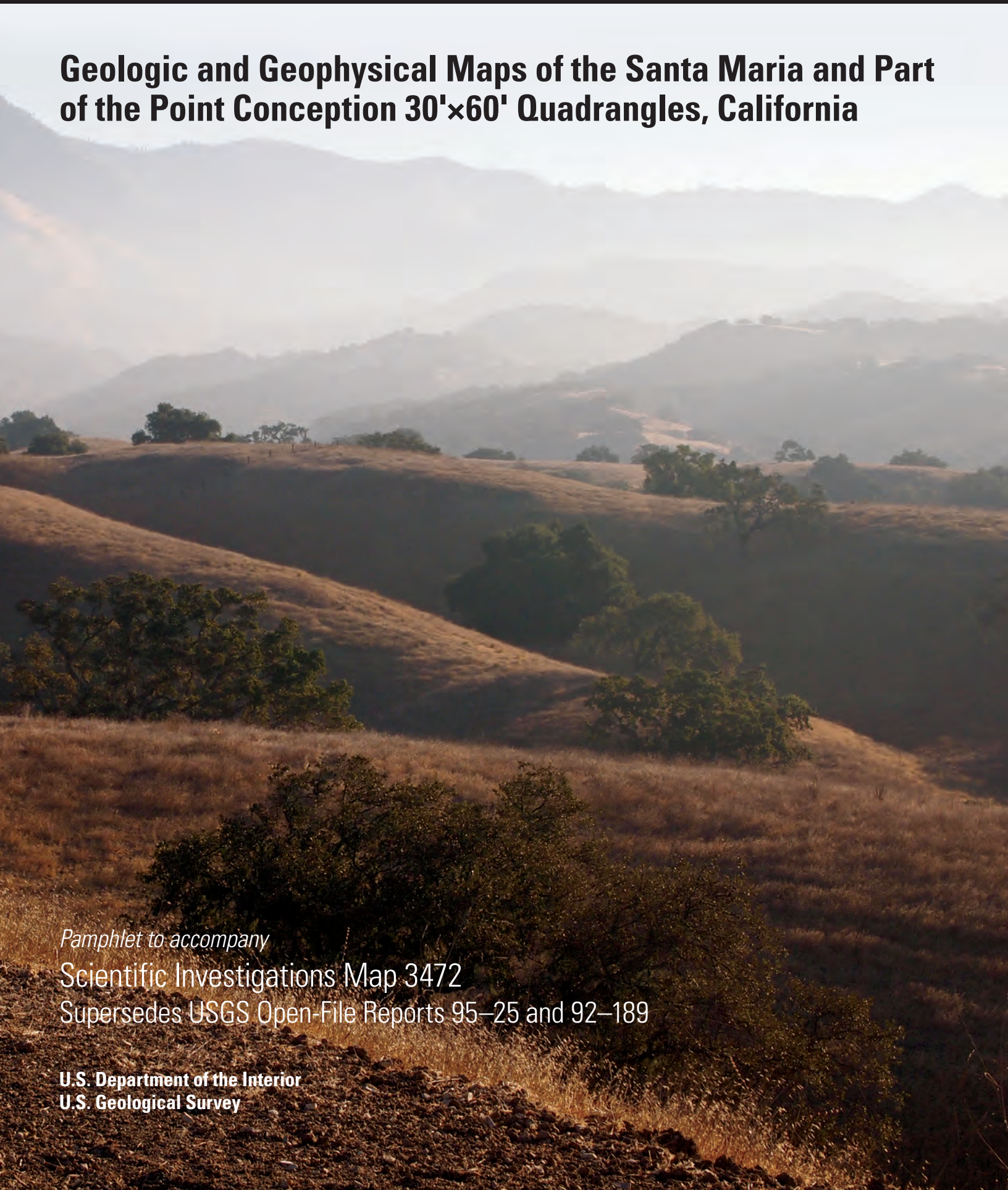

Pamphlet to accompany

Scientific Investigations Map 3472

Supersedes USGS Open-File Reports 95–25 and 92–189

U.S. Department of the Interior
U.S. Geological Survey

Cover. Looking northwest from near Zaca Creek to Zaca Ridge on the east edge of the map area (see pamphlet figure 2 for location of Zaca Creek and Zaca Ridge). Hills in foreground are underlain by gently dipping early Pleistocene and upper Pliocene Paso Robles Formation locally overlain by late Pleistocene fluvial terrace deposits. Zaca Ridge, the high peak on the skyline at left edge of photo, is underlain by folded Miocene Monterey Formation. Photograph taken by Donald S. Sweetkind, U.S. Geological Survey, September 2010.

Geologic and Geophysical Maps of the Santa Maria and Part of the Point Conception 30′×60′ Quadrangles, California

By Donald S. Sweetkind, Victoria E. Langenheim, Kristin McDougall-Reid, Christopher C. Sorlien, Shiera C. Demas, Marilyn E. Tennyson, and Samuel Y. Johnson

Pamphlet to accompany
Scientific Investigations Map 3472
Supersedes USGS Open-File Reports 95–25 and 92–189

U.S. Department of the Interior
U.S. Geological Survey

U.S. Geological Survey, Reston, Virginia: 2021
Supersedes USGS Open-File Reports 95–25 and 92–189

Suggested citation:
Sweetkind, D.S., Langenheim, V.E., McDougall-Reid, K., Sorlien, C.C., Demas, S.C., Tennyson, M.E., and Johnson, S.Y., 2021, Geologic and geophysical maps of the Santa Maria and part of the Point Conception 30'×60' quadrangles, California: U.S. Geological Survey Scientific Investigations Map 3472, 1 sheet, scale 1:100,000, 58-p. pamphlet, https://doi.org/10.3133/sim3472. [Supersedes USGS Open-File Reports 95–25 and 92–189.]

Associated data for this publication:
Sweetkind, D.S., Langenheim, V.E., and McDougall-Reid, K., 2021, Data release—Geologic and geophysical maps of the onshore parts of the Santa Maria and Point Conception 30'x60' quadrangles, California: U.S. Geological Survey data release, https://doi.org/10.5066/P9FU7SJL.

ISSN 2329-132X (online)

Contents

Figures

Table

Conversion Factors

U.S. customary units to International System of Units

Multiply	By	To obtain
	Length	
inch (in)	25.4	millimeters (mm)
foot (ft)	0.3048	meter (m)
mile (mi)	1.609	kilometer (km)
	Volume	
barrel (bbl; petroleum, 1 barrel=42 gal)	0.1590	cubic meter (m^3)
	Mass	
pound, avoirdupois (lb)	0.4536	kilogram (kg)
	Density	
pound per cubic foot (lb/ft^3)	16.02	kilogram per cubic meter (kg/m^3)

International System of Units to U.S. customary units

Multiply	By	To obtain
	Length	
centimeter (cm)	0.3937	inch (in)
meter (m)	3.281	foot (ft)
kilometer (km)	0.6214	mile (mi)
	Volume	
cubic meter (m^3)	6.290	barrel (petroleum, 1 barrel = 42 gal)
	Mass	
kilogram (kg)	2.205	pound avoirdupois (lb)
	Density	
kilogram per cubic meter (kg/m^3)	0.06242	pound per cubic foot (lb/ft^3)

Temperature in degrees Celsius (°C) may be converted to degrees Fahrenheit (°F) as

$$°F = (1.8 \times °C) + 32.$$

Temperature in degrees Fahrenheit (°F) may be converted to degrees Celsius (°C) as

$$°C = (°F - 32) / 1.8.$$

Datum

Vertical coordinate information is referenced to the North American Vertical Datum of 1988 (NAVD 88).

Horizontal coordinate information is referenced to the North American Datum of 1983 (NAD 83).

Altitude, as used in this report, refers to distance above the vertical datum.

Supplemental Information

1 milliGal (mGal) = 10^{-3} of 1 centimeter per second^2 (1 cm/s^2)

1 nanotesla (nT) = 10^{-9} tesla (T)

Calibrated and radiocarbon ages are reported relative to A.D. 1950 (calibrated years before the present, cal yr B.P.)

Paleogene time used in this report[1]			
Period or subperiod	**Epoch**		**Age**
Quaternary	Holocene		0–11.7 ka
	Pleistocene	Late	11.7–132 ka
		Middle	132–788 ka
		Early	788 ka–2.588 Ma
Neogene	Pliocene		2.588–5.332 Ma
	Miocene		5.332–23.03 Ma
Paleogene	Oligocene		23.03–33.9 Ma
	Eocene		33.9–55.8 Ma
	Paleocene		55.8–65.5 Ma

[1]Ages of time boundaries are those of the U.S. Geological Survey Geologic Names Committee (2018) except those for the late-middle Pleistocene boundary and middle-early Pleistocene boundary, which are those of Richmond and Fullerton (1986). Ages are expressed in ka for kilo-annum (thousand years) and Ma for mega-annum (million years).

Geologic and Geophysical Maps of the Santa Maria and Part of the Point Conception 30'×60' Quadrangles, California

By Donald S. Sweetkind,[1] Victoria E. Langenheim,[1] Kristin McDougall-Reid,[1] Christopher C. Sorlien,[2] Shiera C. Demas,[3] Marilyn E. Tennyson,[1] and Samuel Y. Johnson[1]

Introduction

This report presents geologic, gravity, and aeromagnetic maps for the onshore parts of the Santa Maria and Point Conception 30'×60' quadrangles at a compilation scale of 1:100,000. The maps, which are presented as layers in a georeferenced portable document format (PDF), depict the distribution of bedrock units, surficial deposits, paleontological data, geophysical data, and structural features in the Santa Maria basin and the Santa Ynez Mountains to the south (fig. 1), an area corresponding to 26 contiguous 7.5-minute U.S. Geological Survey (USGS) quadrangles. The geologic map also compiles the location of offshore faults and folds. These new maps revise and supersede two earlier mapped versions of the 30'×60' Santa Maria quadrangle that were produced as part of the U.S. Geological Survey's investigations of onshore oil and gas resources of the Santa Maria province (Keller, 1995). The first map was released as a scanned black-and-white image of a hand-drawn compilation (Tennyson, 1992); the second map was a digital release that is no longer available (Tennyson and others, 1995). This new map of the Santa Maria quadrangle also includes the geology of the onshore part of the adjacent Point Conception 30'×60' quadrangle (fig. 1) that encompasses the Santa Ynez Mountains of the western Transverse Ranges. In addition, the digital database that supports this report contains a geospatial map database, magnetic and gravity data, paleontological data, and interpretation of major offshore structural features that bear on the continuity and connection of the mapped onshore structures. The digital database is available as a USGS ScienceBase data release at https://doi.org/10.5066/P9FU7SJL (Sweetkind and others, 2020).

Western Santa Barbara County and parts of southern San Luis Obispo County compose the map area (fig. 1). The landscape includes the northwest-trending Sierra Madre and San Rafael Mountains in the northeast and the east-west trending Santa Ynez Mountains, which form the western part of the Transverse Ranges, in the southern part of the map (figs. 1 and 2). The central part of the map includes the westward-flowing Santa Ynez River and the Casmalia, Solomon, and Purisima Hills. To the north is the broad Santa Maria Valley, drained by the Santa Maria River and its tributary, the Sisquoc River (fig. 2).

The mapped area encompasses the Santa Maria basin, a triangular sedimentary basin bounded on the northeast by the Sierra Madre and San Rafael Mountains, on the south by the Santa Ynez Mountains, and outside of the mapped area on the west, by the offshore Santa Lucia Bank fault (fig. 1; Tennyson, 1995b; Dunkel and others, 1997). The Santa Maria basin is subdivided along the Hosgri fault into onshore and offshore subareas. The onshore basin includes strata and structures that extend offshore to the Hosgri fault; the offshore Santa Maria basin is bounded on the west by the Santa Lucia Bank fault and on the east by the Hosgri fault (fig. 1; Hoskins and Griffiths, 1971; Ogle and others, 1987; Tennyson, 1995b; Dunkel and others, 1997). Within the onshore and offshore parts of the basin, Neogene strata of the Lospe (Tl), Point Sal (Tps), Monterey (Tm), Sisquoc (Tsq), Foxen (Tf), and Careaga (Tc) Formations overlie Mesozoic rocks of the Franciscan Complex (KJf), ophiolite (Jo; included as part of the Coast Range ophiolite of Hopson and others, 2008), and rocks that are correlative to part of the Great Valley Sequence (KJe) (fig. 3). Onshore, the Neogene section is overlain late Neogene (upper Pliocene) and Quaternary (lower Pleistocene) continental sediments (QTpr) and Quaternary deposits (Q) (fig. 3). Total thickness of the Neogene strata exceeds 3,000 meters (m) in the depocenters and thins to less than 1,000 m over intrabasinal uplifts (fig. 3; Woodring and Bramlette, 1950; Dunkel and others, 1997; Behl and Ramirez, 2000).

The Santa Maria basin is one of the oldest oil-producing regions of California (Arnold and Anderson, 1907; Crawford, 1971). As of 2009, the basin produced over 875 million total barrels of oil (MMBO) from the onshore region (California Department of Conservation, 2010), and more than 190 MBO of production offshore (Dunkel, 2001). An additional 1.38 billion barrels (BBO) of potential oil-equivalent resource

[1]U.S. Geological Survey

[2]University of California, Santa Barbara, Calif.

[3]Valdez International Corporation, Denver, Colo.

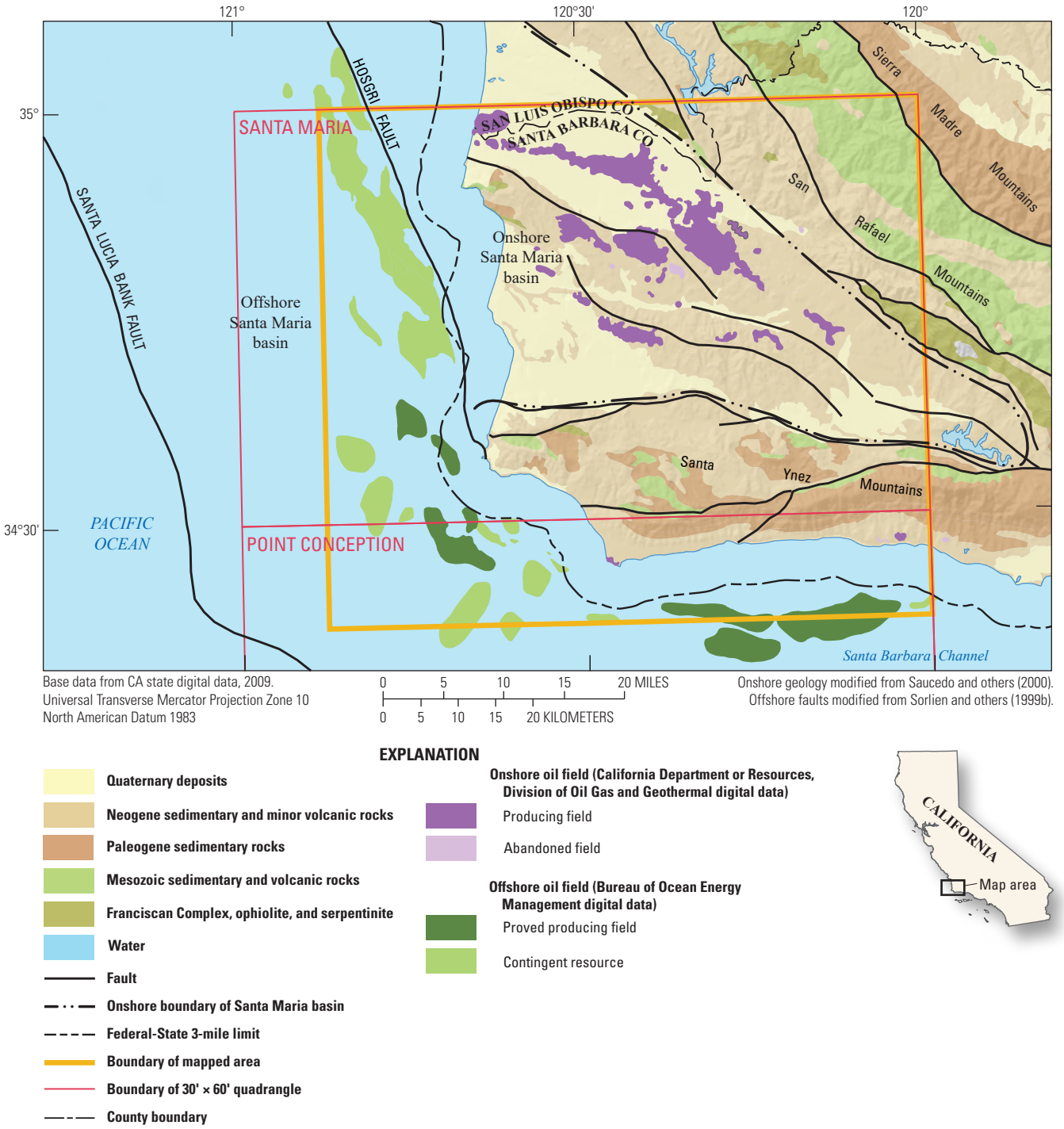

Figure 1. Simplified geologic map of the Santa Maria basin and surrounding areas, California, showing the area mapped within the Santa Maria and Point Conception 30'x60' U.S. Geological Survey quadrangles. Selected major faults shown as thick black lines; the Hosgri fault separates the onshore and offshore parts of the Santa Maria Basin.

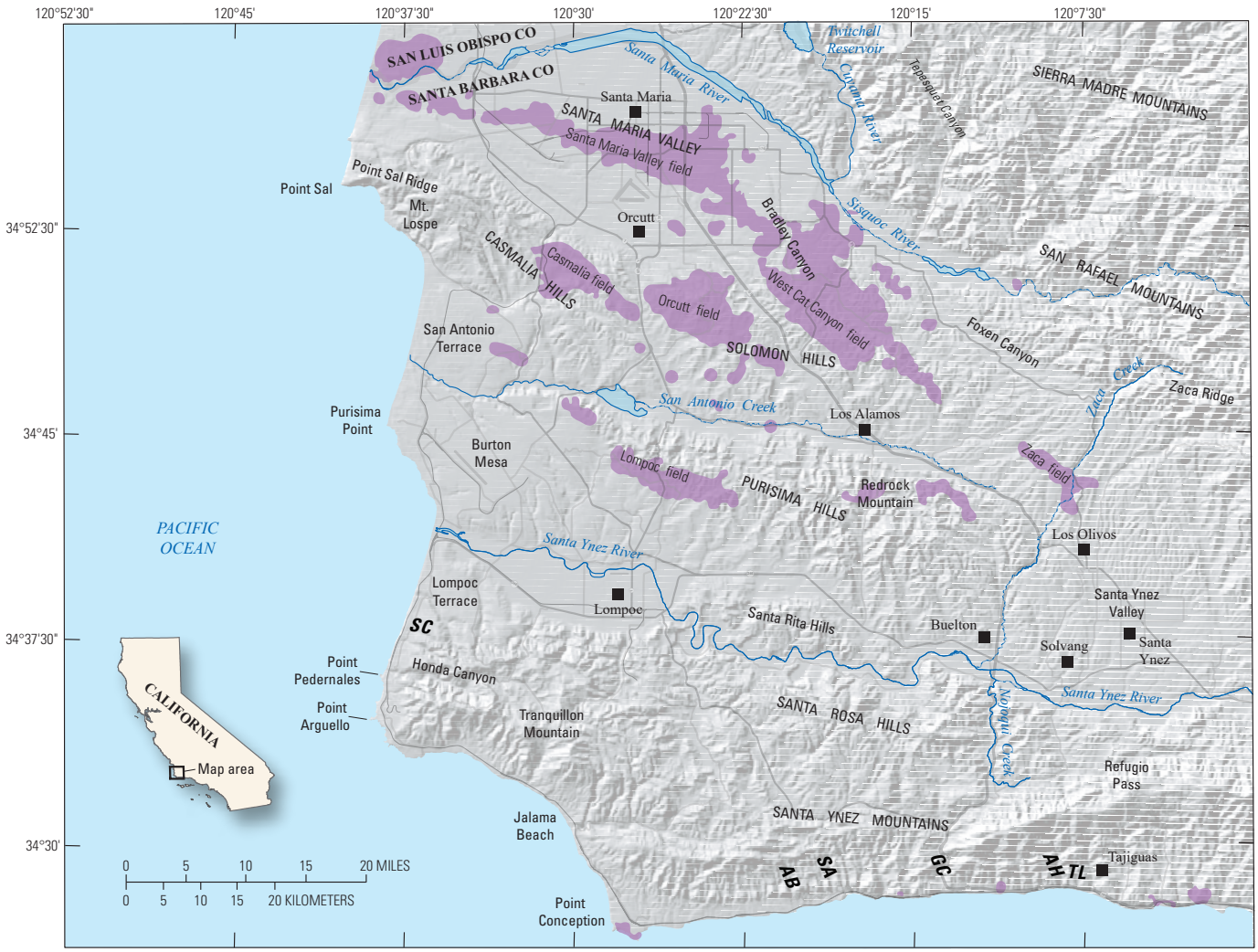

Figure 2. Shaded relief map of the onshore part of the Santa Maria and Point Conception 30'x60' quadrangles, California, annotated with geographic names used in the text. Onshore oil fields shown in purple; topographic features are labeled AH, Arroyo Hondo; GC, Gaviota Canyon; SA, Santa Anita Canyon; SC, Spring Canyon; microfossil sections are labeled AB, Arroyo el Bulito; TL, Tajiguas landfill.

are estimated for the offshore region (Mayerson, 1997; Dunkel, 2001). Almost 60 percent of the total onshore production is from anticlinal traps where the Monterey Formation is overlain by younger sealing strata (the Casmalia, Orcutt, West Cat Canyon, and Lompoc fields, fig. 2) (Crawford, 1971; Tennyson, 1995b). A large part of the remaining production is from stratigraphic traps where the Monterey Formation or other permeable units wedge out beneath less permeable strata at emergent areas on the basin margin (Santa Maria Valley field, fig. 2) (Tennyson, 1995b). Offshore production has come primarily from faulted and fault-bounded anticlines (Dunkel and others, 1997; Mayerson, 1997). The onshore Santa Maria basin also contains the world's largest worked diatomite deposit, located south of Lompoc (Jenkins, 1982).

The Santa Maria basin and rocks in surrounding uplands record multiple phases of Miocene and younger tectonism related to clockwise rotation of the western Transverse Ranges, the evolution of the Pacific–North American plate margin from a transtensional to a transpressional boundary, and the resulting slip on major faults of the central Coast Ranges west of the San Andreas Fault (Hornafius and others, 1986; Luyendyk, 1991; McCrory and others, 1995). Stratigraphic and structural reconstructions of the basin bear on the Neogene tectonic evolution of the central Coast Ranges, the translation and rotation of the western Transverse Ranges, and the partitioning of slip onto a system of faults located to the north of the Transverse Ranges and to the west of the San Andreas Fault (Powell, 1993; Wilson and others, 2005). This new map compilation provides a set of uniform digital geologic and geophysical data that can be used in the analysis of the geologic and tectonic evolution in this region, as well as a geologic basis for the evaluation of energy and water resources and potential geologic hazards.

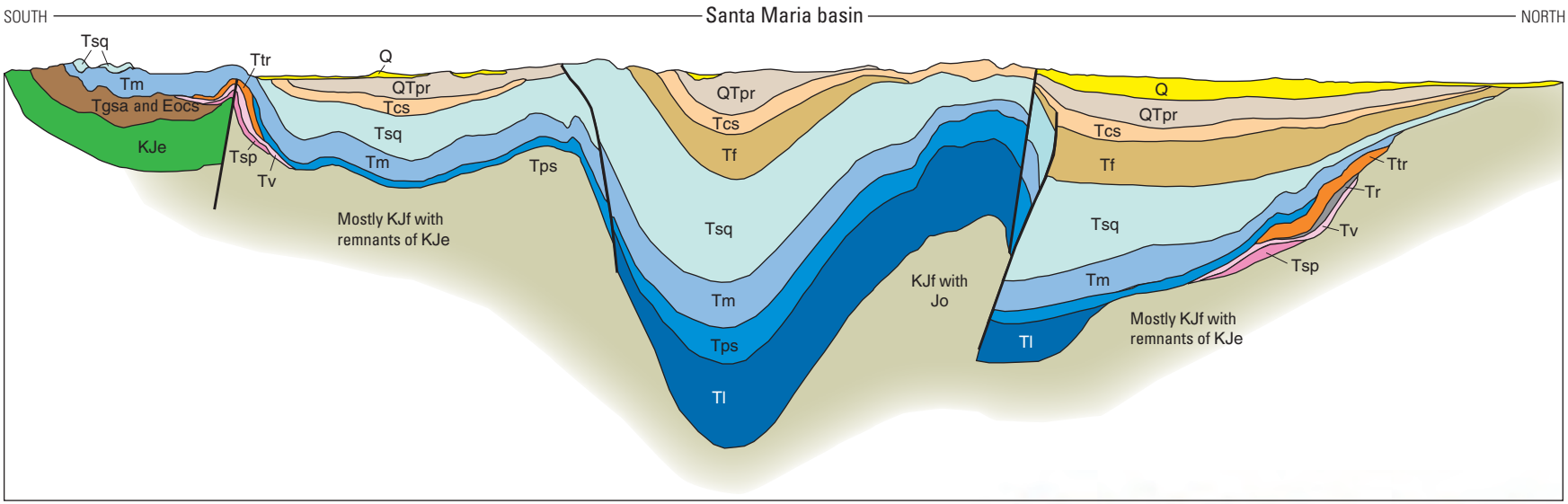

NOT TO SCALE

EXPLANATION

Stratigraphic units shown on section

- Q — Undivided Quaternary deposits
- QTpr — Paso Robles Formation
- Tcs — Careaga Sandstone
- Tf — Foxen Mudstone
- Tsq — Sisquoc Formation
- Tm — Monterey Formation
- Tps — Point Sal Formation
- Tl — Lospe Formation
- Ttr — Miocene volcanic rocks
- Tr — Rincon Shale
- Tv — Vaqueros Formation
- Tsp — Sespe Formation
- Eoc — Eocene units, undivided
- KJe — Espada Formation
- Franciscan Complex and Ophiolite

Generalized units shown on index map

- Quaternary sediments
- Neogene sedimentary and minor volcanic rocks
- Paleogene sedimentary rocks
- Mesozoic sedimentary and minor volcanic rocks
- Franciscan Complex and Coast Range ophiolite

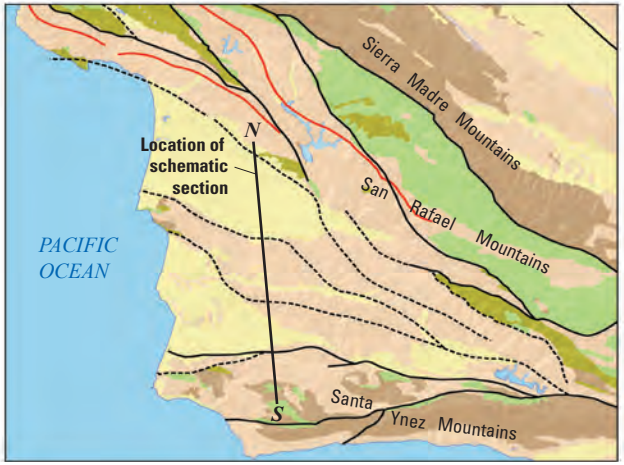

Figure 3. Schematic cross section of the Santa Maria Basin, California. Schematic section modified from American Association of Petroleum Geologists (1959) and Dibblee (1995). The section is intended to illustrate the general configuration of stratigraphic units across the basin; it is not to scale and is a representative structural section.

Previous Mapping

The first geologic map of the Santa Maria basin and the Santa Ynez Mountains was a 1:125,000-scale map published as part of a report on the then-newly producing Santa Maria oil district (Arnold and Anderson, 1907). This map identified the gross distribution of Pliocene, Miocene, and pre-Miocene rocks and defined the traces of the major fold axes and some faults. Mapping at a similar level of detail was compiled for the area surrounding the Santa Ynez River by Nelson (1925). Woodring and others (1943) and Woodring and Bramlette (1950) produced comprehensive studies of the north-central part of the map area between the Santa Ynez River and the Sisquoc River. These studies resulted in geologic mapping at the 1:24,000-scale for the oil-producing regions of the Santa Maria Valley and the Casmalia, Solomon, and Purisima Hills (fig. 2). Dibblee (1950) produced the first comprehensive and detailed maps of the western part of the Santa Ynez Mountains from the southern coast northward to north of the Santa Ynez River at a scale of 1:62,500 [*Fig. 3 on Geologic map PDF Bookmark*]. Dibblee subsequently published four 1:24,000-scale USGS geologic quadrangle maps in the Santa Ynez Mountains in the southeastern part of the study area (Dibblee, 1981a–d) [*Fig. 3 on Geologic map PDF Bookmark*].

Part of the Sierra Madre Mountains near Twitchell Reservoir to the east of the city of Santa Maria (fig. 2) was mapped by Hall (1978) at a scale of 1:24,000. This map provided important geologic relations around the Santa Maria River and West Huasna faults in a region to the east of that mapped by Woodring and Bramlette (1950) [*Fig. 3 on Geologic map PDF Bookmark*]. Hall (1981a) extended this 1:24,000-scale mapping to the southeast in a swath that included the trace of the Little Pine fault and other northwest-striking faults that bound the Santa Maria basin on the northeast side [*Fig. 3 on Geologic map PDF Bookmark*]. Vedder and others (1991) mapped at 1:24,000 scale the geology in the Tepusquet Canyon and Manzanita Mountain quadrangles in the Sierra Madre Mountains in the northeast part of the map area [*Fig. 3 on Geologic map PDF Bookmark*]. Frizzell and Vedder (1986) mapped parts of the San Rafael Mountains in the eastern part of the map area at a scale of 1:250,000 as part of a mineral-resource assessment within the Santa Lucia Wilderness. The Thomas Dibblee Foundation published separate geologic maps at a scale of 1:24,000 of each 7.5-minute quadrangle in the map area except for the Manzanita Mountain quadrangle in the northeast part of the map area (Dibblee, 1988a–f, 1989a–b, 1993a–c, 1994a–c, 1994a–b); these maps were used for reference but due to copyright restrictions were not digitally compiled on the current map.

The extent of alluvial materials and stream terraces were mapped in the Santa Maria River (Worts, 1951), San Antonio Creek (Muir, 1964), and Santa Ynez River (Upson and Thomasson, 1951) drainage basins as part of water-resources investigations. Unconsolidated materials were generally accurately mapped, but deposits were shown in generalized age groupings because detailed age control was unavailable to aid the mapping. Fluvial terrace treads were mapped along selected reaches of the Santa Ynez River by Levish and others (1996) and are similar in shape and relative age to those mapped in this study.

The geology of the Santa Maria 30'×60' quadrangle was initially compiled at 1:100,000 scale from many of the above-cited sources by Tennyson (1992). This map compilation consisted of a scanned raster image of a black-and-white, hand-drawn geologic map showing geologic contacts and major structures with an accompanying explanatory pamphlet. The compilation contained no bedding attitudes and was not released with a geographic information system (GIS) dataset yet presented a useful compilation of maps made by several different workers over the last 50 years. Apart from State geologic maps published by the California Division of Mines and Geology (Jennings 1959; Jennings and others, 1977) at scales of 1:250,000 and 1:750,000, respectively, the geology of the Santa Maria quadrangle had not been previously integrated from the various more detailed geologic maps. A preliminary digital geologic map compilation of the Santa Maria 30'×60' quadrangle (Tennyson and others, 1995) included the geologic mapping of Woodring and Bramlette (1950), Hall (1978, 1981a), and Vedder and others (1991) and serves as an important starting point for the current digital map compilation.

Present Compilation

This report contains the following map layers of the onshore parts of the Santa Maria and Point Conception 30'×60' quadrangles, California, all at 1:100,000 scale: (1) a new geologic map, (2) a tectonic map, (3) two new gravity anomaly maps that differ in their assumption of the density of rocks that make up the topography, (4) a new aeromagnetic anomaly map, (5) two aeromagnetic anomaly maps processed to emphasize shallow and moderate-depth magnetic sources, and (6) a map showing the location of several hundred paleontological localities. Magnetic and gravity data extend to offshore parts of the quadrangles; selected faults are portrayed in the offshore areas to provide context for the geophysical data and the onshore structures. The report also contains a new description of the geologic map units and structural relations in the mapped area.

The geologic map is significantly modified from previous compilations of Tennyson (1992) and Tennyson and others (1995). Three factors led to the decision to remap the area rather than publish the previous compilations in digital form without modification: (1) the western Transverse Ranges are a critical element in the development and subsequent emergence and uplift of the Santa Maria basin (Hornafius, 1985; Hornafius and others, 1986; Onderdonk, 2005), so the geology of the Point Conception 30'×60' quadrangle was added to the map area originally compiled by Tennyson, (2) almost 20 years of new geologic information have been gathered for the offshore part of the map area (Sorlien and others, 1999a,

1999b; Johnson and Watt, 2012; Willingham and others, 2013), allowing interpretation of linkages between faults mapped onshore and offshore, and (3) new aerially consistent and continuous potential-field datasets make it possible to map concealed faults and rock bodies (Langenheim and others, 2013a; Langenheim, 2014). Changes in the geologic map include the following:

1. Integration of the geology of the western Santa Ynez Mountains with the geologic mapping of the Santa Maria basin
2. New mapping of Quaternary surficial deposits throughout the map
3. An updated depiction of several faults, including the Lions Head, Santa Ynez River, and the Oceano-Zaca fault system based on integration of surface mapping, well data, and potential-field geophysical data
4. Revised stratigraphic depiction based on subdivision of stratigraphic domains.
5. New interpretations of basin geometry and location of structures based on potential-field geophysical data
6. Several hundred paleontological localities compiled and interpreted to provide age control for the geological mapping
7. Compilation and interpretation of structures in the offshore part of the map area

Geologic maps from Woodring and Bramlette (1950; 5 pl.) and Dibblee (1950; 2 pl.) were scanned and georeferenced, and the geologic polygons, structures, and bedding attitudes digitized within a GIS. Where the mapping from these two studies overlapped in the Purisima Hills south of 34°45' N, the Woodring and Bramlette (1950) mapping was retained. In the southeast part of the map area, four 1:24,000-scale quadrangles mapped by Dibblee and published by the U.S. Geological Survey (Dibblee, 1981a–d) were digitized and used to replace the earlier mapping of Dibblee (1950). Geology in the San Rafael Mountains was digitized from maps by Hall (1978, 1981a), Frizzell and Vedder (1986), and Vedder and others (1991). The area including San Antonio Terrace to the northeast of Purisima Point was digitized from the mapping of Muir (1964). A small area in the southeast corner of the Foxen Canyon quadrangle not mapped by any of the above studies was mapped from new fieldwork and countywide ortho imagery of 1-m resolution from the National Agriculture Imagery Program (NAIP) for the year 2009 (https://nrcs.app.box.com/v/naip). Geologic features from these various source maps were merged and edge-matched across map boundaries. Additional faults were compiled from the following sources: (1) the Santa Ynez River fault from the trace published in Sylvester and Darrow (1979); and (2) the Los Alamos and Baseline faults in the Los Olivos area digitized from georeferenced images from Guptill and others (1981). Traces of certain subsurface faults, including the Lions Head fault, the Garey fault, and the Oceano-Zaca fault were based primarily on well data (Tennyson, 1995a; Sweetkind and others, 2010) and augmented by the traces shown on subsurface maps by Hall (1982) and Gray (1980). The buried trace of the Casmalia fault is derived from the subsurface mapping of Gray (1980), also compiled by Lettis and others (2004).

Quaternary units were revised from source geologic mapping and augmented with new mapping using a combination of slope maps derived from the digital elevation model (DEM), high-resolution satellite imagery, and soils maps. Alluvial channels and active and stabilized eolian deposits were mapped using countywide ortho imagery of 1-m resolution from the National Agriculture Imagery Program (NAIP) for the year 2009 (https://nrcs.app.box.com/v/naip). Distinction between Holocene and Pleistocene alluvial deposits was based upon interpretation of soil surveys from the Natural Resources Conservation Service (NRCS) for Santa Barbara and San Luis Obispo Counties (https://www.nrcs.usda.gov/wps/portal/nrcs/surveylist/soils/survey/state/?stateId=CA). Soil nomenclature inconsistencies between counties were resolved and polygons on the NRCS digital maps were classified based on (1) geomorphic position in the landscape, (2) shape and orientation of individual mapped deposits, and (3) associated soil series. Relative age of individual soils was determined from the NRCS tabular data by first grouping soils by parent material, then comparing soil horizonation or typical soil profiles, thickness of B horizon, and abundance of secondary carbonate, all of which are soil properties that vary with soil age (Birkeland and others, 1991; Birkeland, 1999). Distinction between Holocene and Pleistocene eolian deposits was based on published age determinations from the Guadalupe and Nipomo dune complexes (Cooper, 1967; Orme, 1992; Knott and Eley, 2006).

The treads of marine and fluvial terraces were identified using a slope map calculated from a DEM with 10-m spatial resolution (https://nationalmap.usgs.gov/; accessed December, 2012). Terraces were identified as surfaces with slopes generally less than 5 degrees, partly bounded by steeper slopes below. Distinction between Holocene and Pleistocene terraces was made based on the relative development of pedogenic, translocated clay as determined from soil survey mapping (https://www.nrcs.usda.gov/wps/portal/nrcs/main/soils/survey/). The relative ages of Pleistocene terraces were distinguished based on each surface's relative elevation above mean sea level and degree of erosional modification. As many as 17 distinct marine terrace levels are present along the south slope of the Santa Ynez Mountains in southwestern Santa Barbara County (Upson, 1951; Kennedy and others, 1992; Rockwell and others, 1992). Terraces underlain by abrasion platforms of known ages were not resolvable at the scale of the current mapping. Instead, two composite geomorphic surfaces, Qto1 and Qto2, are mapped that generally represent the elevations of older and younger Pleistocene marine terraces, respectively, based on comparison with published ages of marine terraces in southwestern Santa Barbara County (Upson, 1951; Clark, 1990; Kennedy and others, 1992; Muhs and others, 1992; Rockwell and others, 1992).

More than 2,700 onshore gravity measurements were used to produce isostatic gravity maps of the study area *[Gravity 2,670 kg/m³ and Gravity 2,000 kg/m³ PDF Bookmarks]*. Offshore gravity data are from a 4-kilometer (km) grid derived from ship track data (Vedder and others, 1974; Beyer, 1980; McCulloch and others, 1989). Sources of onshore data include Rietman and Beyer (1982), Up de Graff (1984), the map of Sauer and Mariano (1990), data compiled by Langenheim (2014), and new data collected by the U.S. Geological Survey in 2009–2013. Gravity measurements are nonuniformly distributed in the region, with an average spacing of 1 km onshore.

Gravity data were reduced to free-air anomalies using standard formulas (for example, Telford and others, 1990). Bouguer, curvature, and terrain adjustments to a radial distance of 166.7 km were applied to the free-air anomaly at each station to determine the complete Bouguer anomalies at a standard crustal reduction density of 2,670 kilogram per cubic meter (kg/m^3) (Plouff, 1977) *[Gravity 2,670 kg/m³ PDF Bookmark]*. Because topography is locally composed of low-density Cenozoic deposits, the data were also processed using a density of 2,000 kg/m^3 *[Gravity 2,000 kg/m³ PDF Bookmark]*. An isostatic adjustment was then applied to remove the long-wavelength effect of deep crustal and (or) upper mantle masses that isostatically support regional topography. The isostatic adjustment assumes an Airy-Heiskanen model (Heiskanen and Vening-Meinesz, 1958) of isostatic compensation. Compensation is achieved by varying the depth of the model crust-mantle interface, using the following parameters: a sea-level crustal thickness of 25 km, a crust-mantle density contrast of 400 kg/m^3, and a crustal density of 2,670 kg/m^3 for the topographic load. These parameters were used because (1) they produce a model crustal geometry that agrees with seismically determined values of crustal thickness for central California; (2) they are consistent with model parameters used for isostatic corrections computed for the rest of California (Roberts and others, 1990); and (3) changing the model parameters does not significantly affect the resulting isostatic anomaly (Jachens and Griscom, 1985). The resulting isostatic residual gravity values should reflect lateral variations of density within the middle to upper crust. Accuracy of the data is estimated to be on the order of 0.1 to 0.5 milliGal (mGal).

The aeromagnetic map [*Aeromagnetic Total PDF Bookmark*] is based on data from three surveys of varying resolution (table 1). The onshore survey (Langenheim and others, 2009), which covers most of the map area, was flown at a nominal height of 305 m (1,000 feet [ft]) above ground along flight lines spaced 0.8 km (0.5 mile [mi]) apart. Accuracy of this modern survey is 1 nanotesla (nT) or better. The offshore surveys are from older, lower-resolution data. Data covering the northwest corner of the map area (McCulloch and Chapman, 1977) were flown at a constant barometric altitude of 610 m along flight lines 1.6 km apart, whereas data along the southern margin of the map area were derived from digitizing a map of a 1961 aeromagnetic survey flown along flight lines 1.6 km apart (Langenheim and others, 1993). All data were adjusted to a common magnetic datum with a gap to mark survey boundaries.

To help delineate structural trends and gradients expressed in the gravity and magnetic fields, a computer algorithm was used to locate the maximum horizontal gradient (Cordell and Grauch, 1985; Blakely and Simpson, 1986). Concealed basin faults beneath the valley areas were mapped using horizontal gradients in the gravity and magnetic fields. We calculated magnetization boundaries on filtered versions of the magnetic field to isolate anomalies caused by sources at varying depths (Blakely, 1995). We used match filtering to separate the data into different wavelength components by modeling the observed spectra as a sum of distinct equivalent source layers at increasing depths (see Phillips, 2001); the resulting depths produced from the match-filtering were 178, 397, and 2,073 meters. Second, the resulting residual aeromagnetic fields were mathematically transformed into magnetic potential anomalies (Baranov, 1957); this procedure effectively converts the magnetic field to the equivalent "gravity" field that would be produced if all magnetic material were replaced by proportionately dense material. The horizontal gradient of the magnetic potential field was then calculated. Gradient maxima occur approximately over steeply dipping contacts that separate rocks of contrasting densities or magnetizations. For moderate to steep dips (45° to vertical), the horizontal displacement of a gradient maximum from the top edge of an offset horizontal layer is always less than or equal to the depth to the top of the source (Grauch and Cordell, 1987).

The trace of the Hosgri fault and faults west of the Hosgri fault were reinterpreted using all two-dimensional (2D) seismic reflection data available in 2013 at the U.S. Geological Survey National Archive of Marine Seismic Surveys (NAMSS) site (https://walrus.wr.usgs.gov/NAMSS/; accessed 2013), along with 180 2D tracks from five 3D seismic reflection volumes, provided by the U.S. Bureau of Safety

Table 1. Specifications of aeromagnetic surveys used to compile the aeromagnetic map for the Santa Maria and Part of the Point Conception 30'×60' Quadrangles, California

[m, meters; NE., north east; SW., south west; N., north; S. south]

Survey	Year flown	Altitude above ground	Flightline spacing (km)	Flightline direction
Paso Robles (Langenheim and others, 2009)	2008	305 m	0.8	NE./SW
Southern California Borderlands (Langenheim and others, 1993)	1961	760 m (estimated)	1.6	N./S.
California Coast (McCulloch and Chapman, 1977)	1976	610 m (barometric)	1.6	NE./SW

and Environmental Enforcement (https://www.data.bsee.gov/; accessed 2013). Tagged image file format (tiff) files (108) were converted to SEG-Y format and interpreted using Kingdom Suite seismic and geological interpretation software (https://ihsmarkit.com/products/kingdom-seismic-geological-interpretation-software.html), while the remaining 72 profiles were used as a check of the mapping by comparison. Additional data from the Hosgri fault are taken from the structural trend map of Willingham and others (2013, pl. 4) and, north of Point Sal, from the mapping of Johnson and Watt (2012). Structures at the south end of the Hosgri fault and between the Hosgri fault and the coast were mapped by us (C.C. Sorlien) based on structure-contour maps of subsurface layers that were constructed using dense grids (~3,000 km) of multichannel seismic reflection data, well logs from 77 hydrocarbon exploration wells, and published geologic and subsurface maps (Sorlien and others, 1999a, b). We remapped strands of the Hosgri fault west through south of Point Arguello and the upper edge of the partly blind North Channel fault for this publication, with parts of these faults imaged near the edges of three-dimensional (3D) seismic reflection surveys.

The traces of the offshore faults should be treated as generalized locations because they are not all mapped at the same stratigraphic horizon. The structural trend map of Willingham and others (2013, pl. 4) is itself generalized; in places, the Hosgri fault is mapped at the seafloor, elsewhere it is projected updip from the top of the early-late Pliocene unconformity. Locational shifts are small because Willingham and others (2013) interpreted the Hosgri fault with a steep dip. Low-angle faults that are associated with uplifts and folds to the west of the Hosgri fault are mapped where the vertical projection of the upper fault tip, or top of the fault ramp for fault-bend folds, would intersect the seafloor (Willingham and others, 2013). Structures east of the south end of the Hosgri fault were mapped at a mid-Sisquoc Formation sequence boundary; farther north, between Purisima Point and Point Sal, structures were mapped within the Monterey Formation where the Sisquoc Formation was removed by erosion (Sorlien and others, 1999a). The map trace is near the seafloor trace because the map horizons at the faults are near the seafloor. Structures at or near the seafloor were compiled from Johnson and others (2015, 2018).

Interactive Portable Document Format (PDF) Map

The geologic, geophysical, and paleontological maps are presented as a single interactive, multilayer PDF, as well as traditional separate map sheets. The various data and base map elements are placed on separate layers, which allow the user to combine elements interactively to create map views in a dynamic fashion not possible with traditional map sheets. For example, fault lines, traditionally part of the geologic map sheet, can be overlain on gravity data to examine the role of the faults as boundaries of bodies with differing density. A layered PDF also allows the user to select simplified views by excluding some of the elements of a traditional map sheet, such as focusing on geologic unit distribution by omitting symbols showing bedding attitude. In addition, a layered PDF allows the user to select either a traditional topographic map base, a topographic shaded-relief base, or even no base at all. Map sheets with a traditional appearance are readily compiled by choosing the associated data layers or by choosing the desired preset map configuration under the Bookmarks panel in the PDF.

Paleontology

Fossils provide considerable understanding of the geology of the map area: microfossils, primarily foraminifers, are present in most of the Tertiary formations. A complete listing of the fossils in the map area is beyond the scope of this report, but we make extensive reference to fossil data in the discussions below. Although most foraminiferal data for the map area are used in the discussion that follows, unused data fall into one of two categories, as described here:

1. Data with a mismatch between unit and fossil related to imprecise location of sample locality and (or) mapped contact. Some localities plot on the “wrong” side of a contact.

2. Data that seem “obviously wrong” (for example, a late Miocene locality in a unit overlain by well-documented middle Miocene strata). We take these age determinations to be errors by earlier workers.

These problems are annotated in the “Notes” field for the locality descriptions of the Chevron outcrops and USGS locations (appendix 1, tables 1.1. and 1.2). We leave resolution to future workers as it is beyond the scope of this study to try to reoccupy the localities to determine whether the locality or contact needs to be relocated.

Cenozoic benthic foraminiferal age interpretations (fig. 4) are based on the California benthic foraminiferal zonations of Kleinpell (1938); Kleinpell and Haller (1980), and Mallory (1959) with modifications as proposed by McDougall (2008) and additional modifications as proposed by Gradstein and

Figure 4 (following page). California Cenozoic biostratigraphic framework based on the California benthic foraminiferal zonations of Kleinpell (1938), Kleinpell and Haller (1980), and Mallory (1959) with modifications as proposed by McDougall (2008) and additional modifications as proposed by Gradstein and others (2012). Ma, million years; Lines on coastal onlap curve indicate sequence boundaries—heavy solid lines are major sequence boundaries, moderate solid lines are medium sequence boundaries, and thin solid lines are minor sequence boundaries. Dashed lines indicate maximum coastal onlap. Pleist., Pleistocene; Cret., Cretaceous; M, Middle; E, Early; ECCE, Eocene Canyon Cutting Event; PCCE, Paleocene Canyon Cutting Event (from McDougall, 2008).

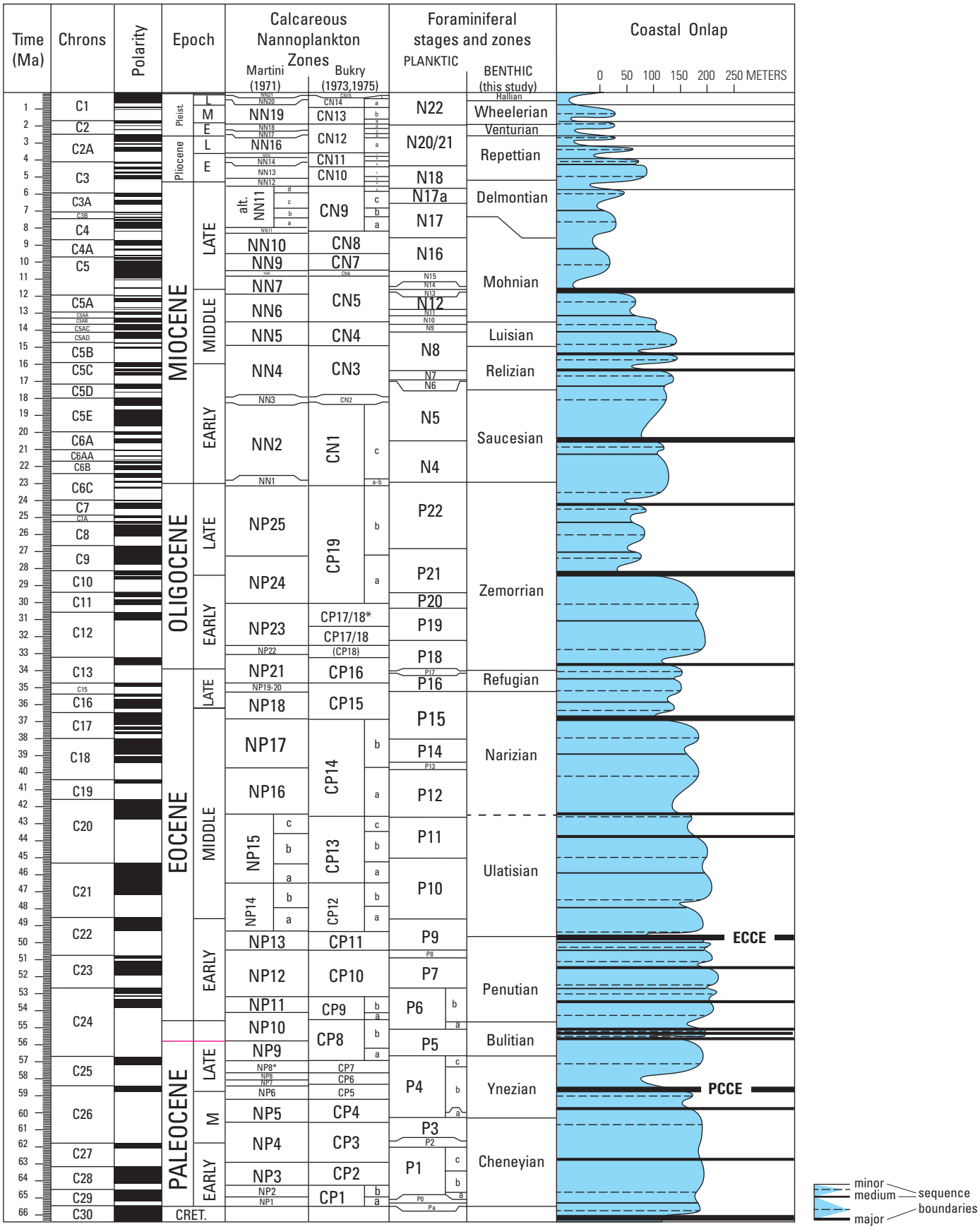
Time (Ma)
Chrons
Polarity
Epoch
Calcareous Nannoplankton Zones
Martini (1971)
Bukry (1973,1975)
Foraminiferal stages and zones
PLANKTIC
BENTHIC (this study)
Coastal Onlap
0 50 100 150 200 250 METERS
Pleist.
Pliocene
MIOCENE
OLIGOCENE
EOCENE
PALEOCENE
CRET.
LATE
MIDDLE
EARLY
Hallian
Wheelerian
Venturian
Repettian
Delmontian
Mohnian
Luisian
Relizian
Saucesian
Zemorrian
Refugian
Narizian
Ulatisian
Penutian
Bulitian
Ynezian
Cheneyian
ECCE
PCCE
minor
medium
major
sequence boundaries

others (2012). Correlation of the benthic foraminiferal stages and zones to the international time scale is discussed in McDougall (2008).

Two important microfossil sections occur in the map area (AB and TL in fig. 2; appendix 1, tables 1.3 and 1.4): AB is the Arroyo el Bulito section of Tipton (1980), which is the type section for the Refugian Stage (late Eocene); and TL is the Tajiguas landfill section (Stanley and others, 1992, 1994; Prothero and Rapp, 2001), which would replace the type section of the Saucesian Stage (early Miocene) on Los Sauces Creek because the Los Sauces Creek section is no longer accessible. Checklists of the benthic foraminiferal assemblages for these sections are included in appendix 2, tables 2.3 and 2.4.

Stratigraphy

The map area includes stratigraphically distinct regions of the central Coast Ranges and the western Transverse Ranges, separated by several major faults known or inferred to have large-scale offset. We have divided the map area into six stratigraphic domains that are primarily divided based on the thicknesses and nature of the Tertiary section [*Fig. 1 on Geologic map PDF Bookmark*]. From northeast to southwest, there are six domains: Nacimiento, Sierra Madre, Huasna, Santa Maria, Santa Rosa Hills, and Santa Ynez [*Fig. 2 on Geologic map PDF Bookmark*]. The more regional study of Lettis and others (2004) generalized the Nacimiento, Sierra Madre, Huasna domains as a southern Coast Ranges domain and combined the Santa Rosa Hills and the Santa Ynez domains as a western Transverse Ranges domain. The Santa Maria domain as used in this report falls within the Los Osos domain of Lettis and others (2004), which was divided by them into distinct structural blocks. Domain boundaries used here [*Fig. 2 on Geologic map PDF Bookmark*] generally follow the same structures used by Lettis and others (2004).

Nacimiento Domain

This domain occupies a small triangular area in the extreme northeast corner of the map area, to the northeast of the Nacimiento fault [*Fig. 2 on Geologic map PDF Bookmark*]. An unnamed marine sandstone of Eocene and (or) Paleocene age (Tus; Vedder and others, 1989a) is the only stratigraphic unit exposed in the map area [*Fig. 1 on Geologic map PDF Bookmark*]. These strata are deformed into northwest-striking, upright, open folds to the east of the map area (Kellogg and others, 2008).

Sierra Madre Domain

The Sierra Madre domain occupies much of the northeast corner of the map area [*Fig. 2 on Geologic map PDF Bookmark*]. This upland area is bounded on the southwest by the East Huasna and Cachuma faults and on the northeast by the Nacimiento fault. The oldest rocks in the Sierra Madre domain are dismembered remnants of the Jurassic Coast Range ophiolite (Hopson and others, 2008), predominantly massive diabase that is locally serpentinized (Dibblee, 1994c). These rocks crop out near the east edge of the map to the north of the Cachuma fault and are associated with magnetic anomalies [*Geologic map PDF Bookmark; Aeromagnetic Total PDF Bookmark*]. The ophiolitic rocks are overlain by Lower Cretaceous marine fine-grained siliciclastic rocks mapped as Espada Formation (KJe) (Vedder and others, 1967; Dibblee, 1994c) and generally correlative to the lower part of the Great Valley Sequence (McLean and Stanley, 1994) [*Fig. 1 on Geologic map PDF Bookmark*]. This domain is characterized by a thick succession of Upper Cretaceous marine turbiditic sandstones (Kus) that are in part correlative with the upper part of the Great Valley Sequence mapped elsewhere in the California Coast Ranges (Howell and others, 1977; McLean and Stanley, 1994; Vedder and Stanley, 2001). An unnamed nonmarine pebble to boulder conglomerate with subordinate sandstone and mudstone that is of Campanian and Maastrichtian age (Kcn) is locally present within the upper part of this section (Vedder and others, 1967, 1977, 1994) [*Fig. 1 on Geologic map PDF Bookmark*]. The Upper Cretaceous section is disconformably and locally unconformably overlain by Oligocene conglomerate and sandstone (Tsi; Vedder and others, 1991); upper Oligocene to lower Miocene unnamed sandstone (Tss) and Monterey Formation (Tm) are preserved along the axes of the larger synclines [*Geologic map PDF Bookmark*]. Near the base of the Upper Cretaceous section is a lens-shaped marine conglomerate of Cenomanian age that contains abundant volcanic-rock clasts (McLean and others, 1977). Strata are deformed into upright, open folds, including the northwest end of the Hurricane Deck syncline of Vedder and others (1967), mapped as the Bald Mountain syncline by Dibblee (1994c).

Huasna Domain

The Huasna stratigraphic domain is bounded on the northeast by the East Huasna and Cachuma faults and on the southwest by a series of northwest-striking faults including the West Huasna, Foxen Canyon, and Little Pine faults [*Fig. 2 on Geologic map PDF Bookmark*]. The oldest rocks in the Huasna domain are ophiolitic rocks of presumed Jurassic age (Jo), predominantly massive diabase and microgabbro that are locally serpentinized (Vedder and others, 1991; Dibblee, 1994b) [*Fig. 1 on Geologic map PDF Bookmark*]. These rock types coincide with magnetic anomalies [*Aeromagnetic Total PDF Bookmark*]. These rocks and small outcrops of unconformably overlying Upper Jurassic and (or) Lower Cretaceous strata (unit KJe) are exposed in an erosional window through Monterey Formation rocks in Tepusquet Canyon. Deformed metasedimentary and metavolcanic rocks and serpentine of the Franciscan Complex (KJf) are exposed in the hanging wall of the Little Pine fault in the eastern part of the map area (Hall, 1981a; Dibblee, 1994b). Hall (1981a) and Dibblee

(1994b) interpreted these Franciscan Complex rocks to be largely separated from Cenozoic units to the northeast by a normal fault mapped as the Camuesa fault. However, outcrops of lower Miocene to upper Oligocene unnamed sandstone locally unconformably overlie the Franciscan Complex with no fault, leading us to interpret the Camuesa fault as a pre-Miocene structure that is truncated by a sub-Miocene unconformity beneath these sandstones, as was mapped in the San Rafael Mountain quadrangle to the southeast (Vedder and Stanley, 2001). Outcrops of volcanic rocks of the Obispo Formation (To) are underlain by Rincon Shale (Tr), Vaqueros Sandstone (Tv), and Simmler Formation (Tsi) adjacent to the West Huasna fault near Twitchell Reservoir (Hall, 1981a) [*Geologic map PDF Bookmark*]. Most of the outcrops in this stratigraphic domain are Monterey Formation overlain by thin siliciclastic, basin-margin facies Todos Santos Claystone and Tinaquaic Sandstone Members of the Sisquoc Formation (Tsqs) [*Geologic map PDF Bookmark*]. The domain is characterized structurally by a series of northwest-striking faults, many of which have reverse offset with northeast-side up. Folds are typically upright and fold axes trend parallel to the fault traces [*Geologic map PDF Bookmark*].

Santa Maria Domain

The Santa Maria stratigraphic domain [*Fig. 2 on Geologic map PDF Bookmark*] composes the central part of the map area and is largely coincident with the onshore Santa Maria basin (fig. 1), a regional-scale syncline located between the San Rafael Mountains to the northeast and the Santa Ynez Mountains to the south. The basin contains a Neogene sedimentary sequence as much as 4.5 km thick (fig. 3; Woodring and others, 1943; Woodring and Bramlette, 1950; Crawford, 1971). These strata record Miocene basin subsidence and the development of the transform plate margin, followed by gradual shoaling and emergence in the late Miocene to early Pliocene during a transition to compressional tectonics associated with Neogene rotation of the western Transverse Ranges on the southern margin of the basin (Hornafius and others, 1986; Luyendyk, 1991; McCrory and others, 1995).

The oldest rocks in the Santa Maria stratigraphic domain are from the Jurassic (~165 Million years [Ma]) ophiolite at Point Sal (Jo) (Hopson and Frano, 1977; Hopson and others, 2008; Mattinson and Hopson, 2008), locally overlain by the Jurassic and Cretaceous Espada Formation (KJe) (Woodring and Bramlette, 1950; Dibblee, 1989b) [*Fig. 1 on Geologic map PDF Bookmark*]. The ophiolite is well exposed along 7 km of coastline from Point Sal southward into the northern part of Vandenberg Air Force Base. From top to bottom, the ophiolitic section includes thick mafic submarine volcanic rocks, subvolcanic sheeted mafic sills, massive gabbro, and an incomplete ultramafic member that is cut off at the base by the post-Miocene Lions Head fault (Hopson and Frano, 1977; Hopson and others, 2008). These rocks are accompanied by prominent gravity and magnetic highs [*Aeromagnetic Total, Gravity 2,670 kg/m³ and Gravity 2,000 kg/m³ PDF Bookmarks*]. Ophiolitic rocks are overlain by thin-bedded, micaceous shales of the Upper Jurassic and Lower Cretaceous Espada Formation [*Geologic map PDF Bookmark*].

Initial subsidence and tectonism within the Santa Maria basin are recorded by lower Miocene nonmarine sedimentary rocks of the Lospe Formation (Tl) that are interpreted to have been shed from uplifted blocks along the basin margin (McLean and Stanley, 1994). Miocene sedimentary rocks of the Point Sal (Tps) and Monterey Formations (Tm) filled in early Miocene extensional lows and onlapped and blanketed structural paleohighs. The deepest subsidence of the basin generally corresponded with deposition of the siliceous, petroliferous, bathyal marine Miocene Monterey Formation (Woodring and Bramlette, 1950). Uppermost Miocene to Quaternary marine and nonmarine siliciclastic rocks including the Sisquoc Formation (Tsqs), Foxen Mudstone (Tf), Careaga Sandstone (Tc), and the Paso Robles Formation (QTpr) record the filling of the basin and the emergence of flanking uplifts (Woodring and others, 1943; Woodring and Bramlette, 1950; Dibblee, 1995). Miocene strata unconformably overlie Jurassic ophiolite, Espada Formation, and Franciscan Complex basement (Gray, 1980; Hall, 1982; McLean, 1991) [*Fig. 1 on Geologic map PDF Bookmark*]. The thick sequences of Paleogene strata that are present in the Santa Ynez Mountains and San Rafael Mountains are absent from this domain [*Fig. 1 on Geologic map PDF Bookmark*].

Uplift and structural inversion of the basin began in the late Miocene, as recorded by an increase in siliciclastic sedimentation and syndepositional thinning of the Sisquoc Formation and Foxen Mudstone over developing anticlinal uplifts (Woodring and Bramlette, 1950; Behl and Ramirez, 2000). Compression resulted in north-vergent reverse faults and folding of Miocene and Pliocene strata (fig. 3), which formed the anticlinal structural traps for much of the petroleum found in this basin (Woodring and Bramlette, 1950; Namson and Davis, 1990; Tennyson, 1995b). As a result of this uplift, upland areas within the domain are underlain by anticlines whereas low-lying valleys are generally underlain by synclines (Woodring and Bramlette, 1950). The Casmalia Hills are a west-northwest-trending upland located south of the Santa Maria Valley and are underlain by a series of en echelon anticlines that continue to the southeast to the Solomon Hills and compose the Casmalia-Orcutt anticlinal trend (Woodring and Bramlette, 1950; Namson and Davis, 1990) [*Geologic map PDF Bookmark*]. The anticlines are typically asymmetric in cross section (Woodring and Bramlette, 1950; Namson and Davis, 1990). Southern limbs are long and gently dipping; northern limbs are moderately to steeply dipping and locally overturned, consistent with northeast-vergent shortening. To the north of the anticlinal trend is the Santa Maria Valley syncline, a large, open upright downwarp known from subsurface exploration (Woodring and Bramlette, 1950; American Association of Petroleum Geologists, 1959; Crawford, 1971; Namson and Davis, 1990). To the south of the Casmalia Hills are the San Antonio and Los Alamos synclines; late Pliocene and Quaternary alluvial deposits have been tilted to vertical or overturned on the faulted south limb of the Los Alamos Valley

syncline (Woodring and Bramlette, 1950; Dibblee, 1993a) [*Geologic map PDF Bookmark*]. This syncline is located along the north limb of another large, north-verging structure, the Lompoc-Purisima anticline. The Santa Rita syncline lies along the south edge of the Santa Maria basin (Dibblee, 1950; Woodring and Bramlette, 1950; Dibblee, 1993a).

Santa Ynez and Santa Rosa Hills Domains

Two stratigraphic domains lie to the south of the Santa Maria basin in the Santa Ynez Mountains: the Santa Rosa Hills domain to the north of the crest of the Santa Ynez Mountains and the Santa Ynez domain on the south flank of the Santa Ynez Mountains [*Fig. 2 on Geologic map PDF Bookmark*]. A thick sequence of predominantly marine sedimentary strata ranging in age from uppermost Jurassic to Pliocene is present in both domains [*Fig. 1 on Geologic map PDF Bookmark*]. In the Santa Ynez domain, these formations are very thick and form a south-dipping homoclinal sequence (Dibblee, 1950, 1982). In contrast, these formations within the Santa Rosa Hills domain are generally much thinner, interrupted by several angular unconformities, and deformed into many folds with axes trending west-northwest (Dibblee, 1950, 1982). Most of the geologic formations and structure of the western end of the Santa Ynez Mountains were described and mapped by Dibblee (1950, 1966), Kelley (1943), and Kleinpell and Weaver (1963). The structurally simpler Santa Ynez domain is discussed first in the text below.

Santa Ynez Domain

The Santa Ynez domain includes rocks exposed in the Santa Ynez Mountains to the south of the Santa Ynez fault [*Geologic map PDF Bookmark*], including Paleogene and Cretaceous marine strata similar to those exposed elsewhere in the western and central Transverse Ranges (Kelley, 1943; Dibblee, 1966; Dickinson, 1995). The aggregate thickness of Upper Cretaceous through Tertiary units exposed on the south flank of the range is as much as 6,700 m thick to the east of Gaviota Canyon; between Gaviota Canyon and Point Conception, this stratigraphic assemblage is about 4,300 m thick (Dibblee, 1950, 1966; Campion and others, 1996). In general, the stratigraphic succession in this domain consists of a largely conformable sequence of Cretaceous and Tertiary marine sandstone and shale [*Geologic map PDF Bookmark*]. The marine sequence is interrupted by the time-transgressive (upper Eocene to middle Oligocene) nonmarine Sespe Formation (Tsp), which interfingers with the marine Gaviota (Tg) and Alegria Formations (Ta) [*Fig. 1 on Geologic map PDF Bookmark*].

The Franciscan Complex is not exposed in the Santa Ynez domain; however, it is exposed along strike in Blue Canyon about 40 km to the east (Dibblee, 1966), suggesting that Franciscan rocks may underlie the exposed section. The oldest exposed rocks in this domain are the Upper Cretaceous Jalama Formation (Kj) composed of at least 900 m of gray micaceous shale with several members of light gray sandstone (Dibblee, 1950, 1982). Cretaceous rocks are overlain by a thick sequence of Paleogene (primarily Eocene) strata with generally conformable contacts [*Fig. 1 on Geologic map PDF Bookmark*]. The Paleocene Anita Shale (Tan) (Kelley, 1943; Mallory and others, 1998) is the oldest Paleogene unit; at its westernmost exposures north of Point Conception, it conformably overlies the Jalama Formation and is composed largely of siltstone and silty shale [*Geologic map PDF Bookmark*]. Overlying Eocene units include, from oldest to youngest, Juncal Formation (Tj), up to 500 m of silty shale and fine sandstone; Matilija Sandstone (Tma), about 650 m thick, composed of beds of well-cemented arkosic sandstone separated by shale partings; Cozy Dell Shale (Tcd), consisting of about 650 m of micaceous shale with thin sandstone beds; Sacate Formation (Tsa), up to 650 m of turbiditic sandstone and mudstone; Gaviota Formation, up to 140 m of fine-grained marine sandstones and mudstones; and the Alegria Formation, 200 to 400 m of shallow marine sandstone and siltstone (Dibblee, 1950, 1982; O'Brien 1972; Van de Kamp and others, 1974; Dickinson, 1995; Campion and others, 1996) [*Fig. 1 on Geologic map PDF Bookmark*].

Dibblee's (1950, 1966) stratigraphic correlations of the Paleogene section between the western and central Santa Ynez Mountains have been questioned by other workers (Bailey, 1952; Stauffer, 1967; Van de Kamp and others, 1974). We have chosen to retain Dibblee's (1950, 1966) formational assignments; revising Paleogene stratigraphic assignments, as suggested by Bailey (1952) and Stauffer (1967), would have required remapping the entire western Santa Ynez Mountains, a task beyond the intended scope of this compilation. Moreover, subsequent work of Campion and others (1996) suggests that Dibblee's (1950, 1966) correlations at San Marcos Pass, 10 km to the east of the map area, were essentially sound. Stratigraphic work by O'Brien (1973) supports the formational assignments of Dibblee (1950); Hornaday and Phillips (1972) discussed faunal evidence from the Cozy Dell and Sacate Formations that tends to support Dibblee's (1950) usage. Paleontological data compiled for this map in most cases lend support to Dibblee's (1950) formational assignments of the Paleogene section.

The uppermost Eocene and middle Oligocene marine units interfinger with the only nonmarine formation of the thick sequence of Cretaceous-Tertiary formations, the Sespe Formation (Bailey, 1947; Howard, 1995) [*Geologic map PDF Bookmark*]. On the south flank of the Santa Ynez Mountains, the Sespe Formation is about 1,000 m thick in the southeastern part of the map area, gradually thinning westward to its disappearance about 10 km northeast of Point Conception (Bailey, 1947) [*Geologic map PDF Bookmark*]. The Sespe Formation is predominantly a fining-upward sequence from red conglomerate of mostly granitic detritus at or near the base to sandstone to mudstone interbeds in the upper part (Bailey, 1947; Howard, 1995). The unit contains an intraformational erosional unconformity; the lower part of the formation is late Eocene (Refugian Stage) in age, and the terrestrial red beds

interfinger with marine rocks of the Gaviota Formation and the lower part of the Alegria Formation in the southeast part of the map area (Howard, 1995). The upper part of the Sespe is late Oligocene (Zemorrian Stage) in age and interfingers with marine rocks of the upper part of the Alegria Formation (Howard, 1995) [*Geologic map PDF Bookmark*].

The Sespe and Alegria Formations are overlain by the 30–50 m thick shallow marine Oligocene (Zemorrian Stage) Vaqueros Sandstone (Dibblee, 1950, 1982; Rigsby, 1998). The Vaqueros Sandstone is conformably overlain by the 500-m thick marine Rincon Shale of early Miocene (late Zemorrian-Saucesian) age (Dibblee, 1982; Rigsby, 1998) [*Fig. 1 on Geologic map PDF Bookmark*]. The Miocene Monterey Formation is conformable on the Rincon Shale throughout areas south of the crest of the Santa Ynez Mountains. This marine siliceous shale unit has generally constant thickness of about 800 m in this area (Dibblee, 1950, 1982). The lower (middle Miocene) part of the Monterey Formation includes thin dolomitic and siliceous strata; the upper (upper Miocene) part is highly siliceous, porcelaneous, and cherty (Dibblee, 1950, 1982). The Monterey Formation is conformably overlain by the upper Miocene and lower Pliocene Sisquoc Formation, which in this domain is dominantly poorly bedded diatomaceous mudstone and shale (Dibblee, 1950, 1982). Thick marine siliciclastic units of Pliocene age crop out to the east of the map area (for example, Tan and others, 2003); within the map area, they are mapped only in the offshore region (Johnson and others, 2015).

The stratigraphic sequence exposed in the Santa Ynez Range and adjacent coastal area is primarily a southward-dipping homoclinal structure [*Geologic map PDF Bookmark*]. The south coastal area is characterized by Miocene and younger formations that dip southward and are disrupted by occasional folds and small-offset, strike-parallel normal faults.

Santa Rosa Hills Domain

The Santa Rosa Hills domain [*Fig. 2 on Geologic map PDF Bookmark*] includes the area to the south of the Santa Maria basin between the Santa Ynez River and the crest of the Santa Ynez Mountains. Stratigraphically, this domain differs from the Santa Ynez domain to the south in that (1) it includes Upper Jurassic to Cretaceous units not exposed in the domain to the south, (2) the Paleogene section is considerably thinner to the north of the Santa Ynez fault, and (3) the Tranquillon Volcanics locally underlie the Monterey Formation (Tm) (Dibblee, 1950, 1982) [*Fig. 1 on Geologic map PDF Bookmark*]. The oldest rocks in the Santa Rosa Hills domain are of presumed Franciscan affinity, exposed near Honda Canyon east of Point Arguello [*Geologic map PDF Bookmark*], consisting of a mélange of sheared black shale, graywacke, chert, and greenstone that are mixed with serpentinite (Dibblee, 1950, 1982). This area also coincides with significant gravity and magnetic highs, as discussed in the potential-field anomalies section [*Aeromagnetic Total PDF Bookmark; Gravity 2,670 kg/m³ PDF Bookmark*]. These rocks are overlain by pervasively sheared dark gray nodular claystone mapped as Honda Formation (KJh) (Dibblee 1950). The Upper Jurassic and Lower Cretaceous Espada Formation (KJe) forms the core of several anticlines in the Santa Rosa Hills domain [*Geologic map PDF Bookmark*]. The Espada Formation is as thick as 2,100 m and is composed of dark gray thin-bedded micaceous shale with thin dark sandstone strata. The base of the unit is only exposed in Honda Canyon where it appears to rest unconformably on the sheared shales of the Honda Formation (Dibblee, 1950).

In contrast to the generally conformable sequence of Upper Cretaceous, Paleogene, and Neogene strata in the Santa Ynez domain to the south, these same strata in the Santa Rosa Hills domain are interrupted by three distinct angular unconformities (Dibblee, 1982; Byrd, 1983) [*Fig. 1 on Geologic map PDF Bookmark*]. From youngest to oldest, the unconformities are (1) the Miocene Monterey Formation overlaps with angular discordance the Oligocene to lower Miocene section of Sespe Formation (Tsp), Vaqueros Formation (Tv), and Rincon Shale (Tr); the degree of angular discordance locally increases such that in areas southwest and south of Lompoc, the Monterey Formation directly overlies rock of Eocene age and at the east edge of the map to the southeast of Santa Ynez, the Monterey Formation directly overlies Upper Cretaceous Espada Formation; (2) the Oligocene to lower Miocene section of Sespe Formation, Vaqueros Formation, and Rincon Shale unconformably overlap the Eocene and Cretaceous section; the degree of angular discordance increases westward in the domain such that at Tranquillon Mountain, the Rincon Shale and Vaqueros Formations overlie successively older Eocene formations and eventually directly overlie the Lower Cretaceous and Upper Jurassic Espada Formation; and (3) the Eocene section unconformably overlaps the Upper Cretaceous Jalama Formation (Kj) and the Lower Cretaceous and Upper Jurassic Espada Formation with increasing angular discordance (Dibblee, 1950, 1982) [*Fig. 1 on Geologic map PDF Bookmark*].

The Paleogene section is deformed into several large west-northwest-trending anticlines [*Geologic map PDF Bookmark*]. These folds expose Cretaceous sandstones of the Espada Formation and, locally, serpentinite in their cores and they terminate east-southeastward against the Santa Ynez fault [*Geologic map PDF Bookmark*]. The overlapping Monterey and Sisquoc Formations are also involved in this folding but are deformed into many small subsidiary folds of similar trends, likely reflecting the rheologic difference between the two stratigraphic packages.

Structures

Onshore faults

Nacimiento Fault

The Nacimiento fault is a fundamental structure of the California Coast Ranges that separates the Jurassic–Cretaceous Franciscan Complex on the southwest from

Cretaceous granitic and metamorphic rocks of the Salinian block to the northeast (Page, 1970; Hall and Saleeby, 2013). The fault was primarily active during Late Cretaceous time (Dickinson, 1983; Yaldezian and others, 1983). Published interpretations vary widely in terms of the fault's sense, magnitude, and timing of slip (Dickinson, 1983; Ducea and others, 2009; Hall and Saleeby, 2013). Most workers suggest that the fault was primarily active during the Late Cretaceous (Dickinson, 1983; Yaldezian and others, 1983) and that motion largely ended by the end of Paleogene time (Jacobson and others, 2011), with minor subsequent Neogene slip (Vedder and Brown, 1968). In the map area, the fault juxtaposes moderately west-dipping Paleogene strata of an unnamed marine sandstone (Tus) on the northeast against variably dipping and locally overturned Upper Cretaceous strata of a marine turbiditic sandstone (Kus) on the southwest (Vedder and others, 1991) [*Geologic map PDF Bookmark*]. Attitude of the exposed fault plane was measured in two places in the map area; in both cases, the fault was observed to dip about 30 degrees to the northeast. Sense of slip is not defined within the map area, but the sinuous mapped trace of the fault is inconsistent with a large amount of strike-slip offset. The timing of offset on this segment of the fault is only constrained to be younger than the poorly defined Paleocene to Eocene age of unit Tus, generally consistent with published minimum slip ages on the fault (Hall, 1991; Dickinson and others, 2005; Jacobson and others, 2011).

East Huasna (Cachuma) Fault

The East Huasna fault, mapped as the Cachuma fault by Dibblee (1966, 1991) is a northwest-trending fault that is regionally upthrown on the northeast, juxtaposing Upper Cretaceous marine turbiditic sandstones (Kus) on the northeast against Monterey Formation on the southwest. Near the east edge of the map, the fault has the appearance of a southwest-vergent thrust, placing northeast-dipping ophiolitic rocks (Jo) and Espada Formation above steeply dipping to overturned Monterey Formation (Dibblee, 1994c) [*Geologic map PDF Bookmark*], although the actual sense of slip is unknown. Similar map relations occur along the fault at Stanley Mountain about 5 km north of the map area (Vedder and others, 1989b). Throughout much of its length within the map area, the trace of the fault is straight, suggesting a steep dip. Hall and Corbató (1967) suggested an unknown amount of strike slip, probably dextral, on the East Huasna fault following deposition of upper Miocene strata in their study 15 km north of the map area. Near the northern edge of the map, the basal contact between Monterey Formation and underlying lower Miocene to upper Oligocene unnamed sandstone (Tss) is offset in map view by at least 2 km of dextral separation [*Geologic map PDF Bookmark*]. Langenheim and others (2013a) suggested the fault could have as much as 26 km of dextral slip based on correlation of offset magnetic anomalies (see additional discussion under "Potential-Field Anomalies" section). The timing of fault offset based on map relations is only constrained as post-middle Miocene offset of the Monterey Formation.

Little Pine Fault

The Little Pine fault in the easternmost part of the quadrangle is mapped at the surface as a 25–38°-northeast-dipping fault thrusting the Franciscan Complex southwest over Pliocene to Pleistocene Paso Robles Formation (Dibblee, 1950; Hall, 1981a; Dibblee, 1993b). Slip indicators on secondary structures near the fault plane and orientation of fold axes in footwall sedimentary units are consistent with reverse displacement with a small dextral component (Cannon, 2013). From the east map edge, similar stratigraphic separation occurs along the fault for about 9 km to the northwest to Zaca Creek, where the surface trace of the Little Pine fault appears to die out in the core of a northwest-plunging anticline within the Franciscan Complex (Hall, 1981a; Dibblee, 1993b) [*Geologic map PDF Bookmark*]. Near Zaca Creek (fig. 2), the Sisquoc Formation that depositionally overlies the Franciscan Complex is unfaulted and outcrops of the Sisquoc Formation wrap around a northwest-striking anticlinal nose at the apparent northwest termination of the Little Pine fault (Cannon, 2013) [*Geologic map PDF Bookmark*]. Hall (1981a) extended the Little Pine fault another 20 km along strike to the northwest beyond this termination, along a structure we map as the Foxen Canyon fault (see also Dibblee, 1994a). The abrupt decrease in stratigraphic separation on the Little Pine fault occurs where gravity and magnetic anomalies veer westward, away from the mapped trace of the Little Pine fault and extend 10–12 km west beneath the basin sediments. These anomalies, interpreted as an upwarp in the basement (see the following section "Relationship of Geophysical Anomalies to Neogene Structure"), may represent a left step on the fault system where slip was transferred onto the concealed Oceano-Zaca fault.

Foxen Canyon Fault

The Foxen Canyon fault is a northwest-striking fault that generally parallels Foxen Canyon for about 25 km from the inferred northwest termination of the Little Pine fault to an inferred intersection with the West Huasna fault near the confluence of the Cuyama and Sisquoc Rivers [*Geologic map PDF Bookmark*]. The fault disrupts only Miocene units at the surface (Hall, 1981a; Dibblee, 1994a). Orientation of closely spaced, en echelon folds in Miocene strata directly adjacent to the fault are consistent with dextral slip on the fault (Cannon, 2013); the generally straight map trace is consistent with strike-slip offset. A small outcrop of unfaulted Careaga Sandstone overlies the southern end of the fault trace, constraining the minimum age of slip on this segment (Dibblee and others, 1994a).

Santa Maria Mesa Fault

The Santa Maria Mesa fault (Hall, 1978, 1981a, 1982; mapped as the Sisquoc River fault by Dibblee, 1994a) is a northwest-striking fault that is generally parallel to, but 3.5 km northeast of, the Foxen Canyon fault [*Geologic map PDF Bookmark*]. Relative motion on the fault is up on the northeast, with Monterey Formation on the northeast juxtaposed against units as young as Careaga Sandstone on the southwest (Hall, 1981a). Fault dip is unknown; Hall (1981a) depicts it as vertical in cross-section view. The Santa Maria Mesa fault dies out to the southeast; to the northwest, it may merge with the West Huasna fault or with the Santa Maria River fault. Hanging wall strata are deformed into a southeast-plunging anticline with a core of Monterey Formation flanked by outcrops of the Tinaquaic Sandstone Member of the Sisquoc Formation (Tsqs) [*Geologic map PDF Bookmark*]. Two additional northwest-striking faults with the same relative sense of offset occur to the northeast of the Santa Maria Mesa fault; both faults place Monterey Formation on the northeast side against Sisquoc Formation on the southwest (Dibblee, 1994a). The fault roughly coincides with the eastern limit of the basin-margin nearshore sand of the Sisquoc Formation.

West Huasna Fault

The offset history of the West Huasna fault is uncertain and probably complex. North of the map area, Miocene sedimentary units on the northeastern block side of the fault are greater than 3,000 m thick and record depositional environments as much as thousands of meters deeper (lower bathyal) than equivalent-aged units on the southwestern side (upper bathyal) (Hall and Corbató, 1967; Tennyson and others, 1991). This pattern suggests that the West Huasna fault may have been active as a down-to-the northeast normal fault during the early Miocene, forming a deep marine depocenter in which Miocene muds accumulated to unusually great thicknesses. However, deeper- and shallower-water sections of about the same age are now at similar elevations on opposite sides of the West Huasna fault in the vicinity of Twitchell Reservoir in the northern part of the Santa Maria quadrangle, indicating substantial post-Miocene reactivation as an up-to-the-northeast reverse fault.

Although the map patterns of many faults in the Huasna domain indicate high-angle reverse offset, many also show evidence for strike-slip motion. Hall (1981a, 1982) pointed to differences in stratigraphic thickness and sequence that could not be explained by pure dip slip faulting as evidence for a largely concealed system of through-going right-lateral faults. Fault kinematic data document right-lateral slip along the Little Pine fault in much of the map area (Cannon, 2012, 2013). Published estimates of right-lateral slip on the West Huasna fault vary from 5 to 8 km (McLean, 1993) to 15 km (Hall and others, 1995). Langenheim and others (2013a) interpret the West Huasna fault to dip steeply northeast to a depth of about 6 km (based on models of potential-field data from north of the map area) and estimate about 25–30 km total right-lateral offset since the Mesozoic by cross-fault correlation of gravity and magnetic anomalies.

Northeast-Striking Faults of the Santa Maria Domain

Along the northeast edge of the Santa Maria domain, we interpret several mostly concealed northwest-striking faults that are similar in structural style to those found in the Huasna domain [*Geologic map PDF Bookmark*]. The Garey fault is mostly covered by alluvium; it is interpreted from limited subsurface data as a steeply northeast-dipping reverse fault cutting units as young as Paso Robles Formation (Hall, 1981a, 1982). Based on well and seismic-reflection data, we interpret a series of northwest-striking faults, referred to as the Oceano-Zaca fault. This fault zone bounds the western edge of the Zaca field (fig. 2; California Department of Conservation, 1992, p. 600–601). Faults along the same trend cut the West Cat Canyon field (fig. 2; California Department of Conservation, 1992, p. 86) and the eastern side of the Santa Maria Valley field (fig. 2; Canfield, 1939; California Department of Conservation, 1992, p. 475). These faults are on-trend with the northwest-striking Oceano fault, a reverse fault recognized in the subsurface from seismic reflection data collected in Santa Maria Valley and immediately north of the map area (Pacific Gas and Electric Company, 1988). The Santa Maria River fault bounds the northeast side of the Santa Maria Valley. Outcrop relations and well data suggest that the fault has up to 100 m of northeast-side-up dip separation (Hall, 1978, 1982).

Casmalia Fault

The Casmalia Hills and Solomon Hills are structurally bounded on their northeast side by a buried, high angle southwest-dipping reverse fault referred to as the Casmalia fault (American Association of Petroleum Geologists, 1959; Hall, 1982). The projected surface trace of the fault is north of exposures of steeply dipping Paso Robles Formation or tilted Orcutt Sand (Qo) (Clark, 1990) [*Geologic map PDF Bookmark*]. The Casmalia fault is best known from subsurface data that document approximately 5,400 m of post-Monterey structural relief and 2,200 m of vertical separation of the base of the upper Pliocene Careaga Formation by a combination of faulting and folding across the fault (Woodring and Bramlette, 1950; American Association of Petroleum Geologists, 1959; Namson and Davis, 1990). Seismic reflection and potential field data show that the Casmalia fault continues offshore to an intersection with the Hosgri fault (Lettis and others, 2004; Willingham and others, 2013); see additional discussion in the “Potential-Field Anomalies Section” of this report.

Baseline-Lompoc Fault

The Baseline fault was mapped by Sylvester and Darrow (1979) along the northeast edge of Lake Cachuma to the east of the map area; they inferred it to extend westward to the Los Alamos fault, a fault with similar orientation and southwest-side-up dip separation mapped by Woodring and Bramlette (1950) near Los Alamos (fig. 2). Although Sylvester and Darrow (1979) extended the fault to the northwest based on similarities in sense of offset with faults in the subsurface in the Orcutt oil field, detailed trenching and photogeologic work suggest that the fault terminates near the town of Los Alamos (Guptill and others, 1981). Analysis of basement elevations from well data suggests a similar termination point for this fault (Gray, 1980; Hall, 1982).

Lions Head Fault

The Lions Head fault is well exposed along the coast south of Point Sal, separating ophiolite to the north from the lower member of the Monterey Formation to the south (Tml) [*Geologic map PDF Bookmark*]. Near Point Sal, the fault is mapped in outcrop as a steeply south-dipping normal fault (Woodring and Bramlette, 1950), although geophysical models suggest the fault may dip steeply to the north at depth (Langenheim and others, 2013a). Potential field and offshore seismic reflection data show that the Lions Head fault extends offshore to the Hosgri fault and bounds a region of elevated basement rock that is uplifted between the Casmalia and Lions Head faults (Lettis and others, 2004). Many generalized maps of the Santa Maria basin portray the Lions Head fault as extending well inland (for example, Gray, 1980; Pacific Gas and Electric Company, 1988; McLean, 1991), but the fault is concealed to the southeast of where it is exposed in outcrop and the fault's location is primarily constrained by drill-hole data (Hall, 1982) and where it is imaged by a seismic-reflection profile (Seeber and Sorlien, 2000). Tying the Lions Head fault mapped south of Point Sal to the subsurface structure attributed as the Lions Head fault to the southeast is problematic on geometric and stratigraphic grounds. Near Point Sal, the fault is steeply dipping with north-side-up dip separation; whereas to the southeast, seismic data are used to interpret the fault as a moderately north-dipping listric normal fault subsequently reactivated as a reverse fault. (Seeber and Sorlien, 2000). Further, the hanging-wall units differ in these two locations with ophiolite occurring at Point Sal and a thick sequence of Monterey and younger units occurring above the fault in the middle of the basin. Basinward projection of the Lions Head fault is discussed in the section "Relationship of Geophysical Anomalies to Neogene Structure."

Santa Ynez River Fault

The existence of a concealed fault that generally lies beneath the course of the Santa Ynez River has been proposed to explain stratigraphic contrasts between Santa Maria basin and the Santa Ynez Mountains (Reed and Hollister, 1936; Sylvester and Darrow, 1979; Hall, 1982). In the Santa Maria basin to the north of the proposed fault, Miocene and younger units unconformably overlie Franciscan Complex basement whereas in the Santa Ynez Mountains to the south of the fault, Miocene units are underlain by a thick section of Paleogene strata, which are underlain by Jurassic to Cretaceous Espada Formation; Franciscan basement is not exposed but is presumed to exist at depth. The Santa Ynez River fault has also been suggested as a way of explaining the westward decrease in the amount of strike separation on the Santa Ynez fault to the west of Lake Cachuma just east of the map area. Sylvester and Darrow (1979) suggested that the fault had an undetermined amount of sinistral separation that was transferred from the Santa Ynez fault.

The Santa Ynez River fault is inferred to lie at the base of the hills just to the south of Lompoc; eastward, the fault generally follows the trace of the Santa Ynez River and lies north of exposures of Espada Formation in the Santa Rosa Hills south of Buellton and Solvang (Sylvester and Darrow, 1979) [*Geologic map PDF Bookmark*]. The inferred map trace is sinuous on a scale of kilometers and is projected to intersect the coast at Spring Canyon (location SC in fig. 2), about 2 km north of Point Pedernales. Offshore, we mapped two splays of the southern end of the Hosgri fault that converge eastward to the coast at Spring Canyon. A gap in coastal outcrop at that location precludes definitive identification of the fault at the coastline. The fault is also expressed as significant gravity and magnetic gradients (see "Potential-Field Anomalies Section").

Subsurface data suggest that the fault dips to the south and has south-side-up, north-vergent, post-Miocene slip. Along the north front of the Santa Rita Hills (fig. 2), well data indicate 1,200 to 1,500 m of south-side up structural relief on the Monterey Formation in a horizontal distance less than 2 km (Tennyson, 1995a; Sweetkind and others, 2010). Nearby, the Rothschild Oil Company Sacramento J.M. #1 well penetrated a fault which places Monterey Formation over Sisquoc Formation and suggests about 300 m vertical component of separation (Tennyson, 1995a; Sweetkind and others, 2010). Additional geologic relations consistent with a mostly buried north-vergent fault system include (1) the presence of tight east-west trending, north-vergent, asymmetric anticlines and south-side-up faults in the western part of the Santa Rita Hills, (2) juxtaposition of informal lower member of the Monterey Formation with Pliocene strata just north of the Santa Ynez River west of the town of Buellton, and (3) near-vertical to overturned dips in the north limb of the Nojoqui anticline on the south side of the Santa Ynez River in the hanging wall of the inferred fault [*Geologic map PDF Bookmark*].

In addition to evidence for post-Monterey Formation convergence, this structure appears to have accommodated other types of displacements in pre-Monterey time. The fault is inferred to have been the boundary between the western Transverse Ranges to the south of the fault that have undergone clockwise vertical-axis rotation of about 100 degrees or more since the early Miocene (Hornafius and others, 1986; Luyendyk, 1991) and the relatively unrotated Santa Maria basin to the north. The presence of the Paleogene section to the south of the fault could be explained by a pre-Monterey down-to-the-south normal fault that either created basin space for the Paleogene section or caused those strata north of the fault to be uplifted and eroded on the north side while being preserved to the south. Although a small amount of strike separation is possible along the fault, the overall sinuosity of the fault trace precludes large magnitude strike-slip offset, unless subsequent compression has significantly modified its trace.

Honda Fault

The Honda fault was mapped by Dibblee (1950) as a steeply south-dipping reverse fault juxtaposing Mesozoic and Eocene units on the south with Monterey Formation on the north [*Geologic map PDF Bookmark*]. Map relations along the coast at Honda Canyon are consistent with south-side-up dip separation (Hornafius and others, 1982) and seismic data from immediately offshore show several east-west faults with similar south-side-up dip separation. The west end of the Honda fault is observed in outcrop as 5–10 m thick shear zones that separate Tranquillon Volcanics from the Monterey Formation; these fault strands have extensive horizontal striations, with evidence for left-lateral motion on some of these surfaces (Hornafius and others, 1982; this study). Sorlien and others (1999a) modeled clockwise rotation of east-west elongate structural blocks bounded by left-lateral faults such as the Honda fault near the southern termination of the Hosgri fault.

Santa Ynez Fault

The Santa Ynez fault is a major east-west striking fault that bounds the north side of the Santa Ynez Range for almost 130 km (Dibblee, 1950, 1966, 1982). The fault zone is generally expressed as a break in slope and topographic depression up to 200 m wide; exposures of the fault typically show a 10–20-m-wide zone of gouge and sheared rock (Dibblee, 1950, 1966). West of Gaviota Canyon (location GC on fig. 2), the Santa Ynez fault divides into two branches: the south branch strikes southwest to the coast and the north branch strikes due west and dips steeply south. Farther west, the north branch of the Santa Ynez fault system may link to the Pacifico fault, a steeply south-dipping fault with about 1,500 m of reverse separation [*Geologic map PDF Bookmark*]. The west end of the Pacifico fault appears to terminate into the generally east-west trending Jalama anticline (Dibblee, 1950, 1982) [*Geologic map PDF Bookmark*].

Within the map area, the fault has a gently sinuous trace and is generally steeply south-dipping with reverse separation, placing Upper Cretaceous to lower Eocene strata in the hanging wall over Eocene through Miocene units in the footwall [*Geologic map PDF Bookmark*]. Maximum dip separation of Eocene sedimentary strata is about 500 m in the map area (Dibblee, 1950), although it may be as much as 2,900 m to the east of the map area (Dibblee, 1966). The slip history of the Santa Ynez fault is poorly understood and controversial. In addition to significant reverse separation, varying amounts and directions of strike-slip displacement have been attributed to the Santa Ynez fault, summarized in Sylvester and Darrow (1979) and Byrd (1983). Estimates of the amount of strike separation across the fault, based on various lithologic correlations, include varying amounts of right-lateral slip (Schmitka, 1973; Hall, 1981a), left-lateral slip (Sylvester and Darrow, 1979), strike-slip of undetermined asymmetry (Page and others, 1951), or a history of right-lateral slip followed by left-lateral slip (Dickinson, 1979).

Within the map area at three locations along the Santa Ynez fault, two faults of different dips are mapped. The largest of these exposures is near the east edge of the map where a linear, steeply dipping northern fault trace that juxtaposes Rincon Shale against the Monterey Formation appears to be overridden by a sinuous, gently south-dipping southern trace that places the Jalama and Juncal Formations above the Rincon Shale [*Geologic map PDF Bookmark*]. Similar relations were mapped by Dibblee (1966) near Lake Cachuma and in the subsurface in the Tecolote Tunnel (Bandy and Kolpack, 1963) about 2 km east of the map area. Based on the age of stratigraphic units involved, these map relations suggest the possibility of late Miocene high-angle, possibly strike slip, offset that is overprinted by Pliocene and younger shortening, with the reverse-separation fault concealing the earlier structure in most places.

Accurate determination of fault offset is hampered by the lack of detailed geologic mapping control along the trace of the fault, stratigraphic variability of supposedly correlative units on either side of the fault, and the absence of unique piercing points on either side of the fault. In general, the magnitudes of dip separation or strike separation along the Santa Ynez fault and the slip history of the fault remain unresolved.

Offshore Structures

Hosgri Fault

The Hosgri fault zone trends subparallel to the coastline and is between 5 and 15 km offshore in most of the map area. The fault is the southern part of the regional San Gregorio-Sur-San Simeon right-slip fault system (Graham and Dickinson, 1978; Sedlock and Hamilton, 1991; Langenheim and others, 2013a). The Hosgri fault forms the boundary between the onshore and offshore Santa Maria basins; these two regions have strongly contrasting structural orientations. Fold axes and fault trends west of the Hosgri fault are subparallel to the

fault, whereas east of the fault the Lions Head and Casmalia faults are oblique to its trend (Willingham and others, 2013) [*Geologic map PDF Bookmark*]. Mapping based on seismic and potential-field data shows that the west-northwest-trending Lions Head and Casmalia faults bend abruptly northward within 1 to 2 km of the Hosgri fault (Johnson and Watt, 2012; Willingham and others, 2013).

In most of the map area, seismic data show that the Hosgri fault is a narrow, linear zone of deformation that typically consists of one or more traces embedded within a complex zone of faulting and folding (Johnson and Watt, 2012; Willingham and others, 2013). In the northwest part of the map area, between the intersections of the Casmalia fault to offshore Purisima Point, the fault zone strikes N.20°W. and generally consists of a single main strand (Johnson and Watt, 2012; Willingham and others, 2013) [*Geologic map PDF Bookmark*]. In this area, the Hosgri fault displays a near-vertical dip in the upper 1.5 seconds (s) of the seismic records. At greater depths, the dip decreases and rotates to the northeast (Willingham and others, 2013).

South of Purisima Point, fault strike changes to a bearing of N.5°W. and the Hosgri fault is composed of two strands with significant vertical separation (Sorlien and others, 1999a; Willingham and others, 2013). The western strand of the Hosgri fault is a moderately east dipping fault with normal separation; the fault is mapped from three-dimensional (3D) seismic reflection data from strong reflection from the fault plane in the top 1–2 s (1–2 km) and stratal reflections that terminate at the fault surfaces (Sorlien and others, 1999a).

The Hosgri fault terminates to the southeast into east-trending folds and reverse-separation faults [*Geologic map PDF Bookmark*]. Three of the offshore faults come ashore at Point Pedernales; the southern two faults are observable in outcrops at the coast. Sorlien and others (1999a) quantified post-Miocene right-lateral slip across the southern Hosgri fault to be 3.5 km and interpreted the slip to be absorbed by folding, thrust overlap, and clockwise vertical-axis rotation of elongate blocks between strands of the fault. One strand of the Hosgri fault comes ashore at Point Arguello where it is observed as a 4-m-thick north-striking zone, with strike-slip striations preserved in hard, degraded asphalt on the fault surface. Based on seismic reflection data, this strand appears to continue south and connect with northwest-striking faults to the south of Point Arguello.

Purisima Structure

The Purisima structure is located west and subparallel to the Hosgri fault (Crouch and others, 1984; Sorlien and others, 1999b; Saenz, 2002) [*Geologic map PDF Bookmark*]. At shallow depths, the structure consists of right-stepping en echelon transpressional folds that converge into, and are ultimately terminated by, the Hosgri fault zone (Sorlien and others, 1999b; Willingham and others, 2013). The folds are associated with northeastward-dipping thrust faults that show strong compressional deformation in Miocene strata but minimal offset at an early–late Pliocene unconformity (Willingham and others, 2013). Seismic reflection data from west of the Hosgri fault show that basins filled with thick sections of Monterey and Sisquoc Formations have been inverted by the Purisima structure (Willingham and others, 2013).

Lompoc Structure

The Lompoc structure forms the west edge of a broad system of mostly east-dipping faults to the west of the Hosgri fault (Sorlien and others, 1999b) [*Geologic map PDF Bookmark*]. At shallow depths, the structure consists of right-stepping en echelon transpressional folds and faults that converge and interconnect in map view southward with the Hosgri fault (Sorlien and others, 1999b; Saenz, 2002). Shallow-level folds and discontinuous faults lie above continuous, east-dipping faults with reverse separation cutting middle Miocene and older horizons (Payne and others, 1979; Crouch and others, 1984).

Amberjack High

The Amberjack High is a northeast-trending uplift forming the southern border of the offshore Santa Maria basin (Crain and others, 1985) [*Geologic map PDF Bookmark*]. Seismic reflection data suggest that the high was present by early Miocene time and influenced the depositional thickness of the Monterey Formation (Crain and others, 1985; Tennyson and Isaacs, 2001).

North Channel Fault

The North Channel fault is a major east-west compressional fault system that parallels the coast a few kilometers offshore (Sorlien and others, 1999b) [*Geologic map PDF Bookmark*]. The fault in general is a north- to northeast-dipping blind fault with thrust separation; the blind fault's upper edge lies a few kilometers south of the coast in the Santa Barbara Channel, in general coinciding with the shelf break (Yerkes and others, 1981; Vedder and others, 1986; McCulloch, 1989; Sorlien and others, 2014). The fault steepens at shallow depths and dies out into folds in the younger part of the section (Tennyson and Kropp, 1998). Strata in the hanging wall, including the Paleogene strata in the Santa Ynez Range, dip southward in the hanging wall of this structure (Tennyson and Kropp, 1998; Sorlien and others, 2014). To the west, the North Channel fault trend curves to the northwest around Point Conception (Sorlien and others, 1999b).

Potential-Field Anomalies

Gravity and magnetic data are useful for projecting the surface geology into the subsurface. Gravity data are processed to reflect density variations within the upper and middle crust and are particularly well suited for determining the shape of Cenozoic basins because of the significant density contrast between dense Mesozoic basement and lighter Cenozoic units. Magnetic data reflect magnetization variations within the crust and are well suited for mapping the distribution of rock types that contain magnetite, such as mafic igneous rocks. Both gravity and magnetic anomalies can be related to rock type, providing a means to map remotely some aspects of the geology. Gravity and magnetic data can also be used to model the location and geometry of faults that juxtapose rocks of differing density and magnetic properties.

Gravity Anomalies

Isostatic gravity anomalies reflect density contrasts in the upper to middle crust. The isostatic gravity map using a reduction density of 2,670 kg/m^3 shows that the most significant density contrast within the Santa Maria and Point Conception quadrangles is between dense Mesozoic basement and overlying, less dense Cenozoic (particularly Neogene) sedimentary rocks and unconsolidated Quaternary deposits *[Gravity 2,670 kg/m^3 PDF Bookmark]*. Not surprisingly, the lowest gravity values are located in the Santa Maria and offshore Ventura basins, loci of thick (>1 km) sections of Cenozoic sedimentary deposits, whereas the highest gravity values correspond to outcrops of Jurassic ophiolite at Point Sal and serpentinite east of Point Arguello, exposures of Franciscan Complex, and Cretaceous sedimentary strata (Kus) along the northeastern part of the map area *[Gravity 2,670 kg/m^3 PDF Bookmark]*. Relatively high gravity values also coincide with thick Paleogene sequences in the Santa Ynez Mountains (labeled “KEs”; *Gravity 2,670 kg/m^3 PDF Bookmark*), indicating that these strata, although Cenozoic in age, are denser than the Neogene and Quaternary section that fills the Santa Maria basin.

The northwest-trending gravity low of the Santa Maria basin reflects thick Neogene basin fill. The gravity field predicted from the basin shape derived from well data by Gray (1980) using a density contrast of −400 kg/m^3 between basin-fill units (2,300 kg/m^3) and basement (2,700 kg/m^3) (fig. 5*A*) is generally similar to that observed (fig. 5*B*), particularly in the position of the major northeastern, western, and southern edges of the basin and in the gentle south-facing gravity gradient north of Point Sal. However, many of the smaller-scale or short-wavelength features superposed on the isostatic gravity low may not reflect changes in basin-fill thickness but are caused by either (1) lateral density variations within the basin fill or (2) artefacts induced by the density assumed to process the gravity data. The isostatic gravity map may overestimate the magnitude of gravity lows where topographic highs (for example, mountains and hills) are composed of materials significantly less dense than 2,670 kg/m^3. Short-wavelength anomalies related to density variations within the basin fill may arise from widely varying densities within the Monterey Formation due to the diagenetic variety of silica (Isaacs, 1980). If the form of silica is opal-A or opal-CT, the density can be significantly less (<1,500 kg/m^3; Isaacs, 1980) than that of typical Santa Maria basin sediments (typically 1,900–2,400 kg/m^3; Beyer and others, 1985). Pockets of low-density Monterey and Sisquoc Formations appear to be responsible for local gravity lows in the Buellton, Solvang, Bradley Canyon, and Lompoc areas (labeled “Bu,” “So,” “BC,” and “Lo,” respectively; *Gravity 2,670 kg/m^3 PDF Bookmark*). Kieniewicz and Luyendyk (1986) identified another possible low-density anomaly in the Lompoc oil field (red dashed line about 8 km north of Lompoc, *Gravity 2,670 kg/m^3 PDF Bookmark*), but wells in this area did not penetrate thick, low-density diatomite.

Another source of short-wavelength gravity lows arises from topography composed of materials that are considerably lower density than that assumed by standard gravity processing (2,670 kg/m^3). Folding and reverse faulting have led to uplift of basin deposits, forming topography composed of materials of densities of ~2,000 kg/m^3, both along the basin margin and in the Purisima Hills, Solomon Hills, and other anticlines within the basin. Many of these anomalies disappear or are diminished when a reduction density of 2,000 kg/m^3 is used, including the local gravity low in the Lompoc oil field (red dashed line) *[Gravity 2,000 kg/m^3 PDF Bookmark]*. For interpretation of basin structure and mapping pockets of anomalously low-density Monterey Formation, the smoother gravity field resulting from a reduction density of 2,000 kg/m^3 is advised. The smoother gravity field over the basin using a reduction density of 2,000 kg/m^3 (fig. 5*C*) more closely resembles the gravity lows predicted from Gray’s (1980) basin configuration (fig. 5*A*) than Gray’s predicted gravity with the isostatic gravity low reduced to 2,670 kg/m^3 (fig. 5*B*). However, using a reduction density of 2,000 kg/m^3 for mountainous areas composed of composed of Jurassic, Cretaceous, and Paleogene strata that are significantly denser than the reduction density (gray diagonal

Figure 5 (following page). Predicted gravity and observed isostatic gravity fields: shaded units and brown contours in milliGal (mGal). *A*, predicted gravity from the basement surface of Gray (1980) computed by assigning a density contrast of −400 kilograms per cubic meter (kg/m^3) between the basement and the basin fill; *B*, Isostatic gravity field using a reduction density of 2,670 kg/m^3; *C*, Isostatic gravity field using a reduction density of 2,000 kg/m^3. Red circles, wells that penetrated basement; dark blue triangles, wells that bottomed in basin fill. Brown contours in middle and bottom panels are gravity contours from top panel for comparison. Solid black lines, faults from geologic mapping; dashed lines, faults from geophysical mapping; heavy blue line is the Pacific coast.

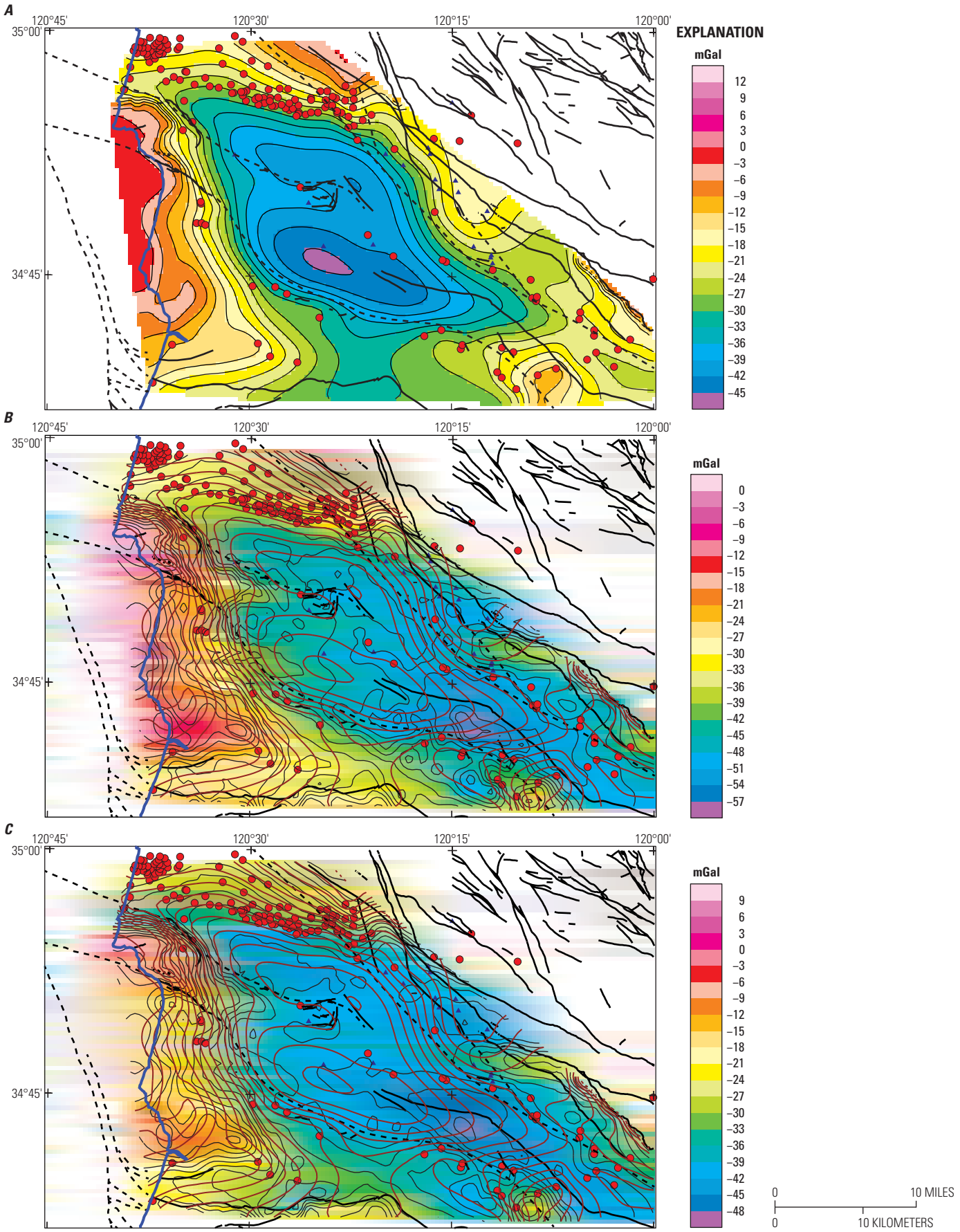
A
120°45'
120°30'
120°15'
120°00'
35°00'
34°45'
EXPLANATION
mGal
12
9
6
3
0
−3
−6
−9
−12
−15
−18
−21
−24
−27
−30
−33
−36
−39
−42
−45
B
mGal
0
−3
−6
−9
−12
−15
−18
−21
−24
−27
−30
−33
−36
−39
−42
−45
−48
−51
−54
−57
C
mGal
9
6
3
0
−3
−6
−9
−12
−15
−18
−21
−24
−27
−30
−33
−36
−39
−42
−45
−48
0
10 MILES
0
10 KILOMETERS

pattern, *Gravity 2,000 kg/m³ PDF Bookmark*) leads to artificially high gravity values that mimic topography and should not be interpreted as arising from subsurface density variations. Such areas include the ridge-like gravity highs in the Santa Ynez Mountains south of the Santa Ynez fault (location labeled "KEs"; *Gravity 2,000 kg/m³ PDF Bookmark*) and high gravity values in the Sierra Madre Mountains where Cretaceous sedimentary rocks are extensively exposed (location labeled "Kus"; *Gravity 2,000 kg/m³ PDF Bookmark*).

The magnitude of gravity lows outside of the Santa Maria basin can be used to estimate the amplitude of synforms in the Neogene section. Low-density Sisquoc and Monterey Formations occupy the core of a southeast-trending syncline that extends to the southeast from the city of Lompoc (location labeled "Lo"; *Gravity 2,670 kg/m³ PDF Bookmark*). These units create a sinuous gravity low of about 12–15 mGal relative to values measured on Eocene and older units (gravity low between the labels "Lo" and "KEs"; *Gravity 2,670 kg/m³ PDF Bookmark*). Assuming a density contrast of −400 kg/m³ based on density measurements from hand samples and well data (Langenheim, 2014), the thickness of Neogene units in the core of the synform is about 700 to 900 m. Superposed on the sinuous gravity low (reduced to 2,000 kg/m³) is an oblong gravity low about 3 km long that may reflect a pocket of diatomite (about 9 km east of location labeled "di"; *Gravity 2,000 kg/m³ PDF Bookmark*).

Another gravity low, located east of Bradley Canyon (fig. 2 and labeled "BC"; *2670 Isostatic gravity map and PDF Bookmark*), may not reflect a synform, but rather a Miocene graben on which younger contractional deformation is superimposed. The north-trending gravity low coincides with folded Miocene strata sandwiched between outcrops of Franciscan Complex to the west (labeled "KJf"; *Gravity 2,670 kg/m³ PDF Bookmark*) and Cretaceous sedimentary rocks (Kus) and an isolated outcrop of Jurassic ophiolite to the east (labeled "Kus" and "Jo," respectively; *Gravity 2,670 kg/m³ PDF Bookmark*). The magnitude of the gravity low is about 20–25 mGal, with a resulting depth to the base of the Neogene section of 1–1.5 km assuming a density contrast of −400 kg/m³, with the deepest part of the sedimentary package located between the Foxen Canyon-West Huasna and Tepusquet faults. The trend of the gravity low is not parallel to the northwest-trending fold axes on the east side of the gravity low, but instead subparallel to the northerly trend of the West Huasna fault, which was probably a Miocene normal fault in its early history. The easternmost strand of the West Huasna fault may be the main basin-bounding structure given its spatial correspondence to a prominent gradient in the gravity reduced to 2,000 kg/m³ (*Gravity 2,000 kg/m³ PDF Bookmark*).

Gravity values measured on outcrops of Franciscan Complex or ophiolite vary by as much as 30–40 mGal, with higher values on the western side of the basin at Point Sal (−10 to 0 mGal, *Gravity 2,670 kg/m³ PDF Bookmark*) compared to values east of the Little Pine fault (−35 to −30 mGal, *Gravity 2,670 kg/m³ PDF Bookmark*). Most of this variation can be attributed to variability in density between diverse types of basement. For example, ophiolite is denser on average than rocks of the Franciscan Complex and a 5-km-thick slab of ophiolite, assuming that it is 100 kg/m³ denser than average Franciscan Complex and of infinite extent, produces a high of about 20 mGal. Lower gravity values measured on basement east of the Little Pine fault may also result from a northeast-dipping fault that places lower-density basin deposits beneath surface exposures of basement. Another possible explanation of lower gravity values measured on basement along the eastern margin of the map area could be an isostatic correction that does not fully account for high topography there. This is unlikely, given that the isostatic correction has a wavelength that is much longer than the width of the Santa Maria basin. Furthermore, values measured on Cretaceous sandstones in the northeastern part of the map area are 10–20 mGal higher than those measured 10 km to the south on Franciscan Complex at lower elevations, opposite of what would be expected if an inaccurate isostatic correction were responsible.

Magnetic Anomalies

Sources of magnetic anomalies are those rocks that contain magnetite or other magnetic iron oxides. In the central Coast Ranges, these rock types are serpentinite, gabbro, and diabase of the ophiolite, some basement rock types within the Salinian block (such as granodiorite exposed in the La Panza Range to the northeast of the Santa Maria 30'×60'quadrangle), metavolcanic rocks of the Franciscan Complex, and, locally, Miocene mafic volcanic rocks (Ttv, To). In general, sedimentary rocks do not produce pronounced aeromagnetic anomalies, but lower-amplitude magnetic highs may be associated with sedimentary strata that are rich in mafic and (or) ultramafic clasts or magnetite grains. In the map area, the Lospe Formation, exposed near Point Sal, can be somewhat magnetic, because it contains recycled ophiolitic clasts, but is too thin and not magnetic enough relative to the ophiolite to produce a prominent anomaly. Where the Lospe Formation crops out (labeled "Tl"; *Aeromagnetic Total PDF Bookmark*), it coincides with a local magnetic low relative to the ophiolite, although it may be responsible for very weak, short-wavelength anomalies that are best seen in the magnetic field filtered to enhance shallow sources (labeled "Tl"; *Aeromagnetic Shallow PDF Bookmark*). Magnetic susceptibility measurements (Langenheim, 2014) indicate that some of the Eocene sandstones are also somewhat magnetic and may be responsible for subtle, short-wavelength magnetic anomalies in the Santa Ynez Mountains. Weak, short-wavelength anomalies in the northeast corner of the map area appear to be caused by locally magnetic Cretaceous sandstone beds (labeled "Kus"; *Aeromagnetic Shallow PDF Bookmark*). Although we do not have magnetic susceptibility measurements to confirm this interpretation in the Santa Maria quadrangle, Cretaceous sandstones in other parts of the California

Coast Ranges are weakly to moderately magnetic and do produce measurable, short-wavelength magnetic anomalies (Langenheim and others, 2006).

Another source of magnetization in sedimentary rocks of the Santa Maria basin are "burnt shales" (Arnold and Anderson, 1907) derived from combustion metamorphism of bituminous-rich shale in the Sisquoc Formation. Ground-magnetic surveys across small outcrops of burnt shale in the Casmalia Hills and Orcutt oil field reveal significant magnetic anomalies with amplitudes as great as 2,000 nT and widths of less than 100 m (Cisowski and Fuller, 1987). The small areal extent of these magnetic outcrops makes them unlikely to be detected by aeromagnetic surveys flown at 800-m line spacing. The largest outcrop of burnt shale (~1,000 m by ~600 m; Woodring and Bramlette, 1950), however, coincides with a small (<2 km width), ~50-nT, semicircular aeromagnetic high centered on Redrock Mountain (labeled "RM"; *Aeromagnetic Shallow PDF Bookmark*), whose gradient suggests that the source is at the surface. According to Cisowski and Fuller (1987), the thermally metamorphosed Sisquoc Formation at Redrock Mountain is strongly magnetic, which they attributed to the conversion of finely disseminated pyrite to magnetite and other magnetic minerals by spontaneous combustion or burning from surface fires of hydrocarbon in the shale.

Some of the short-wavelength anomalies are not caused by natural magnetization contrasts, but by oil field infrastructure and other anthropogenic sources. Short-wavelength anomalies associated with oil fields include the ring-like magnetic highs over the Cat Canyon and Orcutt oilfields (labeled "CC" and "OR," respectively; *Aeromagnetic Shallow PDF Bookmark*). Closely spaced, deeply penetrating well casings present in these oil fields are likely the dominant source of these anomalies, but contributions from natural sources associated with the oil fields cannot be ruled out. For example, the Lompoc oil field (labeled "LO"; *Aeromagnetic Shallow PDF Bookmark*) coincides with a magnetic high that is superposed on a longer magnetic high that crosses the basin. Although part of the magnetic high may be caused by the oil field, the continuation of the magnetic high beyond the oil field supports a natural source. Another example is the short-wavelength magnetic high within the Casmalia oilfield (labeled "CA"; *Aeromagnetic Shallow PDF Bookmark*), which coincides with an anticlinal trend and a small gravity high. Part of the magnetic high could be caused by a sliver of magnetic basement within the core of the anticline.

In the map area, the most prominent anomalies are associated with serpentinite and Jurassic ophiolite. Prominent, short-wavelength magnetic anomalies coincide well with outcrops of ophiolite and serpentinite at Point Sal, southwest of the city of Lompoc (labeled "KJs"), and along the northeast margin of the Santa Maria basin (labeled "Jo" and "KJf"; *Aeromagnetic Total PDF Bookmark*). These short-wavelength anomalies are superposed on broader anomalies, indicating that these scraps of ophiolite are part of a more voluminous body at depth. For example, the highs coincident with the two main outcrops of ophiolite at Point Sal as outlined by magnetization boundaries from the magnetic field filtered to enhance shallow sources (equivalent depth of 1.78 km) *[Aeromagnetic Shallow PDF Bookmark]* appear to be connected at depth, as suggested by the single magnetic high as seen by the magnetic field filtered to enhance medium-depth sources (equivalent depth of 3.97 km) *[Aeromagnetic Medium PDF Bookmark]*. The Point Sal magnetic anomaly can be modeled with the ophiolite body extending to a depth of 5 km (Langenheim and others, 2013a).

The magnetic high at Point Sal extends northwest to the Hosgri fault zone *[Aeromagnetic Total PDF Bookmark]*, which clearly forms the western margin of the magnetic anomaly. The anomaly at Point Sal has been correlated to a magnetic high caused by ophiolite on the west side of the fault ~90 km to the northwest at San Simeon (Langenheim and others, 2013a; original geologic correlation of ophiolite by Hall, 1975). The Point Sal magnetic high also extends ~50 km to the southeast across the Santa Maria basin *[Aeromagnetic Total PDF Bookmark]*. In both directions, the amplitude of the anomaly is diminished as the anomaly broadens, consistent with increasing depth to the top of the magnetic source. The magnetic ridge that extends across the Santa Maria basin is superposed on an even broader magnetic high in the middle of the basin. Well cuttings of ultramafic rock (Gray, 1980) support our interpretation that the curvilinear magnetic ridge that crosses the basin is ophiolite, although the magnetic ridge (and thus by our interpretation, ophiolite) extends farther to the southeast than interpreted from sparse well data by McLean (1991). The basement surface beneath the basin is not comprised everywhere by ophiolite, despite the broad magnetic high beneath the central part of the basin. The lack of similarity between the observed magnetic field (fig. 6*A*) with that predicted assuming that the basement surface of Gray (1980) is the top of a uniformly magnetic body (fig. 6*B*) indicates significant variations in how magnetic the basement rocks are, likely arising from juxtaposition of magnetic ophiolite with weakly magnetic rocks of the Franciscan Complex. The generally shallow basement along the western margin of the basin south of Point Sal, for example, should produce magnetic highs if the basement were uniformly magnetic; instead this region is characterized by smooth magnetic lows.

Relationship of Geophysical Anomalies to Neogene Structure

Many of the prominent Neogene faults in the map area, such as the Hosgri, Santa Maria River, Little Pine, and Santa Ynez River faults, coincide at least in part with prominent gravity and magnetic gradients. The juxtaposition of differing density and magnetization along these faults argues for significant horizontal and (or) vertical displacement. Additionally, the association of magnetic and gravity gradients with Neogene faults suggests that these gradients can be used to extend mapped faults beneath cover such as water, sand dunes, and other surficial deposits. Below, we discuss in more detail the Hosgri, Santa Ynez, Little Pine, and Lions Head faults.

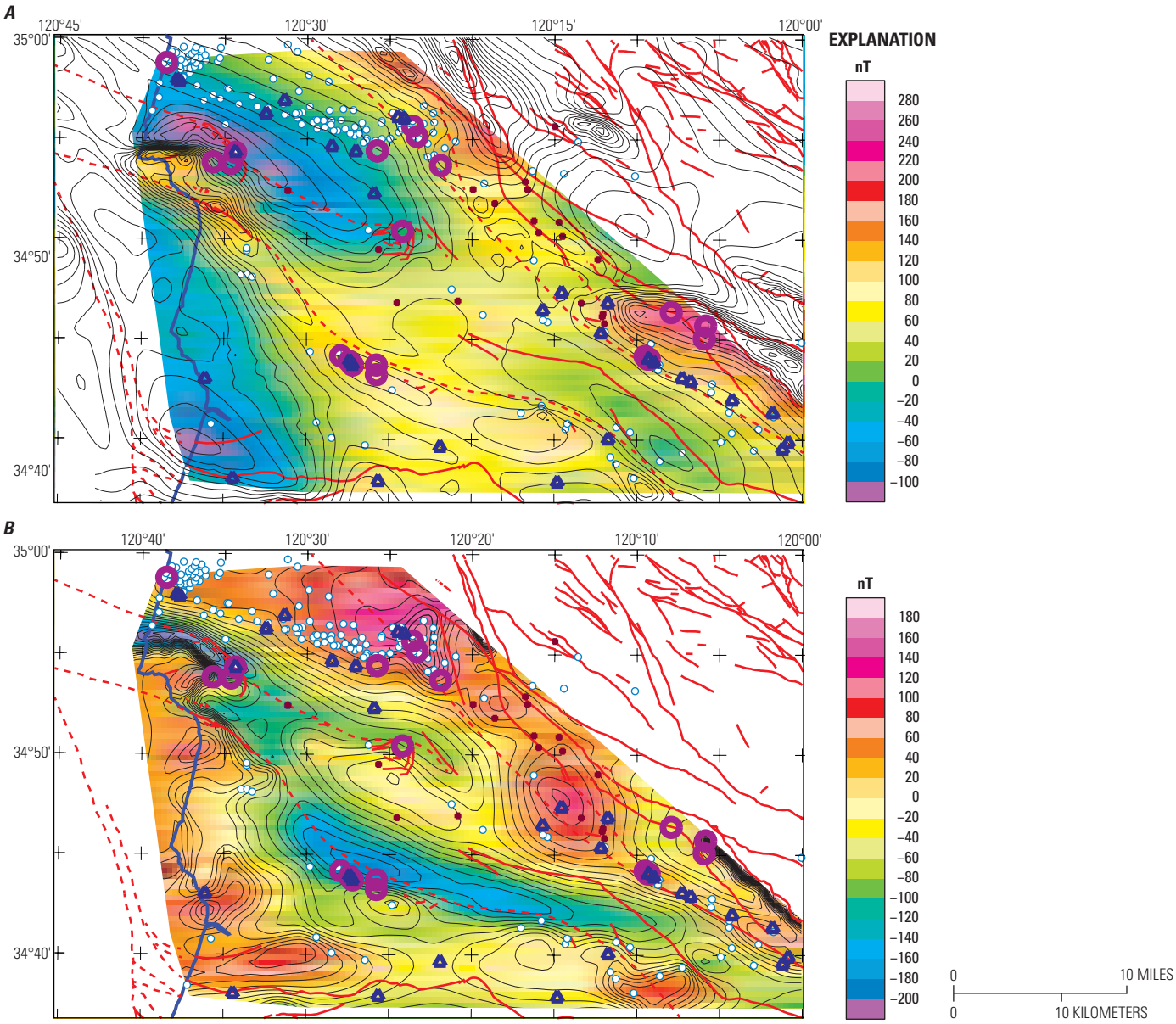

Figure 6. Measured and predicted aeromagnetic maps of the Santa Maria basin; shaded units and contours in nanotesla (nT). *A*, Aeromagnetic map of the Santa Maria basin; *B*, predicted magnetic field arising from uniformly magnetic basement rocks (1 ampere per meter [A/m]) whose top surface is the basement surface of Gray (1980). Blue-rimmed white circles, drill holes that intercepted basement rocks; brown dots, drill holes that bottomed in basin fill; dark blue triangles, drill holes where basement lithology was examined by thin-section petrography; open purple circles, drill holes where basement lithology was identified as ophiolite (symbology from Gray, 1980). Solid red lines, faults from geologic mapping; dashed red lines, faults from geophysical mapping; heavy blue line is the Pacific coast.

The Hosgri fault is well expressed in the potential-field data. It lies entirely offshore in the map area and separates two domains of contrasting magnetic patterns, with northwest-trending anomalies east of the fault and more northerly trending anomalies west of the fault *[Aeromagnetic Shallow PDF Bookmark]*. A two-dimensional (2D) model of gravity and magnetic anomalies across the Hosgri fault near Point Sal indicates a near-vertical fault to a depth of about 10 km, with the data best fit by a very steep northeast dip (Langenheim and others, 2013a). Gravity anomalies, although smoothed and lower resolution because they are based on a 4-km grid, indicate gradients coincident with the fault between Points Arguello and Pedernales in the same places where the seismic-reflection data indicate truncation of pre-Miocene and top of Miocene reflectors (Sorlien and others, 1999a; Willingham and others, 2013).

The Hosgri fault appears to change character where it approaches the Santa Ynez River and Honda faults. A seismic-reflection profile just north of Point Arguello (Sorlien and others, 1999b) indicates a moderate northeast dip of the Hosgri fault accompanied by significant compressional folding to the

northeast of the fault; this same profile shows reverse offset on moderately southwest-dipping strands of the Santa Ynez River fault. Gravity gradients indicating north-side down offset mark both the Honda and Santa Ynez River faults *[Gravity 2,000 kg/m³ PDF Bookmark]*, although the more prominent and persistent gradient is associated with the Honda fault. The position of the gradient relative to the fault strands indicates a near-vertical attitude for the Honda fault and reverse sense of offset for the Santa Ynez River fault. At its south end, the eastern strand of the offshore Hosgri fault curves eastward and projects into an onshore concealed fault that is defined by gradients in the potential field data. Magnetically, the eastern strand of the Hosgri fault appears to curve eastward parallel to folds between the Santa Ynez River and Honda faults *[Geologic Map PDF Bookmark]* and crosses the Santa Ynez River fault 5 km east of the coastline at a highly oblique angle *[Aeromagnetic Total PDF Bookmark]*. The eastern part of the magnetic gradient overlaps with a gravity gradient that extends 7–8 km to the east, to just south of Lompoc (labeled "Lo"; *Gravity 2,000 kg/m³ PDF Bookmark]*. This implies that the complicated structure mapped at the surface may be relatively continuous and simple at depths of 3 km or more. In other words, faults at the surface merge downwards into fewer, larger faults at depth. The western strand of the Hosgri fault appears to horsetail into multiple strands, including the Honda and Santa Ynez River faults, and a strand that projects southward, steps westward 3–4 km, and downdrops to the west magnetic rocks near Point Arguello. In summary, potential-field and seismic-reflection data indicate that the Hosgri fault dies out into a complex network of faults and folds in the vicinity of Point Arguello and thus does not continue south as a major strike-slip fault (Sorlien and others, 1999a; Langenheim and others, 2013a).

The nature of the Santa Ynez River fault (Sylvester and Darrow, 1979), even its very existence, has been a source of controversy. Dibblee (1950) attributed the marked difference in stratigraphy across this enigmatic structure to rapid northward thinning of the Cretaceous and Paleogene sequence accompanied by unconformities, rather than by faulting. However, the fault lies at or near the base of a large gravity gradient of 40–50 mGal *[Gravity 2,000 kg/m³ PDF Bookmark]*. At the west end of this gradient, seismic-reflection data offshore indicate south-dipping faults attributed to the Santa Ynez River fault that offset the Neogene section (Sorlien and others, 1999a,b). Continuity of the gravity gradient along the southern margin of the Santa Maria basin argues for continuity of the fault. Up de Graff and Luyendyk (1989) modeled the gravity gradient south of Buellton (labeled "Bu"; *Gravity 2,000 kg/m³ PDF Bookmark*) as a steep, south-dipping fault marked in the upper 3 km by a density contrast between the low-density Santa Maria basin deposits north of the fault with denser older sedimentary rocks south of it as well as a basement density contrast that extends to about 11 km depth. They attributed the dense basement body south of the fault beneath the Santa Ynez Mountains to mafic crust. Magnetic highs are located just south of much of the fault zone, although the most prominent magnetic high, and presumably the greatest volume of magnetic material, is located south of the western third of the fault zone *[Aeromagnetic Total PDF Bookmark]*. This magnetic high also coincides with the highest gravity values, most likely indicating a large body of dense, mafic ophiolite.

On the southeast margin of the Santa Maria basin, the Little Pine fault is well expressed in the gravity and magnetic data where the fault juxtaposes serpentinite (KJs) and the Franciscan Complex against Paso Robles Formation and younger deposits. The position of the fault at the base of the gravity gradient indicates a moderate northeast dip of the fault, with basement thrust over basin fill; a 2D gravity and magnetic model indicates that the fault becomes near vertical at depths greater than 2 km (Langenheim and others, 2013b). Near Zaca Creek, however, the gravity and magnetic anomalies associated with basement curve to a more westerly orientation and extend across the fault and into the basin *[Aeromagnetic Total PDF Bookmark; Gravity 2,670 kg/m³ PDF Bookmark]*. In this area, serpentinite and the Franciscan Complex are mapped on both sides of the fault, as mapped by Dibblee (1994c). We interpret the gravity and magnetic anomalies that extend about 10–12 km west beneath the basin sediments as an upwarp in the basement caused by transferral of slip from the Little Pine fault to the concealed Garey fault to the west and the West Huasna fault to the northwest. The east-west trend of the basement upwarp is parallel to folds mapped in Paso Robles Formation 2–3 km to the south and folds mapped 3–4 km to the north in the Careaga and Monterey Formations *[Geologic Map PDF Bookmark]*. The east-west trend of these structures interrupts the dominant northwest structural trend and appears localized to the basement upwarp. A left step from the Little Pine fault to the Garey and West Huasna faults would result in transpression if these faults have significant right slip.

Correlating the serpentinite and the Franciscan Complex exposed east of the Little Pine fault with outcrops of these rocks exposed west of the West Huasna fault near Twitchell Reservoir suggests at least 20 km of right slip. This pair of anomalies was one of two anomaly pairs used to infer 25–30 km of right slip on the West Huasna fault by Langenheim and others (2013a). Another pair of anomalies sourced by ophiolite may be offset along the Cachuma and East Huasna faults northeast of the Little Pine and West Huasna faults. An outcrop of ophiolite, exposed beneath Monterey Formation, is in Tepusquet Canyon, 3 km west of the mapped trace of the East Huasna fault. The northwest-trending magnetic anomaly associated with the ophiolite extends in the subsurface to the trace of the East Huasna fault, where the anomaly appears to be truncated *[Aeromagnetic Shallow PDF Bookmark]*. A possibly correlative ophiolite body on the east side of the Cachuma fault is exposed near the eastern margin of the map (labeled "Jo" along the east edge of map, *Aeromagnetic Shallow PDF Bookmark*). This correlation would suggest that the East Huasna and Cachuma faults were connected and have about 10 km of right slip. A previous correlation of magnetic anomalies to the north suggested as much as 26 km of right slip along the East Huasna fault (Langenheim and others, 2013a). The discrepancy could

be explained if right slip is absorbed by shortening east of the fault or by smearing of the ophiolite and its associated anomaly along the fault.

Where it is exposed along the coast south of Point Sal, the Lions Head fault is marked by a prominent magnetic gradient *[Aeromagnetic Total PDF Bookmark]*. A magnetic anomaly crosses the basin southeast of the exposed Lions Head fault; Langenheim and others (2013a) suggested mapping the fault using the southwest edge of the magnetic anomaly. Geometric and stratigraphic dissimilarities between the mid-basin location and the coastal outcrop suggest that the magnetic anomaly may not represent the same fault along its length. Perhaps it is instead the reactivated structural boundary between ophiolite and the Franciscan Complex. In this case, this older structure was reactivated to localize Neogene deformation.

We interpret the change in dip of the Lions Head fault and the magnetic anomaly band that traverses the Santa Maria basin resulting from primarily transtensional offset with significant subsequent overprinting by transpression. Seismic-reflection data about 20 km southeast of where the Lions Head fault is exposed at the coastline (Seeber and Sorlien, 2000) do not show coherent fault-plane reflections across the southern edge of the large magnetic anomaly, consistent with a steeply dipping strike-slip fault zone. If the southern edge of the anomaly reflects a strike-slip fault, it is likely that the fault was originally straighter than its current curved trajectory across the basin. Modification of the main magnetic boundary is suggested by a high in the magnetic field filtered to enhance shallow sources about 3 km south of the magnetic anomaly along the Lions Fault at the coastline *[Aeromagnetic Shallow PDF Bookmark]*. Where the main magnetic anomaly curves to the south, a prong of shallow magnetic material extends parallel to and south of the mapped fault. A hint of a gravity high (*Gravity 2,000 kg/m³ PDF Bookmark*) coincides with the magnetic prong, suggestive of an anticline whose fold axis parallels the fault. Another apparent modification of the main magnetic boundary is located at its southeast end where the main magnetic anomaly curves again to the south. This area is also marked by an elongate gravity high that may reflect a basement-cored anticline. The broad curve in the gravity and magnetic anomaly is parallel to and approximately 5 km to the south of the concealed western part of the Baseline fault (also called the Los Alamos fault at its western end), a Pliocene and (or) Quaternary feature, suggestive of a common origin for folding and modification of the main magnetic anomaly band during the late Neogene and Quaternary.

The northern edge of the magnetic anomaly band across the Santa Maria basin appears to coincide spatially with the north-side-down normal fault as constrained by drill-hole data and imaged by seismic-reflection data (Seeber and Sorlien, 2000). Although this fault has been subsequently reactivated as a reverse fault (north-side-up), the cumulative vertical offset is north-side-down, consistent with the facing direction of a gentle gravity gradient *[Gravity 2,000 kg/m³ PDF Bookmark]*. Using the gravity gradient and the northern edge of the magnetic anomaly band as a guide, the normal fault appears to steepen in dip to the southeast as it curves to the south. To the northwest, the normal fault appears to curve to the north, where it likely played a role in down-dropping the basement from where it is exposed at Point Sal. The relationship of this normal fault to the Pezzoni fault of Woodring and Bramlette (1950), a normal fault that wraps around the northeast part of the Point Sal area, is not known, but perhaps as the Pezzoni fault loses displacement to the southwest, the normal fault that we correlate to the northern edge of the magnetic band picks up displacement.

To the southeast of Point Sal, at least one of the structures responsible for down-dropping the top of the ophiolite into the basin can be identified. The eastern termination of short-wavelength magnetic anomalies about 10 km southeast of Point Sal *[Aeromagnetic Shallow PDF Bookmark]* coincides roughly with a north-trending normal fault (the Pezzoni fault) and gravity gradients *[Gravity 2,670 kg/m³ PDF Bookmark]* that indicate east-side-down displacement. Using the gravity gradient as a guide, the east-side-down, normal fault extends approximately 20 km to the south. Its path is locally sinuous; a southeast-protruding gravity high coincides with the axis of an anticline in the Casmalia Hills and may reflect warping of the fault by subsequent folding. These relationships and others discussed earlier all point to significant compressional or transpressional overprinting of extensional or transtensional structures in the Santa Maria basin.

Acknowledgments

The present mapping effort was funded through the USGS National Cooperative Geologic Mapping Program. We thank Emily Taylor (USGS) for providing guidance and oversight in the subdivision and digital mapping of Quaternary units. We thank Paul Denning (USGS), Michelle Roberts (USGS), and Lauren Shumaker (National Association of Geoscience Teachers [NAGT], USGS summer intern) for their work in digitizing parts of the source geologic maps. Bryanna Sudman (Geographic Information System [GIS] Department, City of Northfield, Minn.) developed and edited GIS datasets while working as a National Association of Geoscience Teachers (NAGT), USGS summer intern. Sorlien's offshore mapping was aided by Richard Behl (California State University, Long Beach) and Nelson Doris (then at California State University, Long Beach); 3D seismic data south and west of the Hosgri fault were provided by Robert Dame (Bureau of Safety and Environmental Enforcement, Pacific Region). We thank Kathleen Gerber (Department of Defense, Vandenberg Air Force Base) for her assistance in obtaining access to Vandenberg Air Force Base and for sharing her knowledge while escorting us at the base. Staff at the State of California Department of Conservation, Division of Oil, Gas, and Geothermal Resources, Santa Maria district office, aided in accessing records for petroleum exploration drill holes and in the scanning of electric logs. Constructive reviews by Joe Colgan, Richard Stanley, Scott Lundstrom, Janet Watt, Julie Herrick, and Darren van Sistine (all USGS) improved the quality of the map, map text, and digital database.

DESCRIPTION OF MAP UNITS

Cenozoic benthic foraminiferal age interpretations are based on the California benthic foraminiferal zonations of Kleinpell (1938, 1980) and Mallory (1959) with modifications as proposed by McDougall (2008) and additional modifications as proposed by Gradstein and others (2012). Correlation of the benthic foraminiferal stages and zones to the international time scale is discussed in McDougall (2008). Foraminiferal assemblages in the Foxen Mudstone are Pliocene and assigned to the Repettian Stage (Ingle, 1985; Behl and Ingle, 1998)

QUATERNARY SURFICIAL DEPOSITS

Qac **Active alluvium (Holocene)**—Sand- to boulder-size, moderately rounded to well-rounded, moderately sorted to well-sorted sediments forming channel and overbank deposits in modern floodplains of the Santa Ynez, Santa Maria, and Sisquoc Rivers. Maximum thickness about 10–13 m (Upson and Thomasson, 1951, p. 49)

Qey **Beach and dune sand (Holocene)**—Fine-grained, very well sorted, sandy eolian and shoreline deposits. Includes inland-lying parabolic dunes that are partly stabilized with vegetation and active transverse dunes in contact with the shore (Cooper, 1967; Orme, 1992). Partly stabilized dunes north of Point Sal yielded uncalibrated ^{14}C ages from buried wood of 1,120±80 years before present (B.P.) and 850±80 B.P.; active transverse dunes were probably activated within last 200 years (Orme, 1992). The Guadalupe Dune sheet along the coast at the north edge of the map yielded an uncalibrated radiocarbon age from a piece of wood at the base of the dune sheet of 3,530±70 B.P. (Knott and Eley, 2006)

Qay **Alluvial fan and fluvial deposits (Holocene)**—Unconsolidated axial valley deposits, floodplains, fluvial deposits in tributary drainages, and alluvial fan deposits. Fluvial deposits include poorly sorted to well-sorted sand, silty sand, and sandy gravel with minor cobbles. Alluvial fan deposits are sand or sandy gravel that generally grade upward to sandy or silty clay.

Floodplain deposits are sandy to silty clay, locally with lenses of silt, sand, and pebbles. Locally includes beach sand and gravel at mouths of alluvial channels along the coast. Holocene age is based on lack of argillic horizon development as determined from soil survey mapping (https://www.nrcs.usda.gov/wps/portal/nrcs/main/soils/survey/)

Qty **Terrace deposits (Holocene)**—Young fluvial deposits capping terraces. Deposits consist of crudely bedded, clast-supported gravels, cobbles, and boulders with a sandy matrix. Holocene terraces occur adjacent to the Santa Ynez River (Upson and Thomasson, 1951). Fluvial terrace deposits form low-relief surfaces that are 3 to 10 m above active stream channel. Holocene age is based on lack of argillic horizon development as determined from soil survey mapping (https://www.nrcs.usda.gov/wps/portal/nrcs/main/soils/survey/)

Qls **Landslide deposits (Quaternary)**—Poorly sorted mixtures of clay, silt, sand, gravel, boulders, and rock masses resulting from slope-movement processes. Includes all levels of activity, from dormant to active. Landslide deposits generally larger than 500 m by 500 m are shown; unmapped smaller areas of landslide deposits commonly overlie a mapped bedrock unit

Qeo **Dune sand (Pleistocene)**—Medium-grained, very well sorted, sandy eolian deposits, occur landward of Holocene dunes and emerging from beneath them (Cooper, 1967). Typically have a well-developed surface soil profile and in some cases, there are two buried soils. Surface morphology of the paleodunes is subdued and gently rolling (Cooper, 1967). Deposits exposed northeast of Point Sal greater than 30 m thick (Orme, 1992). Fluvial deposits immediately underlying these paleodunes yielded a ^{14}C age of 23,560±360 years before present (B.P.) (Orme, 1992)

Qao **Older alluvium (Pleistocene)**—Weakly consolidated, crudely stratified, poorly sorted deposits of gravel, sand, silt, and clay. Channel structures, cross stratification, and pebble imbrication suggest deposition in a fluvial or floodplain environment. Pleistocene age is based on presence of well-developed argillic horizons as determined from soil

survey mapping (https://www.nrcs.usda.gov/wps/portal/nrcs/main/soils/survey/). Unit is identified in drainages tributary to San Antonio Creek where deposits are several meters thick (Muir, 1964; Clark, 1990). Presence of volcanic-rock clasts without a local source suggests these deposits may be remnants of a thorough-going paleo-drainage inset into the Casmalia Hills that had drained from the San Rafael Mountains (Clark, 1990)

Qto2 **Younger terrace deposits (late Pleistocene)**—Terrace deposits on gently sloping surfaces at low elevation along alluvial channels or along coastline. Younger Pleistocene age is based presence of weakly developed argillic horizons as determined from soil survey mapping (https://www.nrcs.usda.gov/wps/portal/nrcs/main/soils/survey/). Fluvial terrace deposits consist of crudely bedded, clast-supported gravels, cobbles, and boulders with a sandy matrix and clay occurring in poorly defined lenses (Worts, 1951). Fluvial terrace deposits lie on gently sloping surfaces that are up to 20–30 m above Qac deposits. Young Pleistocene fluvial terrace deposits are present in the drainages of the Santa Ynez and Sisquoc Rivers where they record an older alluvial system that has been tectonically uplifted above present depositional levels. Occurs in a broad area in the southern half of the Santa Maria Valley near the town of Orcutt, and as smaller remnants to the north of the Sisquoc River. Thickness typically 2–3 m, but locally as thick as 15 m (Worts, 1951).

Marine terrace deposits composed of weakly consolidated pebble-cobble gravel and pebbly sand, in places containing fossil shells of marine mollusks and gastropods, grading upward to sand and silty sand. Commonly overlain by continental alluvial deposits, especially on the landward side of terrace tread. Deposits unconformably overlie bedrock on a wave-cut abrasion platform that is rarely exposed. Marine terrace deposits mapped as Qto2 represent a composite geomorphic surface that combines, at a minimum, the 20-m and 30-m terraces of Upson (1951); corresponding to terraces dated by various methods at 80–125 ka (Muhs and others, 1992; Rockwell and others, 1992)

Qto1 **Older terrace deposits (middle and early Pleistocene)**—Terrace deposits on gently sloping surfaces at high elevations along coastline or above alluvial drainages. Older Pleistocene age is based on presence of well-developed argillic horizons as determined from soil survey mapping (https://www.nrcs.usda.gov/wps/portal/nrcs/main/soils/survey/). Fluvial terrace deposits are like Qto2, consisting of crudely bedded, clast-supported gravels, cobbles, and boulders with a sandy matrix. Fluvial terrace deposits lie on flat surfaces cut a few meters into bedrock that are up to several tens of meters above Qac deposits. Deposits occur at elevations between 80 and 120 m on Burton Mesa and Lompoc Terrace where they form broad, low-relief surfaces. Fluvial terrace deposits occur at elevations between 175 and 240 m in the Solomon Hills.

Terrace deposits Qto2 and Qto1 typically form distinct terrace treads, but locally younger Pleistocene terrace deposits are mapped as directly overlying older Pleistocene terrace deposits; these areas are shown on the map with a stipple pattern. Fluvial terrace deposits lie on gently sloping surfaces that are elevated 5−20 m above active stream channels. Soil survey mapping (https://www.nrcs.usda.gov/wps/portal/nrcs/main/soils/survey/) demonstrates the presence of two ages of soils, with younger terrace overlying older terrace deposits on the same surface. Occurs in the upper Santa Ynez River drainage where younger and older Pleistocene terraces locally overlap.

Marine terrace deposits are similar to Qto2; locally, marine deposits are absent and terrace levels appear only as benches cut in bedrock and level parts of ridge crests that correspond in elevation to nearby abrasion surfaces with demonstrable marine deposits. Marine terrace deposits mapped as Qto1 range in elevation between 60 and 115 m; corresponding to terraces dated by various methods at 340−150 ka (Muhs and others, 1992; Rockwell and others, 1992)

Qo **Orcutt Sand (late Pleistocene?)**—Nonmarine, unconsolidated to loosely compacted sand and sandy gravel. Upper part of formation is medium-grained, well-sorted, massive sand, typically iron stained with minor clay interbeds. Unit grades downward to loosely compacted, gray to white gravel and sand. Gravel clasts in the Santa Ynez River basin are mostly locally derived diatomaceous shale or porcelaneous chert (Upson, 1951); whereas in the Santa Maria Valley and in the Casmalia Hills, clasts also include micaceous sandstone, biotite granite, and rhyolite porphyry sources from outside the

basin (Woodring and Bramlette, 1950). Unit is typically between 15 and 30 m thick, up to 60-m thick in the lower Santa Ynez River Valley (Upson, 1951) and 100 m thick beneath the center of the Santa Maria Valley (Worts, 1951). Unit is a heterogeneous deposit that may have formed in widely varying depositional environments including coalescing alluvial fans, fluvial and eolian environments, and local marine terrace deposits (Clark, 1990). Unit is deformed, with dips of 5–20° on the northeast flank of the Casmalia and Solomon Hills (Woodring and Bramlette, 1950; Worts, 1951). Formation presumed to be upper Pleistocene by Woodring and others (1943) but may be older given the extensive terraces of interpreted upper Pleistocene age developed on the Orcutt Formation (Kitao, 2018)

CENOZOIC SEDIMENTARY ROCKS

QTpr **Paso Robles Formation (early Pleistocene and upper Pliocene)**—Light greenish-gray to buff unconsolidated nonmarine alluvial clayey sand with scattered pebbles and lenses of pebble and cobble gravel. Gravel is typically cross-bedded and composed mostly of clasts of porcelaneous shale pebbles derived from the Monterey Formation, except on south flank of San Rafael Mountains where pebble and cobble clasts include altered mafic volcanic rocks, serpentinite, and jasper (Upson and Thomasson, 1951). Discontinuous beds of clay and freshwater limestone are present in a zone 15–30-m thick that marks the base of the formation and is recognized throughout most of the map area. Unit is up to 600 m thick in the Santa Maria area and as much as 1,400-m thick in the upper Santa Ynez drainage adjacent to the San Rafael Mountains (Woodring and Bramlette, 1950). Conformable with underlying Careaga Sandstone. Largely of Pliocene age (Addicott and Galehouse, 1973); Pleistocene age based on reported presence of vertebrate fossils just north of the map area (Woodring and Bramlette, 1950, p.108)

Tc **Careaga Sandstone (upper Pliocene)**—Fine to coarse-grained gray, buff, or white sandstone and conglomerate containing clasts of quartzite, porphyritic igneous rocks, chert of the Franciscan Complex, and Monterey Formation. Abundant shallow marine fossils. Formation was divided by Woodring and Bramlette (1950) into lower Cebada Member consisting of buff sandstone and sand and upper Graciosa Member consisting of coarse-grained buff sandstone and conglomerate (Woodring and Bramlette, 1950); formation not subdivided on our geologic map. Locally pebbly; shelly intervals at or near base (Dibblee, 1950). Includes fossiliferous calcareous sandstone in Casmalia Hills (Woodring and Bramlette, 1950). Maximum exposed thickness of the Careaga Sandstone is 430 m in the Purisima Hills (Woodring and Bramlette, 1950). The unit is 300-m thick to the north in the San Antonio Creek drainage, and still farther north in the Solomon and Casmalia Hills it is about 200-m thick (Muir, 1964)

Tf **Foxen Mudstone (upper and middle Pliocene; upper Repettian)**—Gray to light olive-gray, slightly consolidated massive mudstone and clayey siltstone and fine-grained sandstone. Unit is marine in origin, in a shallowing-upward sequence. In the Santa Maria oil field, a lower siltstone up to 550-m thick is overlain by up to 150 m of fine sand, which in turn is overlain by up to 20 m of sand and gravel (Canfield, 1939); foraminiferal assemblages in these units also suggest a shallowing-upward depositional environment (Woodring and others, 1943; Behl and Ingle, 1998). Unit is thickest beneath synclinal basins in the map area and is up to 975 m thick in the western part of the Santa Maria oil field (Canfield, 1939; Worts, 1951). Unit is about 250 m thick on the western flanks of the Purisima and Casmalia anticlines but thins eastward and pinches out over the crest of the anticlines. In complete sections, unit gradationally overlies diatomaceous strata of the Sisquoc Formation and is conformably overlain by the basal fine-grained part of the Careaga Sandstone. Foraminiferal assemblages in the Foxen Mudstone are Pliocene and assigned to the Repettian Stage (Ingle, 1985; Behl and Ingle, 1998)

Tsq **Sisquoc Formation (lower Pliocene and upper Miocene; Repettian to Mohnian)**—Laminated to massive brown laminated diatomaceous marine mudstone and claystone, and their diagenetic equivalents porcelaneous and siliceous mudstone, with some

sandstone to white laminated diatomite (Woodring and Bramlette, 1950; Ramirez, 1990; Barron and Ramirez, 1992). Intervals rich in biogenic silica tend to be finely laminated and banded, whereas intervals that contain more terrigenous clastic material tends to be bioturbated and structureless (Henderson and Ramirez, 1990; Ramirez and Garrison, 1998). In comparison with the underlying Monterey Formation, the Sisquoc Formation tends to have higher amounts of terrigenous clastic material and contains a greater proportion of massive beds (Ramirez and Garrison, 1998). The Sisquoc Formation is up to 1,500 m thick in Santa Maria basin (Woodring and Bramlette, 1950) and conformably overlies the Monterey Formation in the center of the Santa Maria basin, but discordantly overlies the Monterey along the basin margins and on certain anticlines within the basin (Woodring and Bramlette, 1950).

Microfossils from the Sisquoc Formation indicate it straddles the Miocene-Pliocene boundary (Arends and Blake, 1986; Dumont and Barron, 1995; Ramirez and Garrison, 1998). Microfossils from the USGS and Chevron outcrop collections indicate an age of late Miocene to Pliocene and are assigned to the Mohnian and Delmontian Stages. Although deposition of the Sisquoc Formation occurred at upper bathyal depths, deposition of this formation is generally at shallower depths than the underlying Monterey Formation (Dumont and Barron, 1995; McCrory and others, 1995)

Tsqs **Todos Santos Claystone Member and Tinaquaic Sandstone Member of Sisquoc Formation, undivided (lower Pliocene and upper Miocene; Repettian to Mohnian)**—Siliciclastic, diatom-poor parts of the Sisquoc Formation that generally underlie fine-grained diatomaceous strata. Fine- to coarse-grained buff or gray sandstone with thin layers of chert pebbles and massive to indistinctly laminated clayey siltstone. Shallow marine megafossils and foraminifers (Woodring and Bramlette, 1950). Includes the Tinaquaic Sandstone Member, a 120- to 440-m-thick marginal basin-edge sandstone facies present in the vicinity of Foxen Canyon on the northeast edge of the Santa Maria basin, and the Todos Santos Claystone Member, a 230- to 530-m thick somewhat porcelaneous claystone part of basin-facies Sisquoc Formation present in the Casmalia Hills (Woodring and Bramlette, 1950). Tinaquaic Sandstone Member is middle Pliocene and Todos Santos Claystone Member is upper Miocene according to Woodring and Bramlette (1950). Foraminifers from Chevron outcrop samples suggest a late Miocene to early Pliocene age and are assigned to the Mohnian Stage

Tm **Monterey Formation (upper, middle, and upper lower Miocene; Mohnian to upper Saucesian)**—Laminated to thin-bedded siliceous shale, calcareous mudstone, dolomite, dolomitic mudstone, marl, diatomaceous shale, diatomite, phosphatic shale, porcelaneous shale, and chert (Bramlette, 1946; Woodring and Bramlette, 1950). Includes sandstone locally at base in the eastern and southern part of map area. Bathyal marine. About 800 m thick in the Casmalia Hills; almost 1,500 m thick on the north flank of the Purisima Hills; about 500 m thick in the Santa Rosa Hills and Santa Ynez Mountains.

Three primary lithofacies packages compose the formation that are generally consistent in their stratigraphic order and age range: (1) a lower calcareous facies, principally massive to thin-bedded calcareous mudstone and shale with some minor sandy beds and concretionary carbonate, ranging from Saucesian to lower Mohnian; (2) a middle unit of phosphatic shale and mudstone grading upward to a transitional zone of cyclically interbedded phosphatic and siliceous rocks, mostly lower Mohnian but in part Luisian and upper Mohnian; and (3) an upper siliceous facies that includes thin- and rhythmically bedded chert, porcelanite, and siliceous shale that grades upward into diatomaceous and clayey mudrock, upper Mohnian (Woodring and Bramlette, 1950; Isaacs, 1980, 1983; Pisciotto, 1981; Pisciotto and Garrison, 1981). Burial diagenesis of these siliceous rocks modifies and in places obscures the primary lithologic variability. Diatomaceous rocks are variably converted to chert, porcelanite, and siliceous mudrocks because of variations in depth and time of burial, host lithology, and geochemical environment (Behl and Garrison, 1994; Behl, 1998, 1999).

Woodring and Bramlette (1950) mapped three informal members of the Monterey Formation, a lower member of phosphatic shale and minor porcelaneous shale, a middle member of chert and cherty shale, and an upper member of porcelaneous shale and

diatomaceous strata. Dibblee (1950, 1981a–d) mapped two informal members of the Monterey Formation, a lower member comprising bedded to massive clayey shale, phosphatic shale, limestone, and laminated siliceous shale, and an upper member of laminated siliceous shale, chert and porcelanite. The Monterey was not subdivided by Vedder and others (1991). Hall (1978) subdivided the Monterey Formation into a lower member of thinly bedded siliceous siltstone and porcelaneous shale and an upper member of porcelaneous siliceous shale, cherty shale, and opaline shale. Hall (1981a) used a similar subdivision, but locally broke out a basal massive siltstone and conglomerate and a diatomaceous siltstone unit. The present compilation subdivides the Monterey Formation into two informal members, upper and lower, where previous mapping allows the distinction. The member boundaries are compiled as shown on the original geologic mapping and have not been reinterpreted. The Monterey Formation is shown as undivided (Tm) where the original mapping did not subdivide the formation (Vedder and others, 1991) or in areas where the originally mapped subdivisions (Hall, 1978, 1981a) could not be confidently correlated to those defined by Woodring and Bramlette (1950) or Dibblee (1950, 1981a–d)

Tmu **Informal upper member of Monterey Formation (upper and middle Miocene; Mohnian to upper Luisian)**—Porcelaneous shale, diatomite, and diatomaceous shale in northern part of map (Woodring and Bramlette, 1950); laminated siliceous shale, cherty shale, diatomite, phosphatic shale, limestone, and local conglomerate and sandstone in western Transverse Ranges (Dibblee, 1950, 1981a–d; Surpless and others, 2009). Equivalent to the informal upper member of Dibblee (1950, 1981a–d) and Woodring and Bramlette (1950). Although foraminifers from this unit are usually middle to late Miocene and assigned to the Mohnian Stage, a few samples contain foraminifers diagnostic of the middle Miocene, Luisian or Relizian Stage. These assemblages may be subsequently found to be in the informal lower member of the Monterey Formation. Thickness 180 to 300 m

Tml **Informal lower member of Monterey Formation (middle to lower Miocene; Mohnian to upper Saucesian)**—Siliceous mudstone, siltstone, thin-bedded sandstone, phosphatic shale, calcareous mudstone, porcelaneous shale, limestone in northern part of map (Woodring and Bramlette, 1950); siltstone, silty siliceous shale, limestone, phosphatic shale and minor porcelaneous and cherty shales in western Transverse Ranges (Dibblee, 1950). Equivalent to the informal lower member of Dibblee (1950, 1981a–d) and the lower and middle members of Woodring and Bramlette (1950).

Foraminiferal assemblages are primarily early to middle Miocene and assigned to the Saucesian, Relizian, and Luisian Stages, although this group is highly variable. Assemblages assigned to the early Miocene Saucesian Stage will probably prove to be from the Rincon Shale and the late Miocene Mohnian assemblages will probably prove to be from the informal upper member of the Monterey Formation. Thickness 60 to 275 m

Tps **Point Sal Formation (lower middle Miocene to upper lower Miocene; Relizian to Saucesian)**—Mudstone, siltstone, and fine-grained sandstone; bathyal marine. Mainly of dark gray to black, brown-weathering, silty shale with thin (2-10 cm) interbeds of medium-grained brownish, locally calcareous sandstone. More than 450 m thick near Point Sal (Stanley and others, 1996) although local thickness may be considerably less (Woodring and Bramlette, 1950; Crawford, 1971). Fine-grained rocks are hard, fissile, and calcareous, with laminations and calcareous microfossils that suggest deposition in oxygen-poor environments at bathyal water depths (Stanley and others, 1996). Sandstones are turbiditic and probably represent submarine fan deposition (Lagoe, 1987). Lower part of formation contains benthic foraminifers of the lower Miocene Relizian Stage (Woodring and Bramlette, 1950; appendix 1, table 1.1); the Saucesian-Relizian benthic foraminiferal stage boundary is identified about 2 m above the base of the formation (Stanley and others, 1991). Formation locally intruded by diabase sills (Woodring and Bramlette, 1950; Cole and Stanley, 1998)

Tl **Lospe Formation (upper lower Miocene; Saucesian)**—Red and green conglomerate, sandstone, siltstone, and mudstone with minor water-laid rhyolitic tuff. Nonmarine (alluvial fan and lacustrine) to shallow marine. Informally subdivided into a nonmarine

lower member consisting of alluvial fan and fan-delta red and green conglomerate, sandstone, and mudstone and a lacustrine to shallow-marine upper member consisting of greenish-gray sandstone, siltstone, and gypsiferous mudstone (Woodring and Bramlette, 1950; Johnson and Stanley, 1994; Stanley and others, 1996). Conglomerates contain assemblages of clasts derived from Mesozoic basement rocks including gabbro, diabase, and serpentinite from underlying ophiolite, and sandstone clasts derived from both the Franciscan Complex and from Jurassic and Cretaceous sedimentary rocks equivalent to the upper part of the Great Valley Sequence (McLean and Stanley, 1994). Tuffs range from a few centimeters (cm) to 20 m thick and were deposited by high density turbidity flows that closely followed pyroclastic eruptions (Cole and Stanley, 1994).

The Lospe Formation is as thick as 830 m and is exposed at the west end of the Casmalia Hills on Point Sal Ridge and to the south of Mt. Lospe. The Lospe Formation is present in the subsurface within a narrow, northwest-trending band that underlies the Casmalia, Solomon, and Purisima Hills (Hall, 1982) that may represent localized deposition within a narrow, fault-bounded initial phase of the Santa Maria basin (Johnson and Stanley, 1994). The formation nonconformably overlies igneous rocks of the Jurassic ophiolite at Point Sal (Hopson and others, 1975; Hopson and Frano, 1977) and overlies with an angular unconformity Jurassic and Cretaceous sedimentary rocks mapped as Knoxville by Woodring and Bramlette (1950). The formation is conformably overlain by the Point Sal Formation. Age determinations from interbedded tuffs suggest unit was deposited about 18–17 Ma (Stanley and others, 1991, 1996). Microfossil assemblages indicate the formation is late early Miocene; the type Lospe Formation contains lower Miocene (Saucesian) foraminiferal assemblages (Stanley and others, 1996; appendix 1, table 1.1)

Tss **Unnamed sandstone (lower Miocene? to upper Oligocene?; Saucesian to Zemorrian)**—Marine fine- to coarse-grained, thick-bedded to massive quartzofeldspathic sandstone, generally calcareous, commonly glauconitic. Fossils were not previously reported in the map area (Vedder and others, 1991), but unit in adjoining areas to the north contained middle Miocene pectenids (Vedder and others, 1989a). Microfossils in the Chevron outcrop samples from Sierra Madre domain are early Miocene to Oligocene and assigned to the Saucesian and Zemorrian Stages. This unit may be equivalent in part to the Rincon Shale and locally equivalent to lower Miocene–upper Oligocene Vaqueros Formation mapped in adjacent areas (Hall and Corbató, 1967; Hall, 1978)

Tr **Rincon Shale (lower Miocene; Saucesian)**—Brown, gray, or buff silty claystone or mudstone with orange-weathering dolomite concretions and tabular beds. Generally, bioturbated and poorly bedded to massive. Locally includes 5–10 cm thick sandstone beds. Unit is 500 m thick in the western Santa Ynez Mountains (Dibblee, 1950). Bathyal marine, based on benthic foraminiferal assemblages (Edwards, 1972; Finger, 1983; appendix 1, table 1.1). Typically forms gentle, grass-covered slopes and weathers to a clayey adobe soil.

The contact with underlying Vaqueros Formation is conformable; lithologic transition from coarse sandstone to mudstone occurs over an interval of about 5 m (Edwards, 1972). On the southern flank of the Santa Ynez Mountains, the Rincon Shale is conformably overlain by the Monterey Formation. In the western Santa Ynez Mountains at Tranquillon Mountain, the Rincon Shale is separated from the underlying Vaqueros Formation by the Tranquillon Volcanics. Rincon Shale is also present in the Huasna domain along the West Huasna fault where it unconformably overlies unnamed Upper Cretaceous sandstone and underlies volcanic rocks of the Obispo Formation (Hall, 1978).

Several workers have suggested that the Rincon Shale spans an age range from latest Oligocene through early Miocene, based on age ranges defined by molluscan zones (Kleinpell and Weaver, 1963), foraminiferal assemblages (Edwards, 1972), and marine ostracodes (Finger, 1983). However, detailed biostratigraphic analysis of samples from a well-exposed section at the Tajiguas landfill (location TL in fig. 2) demonstrates that the Rincon Shale at this location is entirely of early Miocene (Stanley and others, 1992, 1996)

Tsi **Simmler Formation (lower Miocene to upper Oligocene?; Saucesian to Zemorrian)**—Nonmarine conglomerate, sandstone, and mudstone. Red, green, greenish-yellow, or greenish brown; conglomerate contains abundant clasts of biotite-rich sandstone. Fluvial, locally channeled, unconformity at base. Occurs in the Sierra Madre domain in the San Rafael Mountains to the southwest of the Nacimiento fault and northeast of the East Huasna fault. Formerly assigned to Sespe Formation by Crandall (1961) and Redwine and others (1975). Mapped as Simmler Formation by Vedder and others (1991) based on similarity to mapped Simmler Formation in adjoining areas to the north (Vedder and others, 1988) and a difference in clast composition from Sespe in the Santa Ynez Mountains. Exact age uncertain because of rarity of fossils; interpreted as Oligocene(?)-early Miocene in the southern Cuyama Valley area (Blake, 1982; Ballance and others, 1983).

Small outcrops of nonmarine conglomerate, sandstone, and silty claystone near the West Huasna fault, which Hall (1978) designated as Lospe Formation, are lithologically unlike and demonstrably older than the type Lospe Formation (Stanley and others, 1996). These outcrops are tentatively correlated with the Simmler Formation based on lithology, pre-early Miocene, and proximity to outcrops mapped as Simmler in the nearby San Rafael Mountains (Vedder and others, 1991)

Tv **Vaqueros Formation (upper Oligocene; Zemorrian)**—Gray or buff fine- to coarse-grained quartzofeldspathic sandstone, pebble conglomerate, pebbly sandstone, and shell debris. In the western part of the Santa Ynez Mountains, the unit is typically about 30 m thick and consists of a greenish-brown, coarse-grained, matrix-supported, variably fossiliferous conglomerate containing clasts predominantly derived from the Franciscan Complex overlain by buff, extensively bioturbated, locally cross-bedded, coarse- to fine-grained sandstone (Dibblee, 1950; Rigsby, 1998). These strata have been interpreted as fan-delta deposits (Rigsby, 1998). From approximately Gaviota Canyon (location GC in fig. 2) eastward, the unit consists of a lower unit of light gray, friable to hard, calcareous, cross-bedded, medium- to coarse-grained sandstone and conglomerate overlain by planar-laminated, coarse-grained sandstone. Mollusks are abundant in the sandstone. These strata are interpreted to represent a prograding shoreface-beach environment (Miles and Rigsby, 1990; Rigsby, 1998). The Vaqueros thins to as little as 5 m at Gaviota Canyon but thickens eastward to about 125 m near Refugio Pass (Edwards, 1972). The Vaqueros Formation is thickest on the north flank of the Santa Ynez Mountains near Nojoqui and Alisal Creeks where it is up to 200 m thick and consists of buff, fine- to medium-grained sandstones interbedded with light brown, thinly bedded siltstone with local beds of conglomerate, coquina, and fossil hash (Dibblee, 1950; Byrd, 1983). Hall (1978) mapped a thin outcrop band of Vaqueros Formation in the Huasna domain to the west of Twitchell Reservoir where it underlies volcanic rocks of the Obispo Formation.

In the Santa Ynez domain to the east of Gaviota Canyon, the Vaqueros lies conformably on the Sespe Formation. As the Sespe Formation thins and grades westward into paralic and shelf facies of the Alegria Formation, the Vaqueros Formation gradually overlaps the upper part of the Alegria Formation (Rigsby, 1998). The contact becomes unconformable and angular in the western part of the Santa Ynez Mountains where the Vaqueros Formation overlies the Alegria and Sacate Formations (Rigsby and Schwartz, 1990; Rigsby, 1998).

The Vaqueros is considered to be late Oligocene on the basis of stratigraphic position between the upper Oligocene upper part of the Sespe Formation and lower Miocene Rincon Shale (Minor and others, 2009). Rigsby (1998) reported a strontium-isotope date of 24±1 Ma (latest Oligocene) from oyster shells in Vaqueros Formation from the south slope of the Santa Ynez Mountains west of Gaviota Canyon. Microfossils in the Chevron outcrop samples (appendix 1, table 1.1) are Oligocene and assigned to the Zemorrian Stage, which is consistent with the regional interpretation of foraminiferal faunas that place the Vaqueros in the Zemorrian Stage (Kleinpell and Weaver, 1963; Edwards, 1972)

Ta **Alegria Formation (Oligocene and upper Eocene; Zemorrian and Refugian)**—Shallow marine sandstone and green siltstone. Unit subdivided by Dibblee (1950) into seven informal members that are not shown on this map. Sandstone members are buff to gray, medium- to coarse-grained, thick-bedded to massive, friable, and generally fossiliferous. Siltstone members are greenish-brown to grayish-brown, poorly to well-bedded, clayey siltstone. Members vary along strike in lithology and thickness.

Alegria Formation crops out only on the south flank of the Santa Ynez Mountains; thickness varies between 200 and 400 m. Conformably overlies the Gaviota Formation. East of Gaviota Canyon, it is overlain gradationally by alluvial red siltstones of the Sespe Formation, whereas to the west it is overlain unconformably by the Vaqueros Formation (Dibblee, 1950; O'Brien, 1972). East of Gaviota Canyon and the south branch of the Santa Ynez fault, the Alegria Formation grades eastward into nonmarine strata of the Sespe Formation (Dibblee, 1988d, 1988e; Howard, 1995). Microfossil assemblages are upper Eocene to Oligocene and assigned to the Refugian and Zemorrian Stages (appendix 1, table 1.1)

Tsp **Sespe Formation (Oligocene to upper Eocene; Zemorrian and Refugian)**—Sandstone, siltstone, shale, and conglomerate; continental fluvial and delta plain. On the south slope of the Santa Ynez Mountains, the map unit consists of about 700 m of pinkish-gray to buff, friable, laminated sandstone interbedded with red and green shale and siltstone. Typically, 10- to 30-m-thick intervals of fining-upward sequences of sandstone and siltstone alternate with fissile claystone (Howard, 1988). In the Santa Rosa Hills, the Sespe is about 150 m thick and consists of an upward-fining sequence of a coarse conglomerate containing with clast lithology predominantly of the Franciscan Complex, overlain by red and green friable sandstone and interbedded red and green shale and siltstone (Dibblee, 1950).

The Sespe consists of two of fining-upward depositional sequences that are separated by a regional unconformity that places upper Oligocene rocks on upper Eocene strata. The lower sequence is middle to late Eocene and grades westward into the Gaviota Formation (Howard, 1995); this sequence is present in the eastern part of the map area east of Refugio Pass (Dibblee, 1988d). The upper sequence is late Oligocene and grades westward into the Alegria Formation (Howard, 1995). Lower Oligocene strata have not been identified and are presumably missing along the mid-Sespe unconformity. The upper sequence of the Sespe Formation wedges out to the west of Gaviota Canyon (location GC in fig. 2), where it in part grades into the marine Alegria Formation and in part is overlapped and truncated by the overlying Vaqueros Formation (Bailey, 1947). Foraminiferal assemblages from samples in the Sespe Formation east of Arroyo Hondo (location AH on fig. 2) are Oligocene and assigned to the Zemorrian Stage. Samples in Santa Anita Canyon contain only broadly ranging species indicating a late Eocene to Oligocene age (appendix 1, table 1.1, field nos. 4827 and 4828, Sacate 7.5' quadrangle). These Chevron samples are probably from the marine Alegria Formation which interfingers with the Sespe Formation

Tg **Gaviota Formation (upper Eocene; Refugian)**—Sandstone and siltstone. Shallow marine, regressive. Divided into three informal members over much of its outcrop area (Dibblee, 1950; O'Brien, 1972, 1973). Lower member: massive, soft, gray siltstone; middle member: light buff, thick-bedded, bioturbated well-sorted, fine- to medium-grained upward-coarsening sandstone; upper member: gray sandy mudstone and siltstone with interbedded fine-grained sandstone (Dibblee, 1950; O'Brien, 1972).

The formation is about 500 m thick near its type section to the west of Gaviota Canyon. Lower member has a maximum thickness of 140 m and thins eastward by lateral gradation into shallow-water marine sandstones (O'Brien, 1972, 1973). The middle member has an average thickness of 230 m. Upper member up to 200 m thick but thins and grades eastward into shallow-water marine sandstones. East of Refugio Pass, almost the entire formation is sandstone with only minor siltstone and conglomerate interbeds (Weaver, 1965; O'Brien, 1972). East of the map area, the entire Gaviota Formation grades into the continental Sespe Formation (Dibblee, 1966; Hornaday and Phillips, 1972).

The formation is late Eocene and assigned to the Refugian Stage (Tipton, 1980; appendix 1, tables 1.1 and 1.2)

Tgsa **Gaviota and Sacate Formations, undivided (upper to middle Eocene; Refugian to Narizian)**—Gaviota Formation and Sacate Formation, undifferentiated. In the Santa Rosa Hills domain north of the Santa Ynez fault, the Sacate and the overlying Gaviota Formation are not readily distinguishable. The lower part of the interval is like the Sacate Formation, predominantly shale with thin sandstone interbeds. This unit grades upward into sandstone similar to the Gaviota Formation. Due to poor exposures and lack of faunal control, this interval is defined cartographically as "Undifferentiated Gaviota-Sacate," following the usage of Dibblee (1950). Foraminiferal assemblages range in age from upper to middle Eocene and are assigned to the Narizian and Refugian Stages (Weaver and Molander, 1964; appendix 1, table 1.1).

Tcd **Cozy Dell Shale (upper and middle Eocene; lower Refugian to Narizian)**—Thin-bedded clay shale with subordinate thin sandstone interbeds, marine. About 220 m of well-bedded gray clay shale. Contains one and locally several thin beds of hard greenish sandstone about 60 m above the base of the unit. Upper part of unit contains same shale but includes two beds of thin-bedded, siliceous, resistant brown clay shales (Kelley, 1943; Dibblee, 1950). In the map area, Cozy Dell Shale grades upward through a series of thin sandstone interbeds into the overlying Sacate Formation; east of the map area, the lower Sacate grades laterally into the upper part of the Cozy Dell Shale. Megafossil assemblages suggest a middle or late Eocene age in the map area (Kelley, 1943; Dibblee, 1950, 1966). Microfossil assemblages suggest a middle to late Eocene age and are assigned to the Narizian and Refugian Stages, Zones A–1 and A–2 of Laiming (1939) (Weaver, 1962; Weaver and Molander, 1964). Magnetostratigraphic data also suggest a middle Eocene age (Prothero and Britt, 1998; Prothero, 2001)

Tsa **Sacate Formation (upper and middle Eocene; upper Narizian)**—Marine sandstone, siltstone, and shale, neritic to bathyal. The Sacate Formation, originally described by Kelley (1943), is exposed on the southern flank of the western Santa Ynez Mountains and at several localities in the Santa Rosa Hills domain.

The Sacate is informally subdivided into a lower sandstone member and mudstone-rich upper member (Kelley, 1943; O'Brien, 1972, 1973; Dibblee, 1988d). Lower member consists of massive, hard, fine- to medium-grained light gray to brown sandstone with local conglomerate lenses, separated by thin siltstone and brown micaceous shale. Upper member consists of massive- to thin-bedded and laminated brown shale and siltstone with occasional, nonpersistent sandstone beds.

The Sacate Formation is consistently more than 600 m thick east of Gaviota Canyon and is generally conformable with both the overlying Gaviota Formation and underlying Cozy Dell Shale (Dibblee, 1950). West and north of Gaviota Canyon, the Sacate locally disconformably overlies the Matilija Sandstone where the intervening Cozy Dell Shale is absent (Campion and others, 1988; Campion and others, 1996). North of Point Conception in the western Santa Ynez Mountains the Sacate is generally less than 200 m thick (Dibblee, 1950).

The age of the Sacate Formation is middle and late Eocene (Narizian) based on numerous foraminiferal and molluscan studies (Hornaday, 1961, 1965; Weaver and Weaver, 1962; O'Brien, 1973; Tipton, 1980; appendix 1, tables 1.1 and 1.2). The Sacate Formation interfingers with and grades laterally into the Coldwater Sandstone and the Cozy Dell Shale in the central Santa Ynez Mountains to the east of the map area (Hornaday and Phillips, 1972; O'Brien, 1973; Dickinson, 1995; Campion and others, 1996)

Tma **Matilija Sandstone (middle Eocene; lower Narizian to Ulatisian)**—Arkosic sandstone and interbedded shale, marine. Consists of a succession of beds up to 5–15 m thick of laminated to cross-bedded, medium-grained, fairly hard, buff to bluish-white sandstone. The sandstone beds are separated by thin partings of greenish gray, micaceous, silty, slightly calcareous shale (Dibblee, 1950). The basal part is locally pebbly sandstone and contains rounded pebbles of quartzite and granitic rocks (Kelley, 1943).

Unit is about 120 m thick at Refugio Pass but thickens eastward to 600 m at the eastern boundary of the map area. On the south-facing slope of the western Santa Ynez Mountains between Las Cruces and Jalama Canyon, the Matilija is 150–300 m thick. In the Santa Rosa Hills, the Matilija is less than 100 m thick. Thickness variations may be in part the result of lithofacies changes where the lower, deep-water part of the unit is not present in the western areas (Link, 1975; Link and Welton, 1982). Nannofossil (Almgren and others, 1988), foraminiferal (Weaver, 1962), and magnetostratigraphic (Prothero, 2001) data suggest a middle Eocene age for this unit

Tj **Juncal Formation (middle to lower Eocene; Ulatisian)**— Interbedded marine sandstone and shale; turbiditic. Less than 500 m thick east of the Santa Ynez Valley (Dibblee, 1966). Silty shale, shale and thin sandstone beds, and fine sandstone with thin shale interbeds; Varying proportions of silty shale and thin-bedded arkosic sandstone result from varying submarine fan depositional environments (Dickinson, 1995). Conformable on the Sierra Blanca Limestone, where present, otherwise unconformably overlies Upper Cretaceous strata (Vedder, 1972). Present in southeast part of map area at the base of the northern slope of the Santa Ynez Mountains where it overlies Jalama Formation and is continuous with exposures in the central Santa Ynez Mountains (Dibblee, 1966)

Tan **Anita Shale (lower Eocene to Paleocene; Ulatisian to upper Bulitian)**—Dark gray silty shale, with subordinate thin sandstone interbeds. Often consists of a lower unit of greenish gray silty shale with thin beds of micaceous sandstone, a middle unit of green to reddish brown foraminiferal clay shale (the so-called Poppin Shale of Dibblee, 1950, p. 26), and an upper unit of gray to buff silty shale with common interbeds of arkosic sandstone (Kelley, 1943; Gibson, 1972). Lower part of the formation includes a nonpersistent horizon of nodules and lenses of detrital limestone previously mapped as Sierra Blanca Limestone (Keenan, 1932; Dibblee, 1950). Unit is approximately 300 m thick on the southern slopes of the Santa Ynez Mountains, but thins northward and is 50-m thick or less near Nojoqui Creek (Dibblee, 1950; Gibson, 1972). The Anita disconformably overlies the Upper Cretaceous Jalama Formation, except for a single location where the Sierra Blanca Limestone rests on the Jalama Formation and is concordantly but disconformably overlain by Matilija Sandstone (Kelley, 1943; Gibson, 1972). The unit ranges in age from Paleocene to early Eocene based on microfossils (Gibson, 1972; McDougall, 2008; appendix 1, table 1.1)

Tus **Unnamed sandstone (Eocene? and (or) Paleocene?; Ulatisian? to Ynezian?)**—Marine sandstone with subordinate conglomerate, and minor mudstone and algal limestone. Lenticular bedding, interpreted as submarine fan deposits (Vedder and others, 1989a, 1991). Sandstone is quartzofeldspathic and micaceous; conglomerate includes abundant siliceous metavolcanic clasts. Contains sparse Paleocene and early Eocene(?) sporomorphs and foraminifers (Vedder and others, 1989a). Unit occurs northeast of Nacimiento fault at extreme northeast corner of map area; thickness at least 500 m (Vedder and Dibblee, 1991)

Tsb **Sierra Blanca Limestone (lower Eocene to upper Paleocene; Penutian to upper Bulitian)**—White to light gray algal limestone, locally sandy to clayey, massive- to thin-bedded, glauconitic. Shallow marine.

Continuous exposures of the formation lie to the north of the Santa Ynez fault in the upper Santa Ynez River drainage and in the southern San Rafael Mountains, 30 km east of the map area (Walker, 1950; Dibblee, 1966; Vedder and others, 1998). In parts of this area, the unit is as much as 70 m thick, and consists of nearly pure, dense, buff to white algal limestone that rests unconformably on underlying rocks of Late Cretaceous or older age (Keenan, 1932; Walker, 1950; Dibblee, 1966); however, in places, the unit consists of discrete beds of limestone, interpreted as turbidity current deposits, that are interstratified with mudstone beds containing middle to lower bathyal foraminiferal assemblages (Vedder and others, 1998).

In the map area, the Sierra Blanca Limestone is represented by a single map polygon near Nojoqui Creek (the “Moonshine Canyon” locality of Gibson (1972) and the “Live Oak Ranch dairy section” of Dibblee, 1950; see also Whidden and others, 1995).

At this locality, the formation consists of about 15 m of gray-white, hard, sandy, algal limestone that overlies the Jalama Formation with an angular unconformity and underlies Anita Shale that contains upper Paleocene benthonic fossil assemblages (Dibblee, 1950; Gibson, 1972). Two other localities within the map area have been previously described as Sierra Blanca Limestone (Keenan, 1932; Dibblee, 1950); in both cases, impure, sandy to pebbly limestone occur as lenticular bodies within the Anita Shale and are compiled as Anita Shale on this map. These lenticular bodies were interpreted as turbidite deposits that were shed off an algal limestone bank that lay to the north and east (Schroeter, 1972; Van de Kamp and others, 1974)

CENOZOIC VOLCANIC ROCKS

To **Obispo Formation (uppermost lower Miocene; Relizian to upper Saucesian)**—Vitric, pumiceous reworked nonwelded rhyolitic tuff, tuff breccia, tuffaceous sandstone and siltstone and local diabase and basalt. Tuff units are fine- to coarse-grained, white, nonwelded, crystal-bearing and occur as thick, massive, poorly sorted intervals and well-bedded tuff and pumice lapilli tuff. Tuff is locally zeolitized or silicified and forms resistant outcrops to the south of Twitchell Dam (Hall, 1978). Medium- to coarse-grained diabase occurs locally as dikes or sills (Hall, 1978); aphanitic basalt flows and pillow basalts occur locally in the upper part of the formation (Cole and Stanley, 1998). Tuffaceous rocks interpreted to have been erupted from an unidentified volcanic source to the northwest of the map area and deposited as subaqueous debris flows or turbidites (Schneider and Fisher, 1996).

In the map area, unit occurs in the vicinity of Twitchell Dam and the lower Cuyama River to its junction with the Sisquoc River. Exposures near Twitchell Dam as thick as 600 m (Hall, 1978). Includes small exposures of interbedded basalt, tuff, and tuff breccia along the Camuesa fault to the southwest of Zaca Peak (Hall, 1981a). Outside the map area, the unit forms a northwest-southeast-trending belt of outcrops that extends almost 40 km northwest of the map area and as thick as 1,500 m (Hall and Corbató, 1967; Cole and Stanley, 1998). Dated 15.7±0.5 to 16.9±0.8 Ma (K-Ar on plagioclase; Turner, 1970; recalculated ages as reported by Cole and Stanley, 1998). Microfossil assemblages from exposures near Twitchell Dam suggest an age of early to middle Miocene and are assigned to the Saucesian and Relizian Stages (appendix 1, table 1.1). Conformably overlies Rincon Shale and is conformably overlain by the Point Sal Formation and Monterey Formation

Ttv **Tranquillon Volcanics (uppermost lower Miocene; Relizian and Saucesian)**—Nonwelded to welded rhyolitic tuff, lapilli tuff, and minor basalt. Variably welded rhyolitic tuff (average SiO_2 77 percent) is gray-white to pinkish white, and contains 15–40 percent pumice, 5–15 percent quartz and sanidine phenocrysts, and less than 5 percent lithic fragments (Robyn, 1980). Welded tuff intervals display eutaxitic texture where pumice grains and glass shards are aligned and flattened parallel to bedding. Glass in nonwelded tuff and lapilli tuff diagenetically altered to zeolite minerals including analcime and clinoptilolite. Glass in welded tuff devitrified to potassium feldspar and quartz except for basal vitrophyre near base of the volcanic section (Robyn, 1980).

Originally mapped and described by Dibblee (1950) who proposed a type section between Tranquillon Mountain and Point Arguello. Subsequent mapping and stratigraphic analysis by Robyn (1980) show that these volcanic rocks are likely pyroclastic flows and pyroclastic fallout deposits. Robyn (1980) interpreted two distinct pyroclastic flow cooling units that are moderately to densely welded at the base and transition upward to nonwelded deposits. Map unit is up to 150 m thick to the south of Tranquillon Mountain but more typically 50–60 m thick over much of its outcrop area (Robyn, 1980). Unit thins rapidly to the southeast; on the southern flank of the Santa Ynez Mountains, the Tranquillon Volcanics are represented by a 50-cm to 1.8-m-thick tuff or bentonite bed that was included by Dibblee (1966) within the lowest part of the Monterey Formation, directly above the contact between the Monterey Formation and Rincon Shale. This bed contains angular, gray, pumiceous rock fragments (Edwards,

1972) and may be traced from the vicinity of Jalama Beach on the west through Tajiguas (Carson, 1965; Stanley and others, 1994) and eastward to the city of Santa Barbara (Minor and others, 2009). The map unit is present in the Lompoc Hills domain; wells to the north of the Santa Ynez River fault and south of the Lions Head fault intersect up to 60 m of volcanic rocks that may correlate to the Tranquillon Volcanics (Cole and Stanley, 1998; Sweetkind and others, 2010).

The Tranquillon Volcanics are disconformable on the underlying Rincon Shale and are unconformably overlain by the Monterey Formation (Dibblee, 1950; Dunham and Blake, 1987). Sanidine from welded tuff near the top of Tranquillon Mountain yielded a single crystal laser fusion argon/argon ($^{40}Ar/^{39}Ar$) age of 17.80±0.05 Ma (Stanley and others, 1996), an age consistent with its stratigraphic position between the two Miocene formations. The age of the Monterey Formation overlying the Tranquillon Volcanics is middle Miocene and assigned to the Relizian Stage (Finger, 1995; appendix 1, table 1.1, field nos. 11080 and 11081, Tranquillon Mountain USGS 7.5' quadrangle).

Isolated exposures of basaltic rocks mapped as Tranquillon Volcanics (Dibblee, 1950) crop out about 25 km east of Tranquillon Mountain along the Santa Ynez River drainage to the southwest of Buellton. These exposures are of basaltic andesite breccia that stratigraphically overlies the Rincon Shale and underlies the Monterey Formation. The basalt yielded a whole-rock potassium/argon (K/Ar) radiometric date of 17.4±1.2 Ma (Turner, 1970; corrected age reported by Cole and Stanley, 1998). Cole and Stanley (1998) interpreted these rocks as subaqueous lava flows likely derived from a nearby source, based on blocky, angular texture and incorporation of mudstones possibly derived from the underlying Rincon Shale within the breccia

MESOZOIC SEDIMENTARY ROCKS

Petrofacies equivalents to Great Valley Sequence—Divided into:

Kj **Jalama Formation (Upper Cretaceous)**—Argillaceous to silty shale and hard gray to buff sandstone, marine. Pebble-cobble conglomerate lenses near top, with clasts of quartzite, granitic rocks, porphyritic igneous rocks, chert, shale, and sandy limestone. Formation is at least several hundred meters thick and its base is not known (Dibblee, 1950; Bottjer and Link, 1984). Interpreted as dominantly turbidites deposited in a mid-outer deep-sea fan, but sediments deposited in shallow marine and brackish-water environments are locally present (Browning, 1983). Sandstone petrofacies are comparable to rocks in the upper part of the Great Valley Sequence in central California (MacKinnon, 1978; Dickinson, 1995). The relationship between the Jalama Formation and overlying Anita Shale is variable: south of the Santa Ynez fault system, the Anita Shale overlies the Jalama Formation with no apparent angular discordance, but to the north in the Santa Rosa Hills, the Anita Shale unconformably overlaps the Jalama Formation (Dibblee, 1982). Both the foraminifer and molluscan assemblages indicate a late Campanian or Maastrichtian age (Dailey and Popenoe, 1966; Almgren, 1973)

Kus **Unnamed sandstone (Upper Cretaceous)**—Marine turbiditic sandstone, mudstone, and conglomerate. Various rock types form lenticular turbidite sequences with few distinguishing marker beds; interpreted as submarine fan deposits (Vedder and others, 1989a, 1991). Sandstone is quartzofeldspathic and micaceous. Contains rare Late Cretaceous foraminifers and mollusks (Vedder and others, 1989a, 1991). Extensive outcrops of unit in the San Rafael Mountains to the southwest of the Nacimiento fault and northeast of the East Huasna fault; scattered exposures west of the East Huasna fault to the West Huasna fault. In part equivalent to the Cachuma Formation of Dibblee (1991); sandstone petrofacies are comparable to rocks in the upper part of the Great Valley Sequence in central California (MacKinnon, 1978). Vedder and Stanley (2001) report thickness is unknown but possibly as much as 2,300 m to the east of the map area

KJe **Espada Formation (Lower Cretaceous and Upper Jurassic)**—Dark greenish-brown, well-bedded argillaceous silty to sandy shale and thin interbeds of fine-grained sandstone (Dibblee, 1950). Local thin lenses of pebble to cobble conglomerate with clasts of quartzite, chert, and volcanic clasts. Deep marine, submarine fan deposits. Sandstone

petrofacies are comparable to rocks in the lower part of the Great Valley Sequence in central California (MacKinnon, 1978; Dickinson, 1995).

Occurs in the Santa Ynez Mountains to the south of the Santa Ynez River fault and in the San Rafael Mountains to the northeast of the Camuesa fault; also includes rocks mapped as Knoxville Formation in vicinity of Point Sal (Woodring and Bramlette, 1950). Thickness 1,200 m in the western Santa Ynez Mountains but as thick as 2,100 m in the southern San Rafael Mountains (Vedder and others, 1982; Dibblee, 1991; McLean and Stanley, 1994). Unconformably overlies Honda Formation in the western part of the Santa Rosa Hills domain in the extreme western Santa Ynez Mountains; disconformably overlies ophiolitic rocks at Point Sal and in the southern San Rafael Mountains. Locally, conformably overlain by Upper Cretaceous sandstones of the Jalama Formation in Nojoqui Creek and Upper Cretaceous sandstones in the San Rafael Mountains; elsewhere, unconformably overlain by younger strata.

Age of the lower part of the Espada Formation based on the identification of pelecypod macrofossils *Buchia piochii* and *Buchia crassicollis* to the east of the map area (Dibblee, 1966)

KJh **Honda Formation (Lower Cretaceous and Upper Jurassic)**—Dark greenish-brown clay shale containing calcareous concretions and local thin beds of fine-grained sandstone. Marine. Shale is poorly bedded and intensely sheared. Exposed only in the western part of the Santa Rosa Hills domain in the extreme western Santa Ynez Mountains; exposed thickness 460 m (Dibblee, 1950; Vedder and others, 1982). Base not exposed, unconformably overlain by Espada Formation (Dibblee, 1950). Sandstone petrofacies are comparable to rocks in the lower part of the Great Valley Sequence in central California (MacKinnon, 1978; McLean and Stanley, 1994).

Tentatively assigned a Jurassic age by Dibblee (1950) based on the presence of a small, indeterminate species of *Aucella*. However, lithologic similarity to Espada Formation and rocks mapped as Knoxville Formation near Point Sal (Woodring and Bramlette, 1950) suggest that the Honda Formation may be Late Jurassic to Early Cretaceous, overlapping in age with occurrences of the Espada Formation distant from the western Santa Ynez Mountains (Vedder and others, 1982; McLean, 1991)

Kcn **Unnamed conglomerate (Upper Cretaceous)**—Nonmarine pebble to boulder conglomerate with subordinate sandstone and mudstone. Conglomerate is massive to thick-bedded, poorly sorted, and interbedded with lenticular yellowish-gray sandstones. Conglomerate is channeled at base and internally. Clasts are rounded, imbricated, predominantly porphyritic siliceous volcanic rock, with common clasts of granite and quartzite (Vedder and others, 1991, 1994). Non-fossiliferous; correlated with Upper Cretaceous marine sandstones based on stratigraphic position and possible interfingering relations (Vedder and others, 1977). Occurs in the San Rafael Mountains immediately southwest of the Nacimiento fault (Vedder and others, 1991, 1994)

Kuc **Unnamed conglomerate (lowermost Upper Cretaceous; Cenomanian)**—Pebble to boulder conglomerate, thick-bedded to massive. Clasts are predominantly mafic volcanic rocks set in a matrix of clayey sandstone (Vedder and others, 1967; McLean and others, 1977). Unit is lens shaped, thickening southeastward to as much as 650 m (McLean and others, 1977). Age based on presence of Cenomanian marine macrofossils (McLean and others, 1977)

MESOZOIC MELANGE, SERPENTINITE, AND OPHIOLITIC ROCKS

Franciscan Complex (Cretaceous and Jurassic)—Divided into:

KJf **Franciscan Complex (Cretaceous and Jurassic)**—Tectonic mélange containing chaotic assemblage of tectonic blocks of graywacke, chert, metavolcanic rocks, greenstone, blueschist, serpentinite, and other rock types in a matrix of pervasively sheared shale, sandstone, and serpentinite (Wahl, 1998). Exposed to the west of the West Huasna fault near Twitchell Reservoir and along the Little Pine fault northwest of Zaca Ridge and known from drill-hole data to underlie much of Santa Maria and Huasna domains (McLean, 1991; Sweetkind and others, 2010). Near Twitchell Reservoir, blocks of gray-

wacke or chert within Franciscan Complex large enough to be portrayed on the map are shown as separately mapped units. Thickness unknown. Limited fossil evidence suggest age range from Jurassic to Cretaceous (Pessagno, 1977; Wahl, 1998)

KJfc **Chert blocks (Cretaceous and Jurassic)**—Blocks of chert within Franciscan Complex large enough (at least 100 m x 100 m) to be portrayed on the map

KJfg **Graywacke blocks (Cretaceous and Jurassic)**—Blocks of graywacke within Franciscan Complex large enough (at least 100 m x 100 m) to be portrayed on the map

KJs **Serpentinite (Cretaceous? and Jurassic)**—Serpentinized mantle peridotite and serpentinite matrix. Forms bands within the tectonic mélange of the Franciscan Complex or along faults; interpreted to be mobilized during tectonism and structurally emplaced (Wahl, 1998)

Jo **Ophiolite (Upper Jurassic; Callovian)**—Pillow basalt, greenstone, diabase dikes and sills, gabbro, diorite, plagiogranite, and ultramafic rocks, including serpentinite, harzburgite, and pyroxenite (Hopson and others, 1975, 2008; Hopson and Frano, 1977). At Point Sal, rocks form an ophiolitic sequence that represents an approximately 3-km thickness of oceanic crust, including a 1.3-km thick volcanic section of massive and pillowed submarine basaltic lavas underlain by a sheeted dike or sill complex, a 1-km thick plutonic member of diorite and gabbro, and a basal member of ultramafic rocks (Hopson and Frano, 1977; Hopson and others, 2008). Hopson and others (2008) reported a CA-TIMS age from zircon 165.48±0.13 Ma for plagiogranite within the ophiolite at Point Sal. Unit also includes massive diabase and serpentinite diabase that underlie Espada Formation to the northeast of the Cachuma fault in the San Rafael Mountains (Dibblee, 1994c) and in Tepusquet Canyon (Dibblee, 1994b). Age of these ophiolitic remnants and relation to ophiolite at Point Sal is not determined

References Cited

Addicott, W.O., and Galehouse, J.S., 1973, Pliocene marine fossils in the Paso Robles Formation, California: Journal of Research of the U.S. Geological Survey, v. 5, no. 1, p. 509–514. [Also available at https://pubs.usgs.gov/journal/1973/vol1issue5/report.pdf.]

Almgren, A.A., 1973, Upper Cretaceous foraminifera in southern California, *in* Dibblee, T.W., Jr., ed., Cretaceous stratigraphy of the Santa Monica Mountains and Simi Hills—Pacific Section, Society of Economic Paleontologists and Mineralogists Guidebook for Field Trip, Fall 1973 p. 31–44.

Almgren, A.A., Filewicz, M.V., and Heitman, H.L., 1988, Lower Tertiary foraminiferal and calcareous nannofossil zonation of California—An overview and recommendation, *in* Filewicz, M.V., and Squires, R.L., eds., Paleogene Stratigraphy, West Coast of North America, West Coast Paleogene Symposium: Society of Economic Paleontologists and Mineralogists Pacific Section, v. 58, p. 83–105. [Also available at https://archives.datapages.com/data/pac_sepm/075/075001/pdfs/83.pdf.]

American Association of Petroleum Geologists, 1959, Correlation section across Santa Maria basin from Cretaceous outcrop in Santa Ynez Mountains northerly to Franciscan outcrop north of Santa Maria River, California: Pacific Section, American Association of Petroleum Geologists, Correlation Section 12, scales 1:12,000 and 1:48,000. [Also available at https://www.psaapg.org/cross-sections/.]

Arends, R.G., and Blake, G.H., 1986, Biostratigraphy and paleontology of the Naples Bluff coastal section based on diatoms and benthic foraminifera, *in* Casey, R.E., and Barron, J.A., eds., Siliceous microfossils and microplankton—Studies of the Monterey Formation and modern analogs: Tulsa, Okla., Pacific Section Society of Economic Paleontologists and Mineralogists Special Publication, p. 121–135. [Also available at https://archives.dataages.com/data/pac_sepm/061/061001/pdfs/121.pdf.]

Arnold, R., and Anderson, R., 1907, Geology and oil resources of the Santa Maria oil district, Santa Barbara California: U.S. Geological Survey Bulletin 322, 161 p. [Also available at https://doi.org/10.3133/b322.]

Bailey, T.L., 1947, Origin and migration of oil into Sespe redbeds, California: The American Association of Petroleum Geologists Bulletin, v. 31, p. 1913–1935. [Also available at https://archives.datapages.com/data/bulletns/1944-48/images/pg/00310011/1900/19130.pdf.]

Bailey, T.L., 1952, Review of geology of southwestern Santa Barbara County, California by T.W. Dibblee: The American Association of Petroleum Geologists Bulletin, v. 36, no. 1, p. 176–178.

Ballance, P.F., Howell, D.G., and Ort, K., 1983, Late Cenozoic wrench tectonics along the Nacimiento, South Cuyama, and La Panza faults, California, indicated by depositional history of the Simmler Formation, *in* Andersen, D.W., and Rymer, M.J., eds., Tectonics and sedimentation along faults of the San Andreas system: Tulsa, Okla., Pacific Section of Society for Sedimentary Geology, p. 1–9. [Also available at https://archives.datapages.com/data/pac_sepm/045/045001/pdfs/1.htm.]

Bandy, O.L., and Kolpack, R.L., 1963, Foraminiferal and sedimentological trends in the Tertiary section of Tecolote tunnel, California: Micropaleontology, v. 9, no. 2, p. 117–170. [Also available at https://doi.org/10.2307/1484566.]

Baranov, V.I., 1957, A new method for interpretation of aeromagnetic maps—Pseudo-gravimetric anomalies: Geophysics, v. 22, no. 2, p. 359–383. [Also available at https://doi.org/10.1190/1.1438369.]

Barron, J.A., and Ramirez, P.C., 1992, Diatom stratigraphy of selected Sisquoc Formation sections, Santa Maria basin, California: U.S. Geological Survey Open-File Report 92–197, 23 p. [Also available at https://doi.org/10.3133/ofr92197.]

Behl, R.J., 1998, Relationships between silica diagenesis, deformation, and fluid flow in Monterey Formation cherts, Santa Maria basin, *in* Eichhubl, P., ed., Diagenesis, deformation, and fluid flow in the Miocene Monterey Formation—Tulsa, Okla., Pacific Section, Society for Sedimentary Geology Special Publication 83: California, p. 77–83. [Also available at https://archives.datapages.com/data/pac_sepm/101/101001/pdfs/77.htm.]

Behl, R.J., 1999, Since Bramlette (1946)—The Miocene Monterey Formation of California revisited, *in* Moores, E.M., Sloan, D., and Stout, D.L., eds., Classic cordilleran concepts—A View from California—Boulder, Colo: Geological Society of America Special Paper 338, 489 p. [Also available at https://doi.org/10.1130/0-8137-2338-8.301.]

Behl, R.J., and Garrison, R.E., 1994, The origin of chert in the Monterey Formation of California (USA), *in* Iijima, A., Abed, A., and Garrison, R., eds., Siliceous, phosphatic and glauconitic sediments of the Tertiary and Mesozoic, Proceedings of the 29th International Geological Congress, Part C, August 23–September 3, 1992: Utrecht, The Netherlands, VSP, p. 101–132.

Behl, R.J., and Ingle, J.C., Jr., 1998, The Sisquoc-Foxen Mudstone boundary in the Santa Maria basin, California—Sedimentary response to the new tectonic regime, chap V *of* Keller, M.A., ed., Evolution of sedimentary basins/onshore oil and gas investigations—Santa Maria Province: U.S. Geological Survey Bulletin 1995–V, 16 p. [Also available at https://doi.org/10.3133/b1995TUV.]

Behl, R.J., and Ramirez, P.C., 2000, Field guide to the geology of the Neogene Santa Maria basin—From Rift to Uplift: Pacific Section Society for Sedimentary Geology, book 86, p. 1–31. [Also available at https://archives.datapages.com/data/pac_sepm/104/104001/pdfs/i.pdf.]

Beyer, L.A., 1980, Offshore southern California, *in* Oliver, H.W., ed., Interpretation of the gravity map of California and its continental margin—California Division of Mines and Geology Bulletin 205 p. 8–15. [Also available at https://www.conservation.ca.gov/cgs/Pages/Publications/statewide_references.aspx.]

Beyer, L.A., Robbins, S.L., and Clutson, F.G., 1985, Basic data and preliminary density and porosity profiles for twelve borehole gravity surveys made in the Los Angeles, San Joaquin, Santa Maria, and Ventura basins, California: U.S. Geological Survey Open-File Report 85–42, 69 p. [Also available at https://doi.org/10.3133/ofr8542.]

Birkeland, P.W., 1999, Soils and Geomorphology 3rd ed.: New York, Oxford University Press, 430 p.

Birkeland, P.W., Machette, M.N., and Haller, K.M., 1991, Soils as a tool for applied Quaternary geology: Utah Geological and Mineral Survey, Miscellaneous Publication 91–3, 63 p. [Also available at https://ugspub.nr.utah.gov/publications/misc_pubs/MP-91-3.pdf.]

Blake, T.F., 1982, Depositional environments of the Simmler Formation in southern Cuyama Valley, Santa Barbara & Ventura Counties, California, *in* Ingersoll, R.V., and Woodburne, M.O., eds., Cenozoic non-marine deposits of California and Arizona: Tulsa, Okla., Pacific Section Society of Economic Paleontologists and Mineralogists, p. 35–50. [Also available at https://archives.datapages.com/data/pac_sepm/037/037001/pdfs/35.pdf.]

Blakely, R.J., 1995, Potential theory in gravity and magnetic applications: Cambridge, U.K., Cambridge University Press, 441 p. [Also available at https://doi.org/10.1017/CBO9780511549816.]

Blakely, R.J., and Simpson, R.W., 1986, Approximating edges of source bodies from magnetic or gravity anomalies: Geophysics, v. 51, p. 1494–1498. [Also available at https://doi.org/10.1190/1.1442197.]

Bottjer, D.J., and Link, M.H., 1984, A synthesis of Late Cretaceous southern California and northern Baja California paleogeography, *in* Crouch, J.K., and Bachman, S.B., eds., Tectonics and sedimentation along the California margin—Pacific Section v. 38: Los Angeles, Calif., Society of Economic Paleontologists and Mineralogists, p. 171–188. [Also available at https://archives.datapages.com/data/pac_sepm/054/054001/pdfs/171.pdf.]

Bramlette, M.N., 1946, The Monterey Formation and the origin of its siliceous rocks: U.S. Geological Survey Professional Paper 212, 57 p. [Also available at https://doi.org/10.3133/pp212.]

Browning, J.V.B., 1983, Paleoecology and paleoenvironments of the Jalama Formation (Upper Cretaceous), western Santa Ynez Mountains, California: Los Angeles Calif., University of Southern California, M.S. thesis, 204 p. [Also available from the University of Southern California Libraries at http://digitallibrary.usc.edu/cdm/ref/collection/p15799coll30/id/121207.]

Byrd, J.O.D., 1983, Geology of the Alisal Ranch area, south of Solvang, Santa Barbara County, California: Santa Barbara, Calif., University of California, M.A. thesis, 169 p. [Also available through the University of California Santa Barbara Library, call number QE47.3.C2 S25 BYRD 1983.]

California Department of Conservation, 1992, California oil and gas fields, volume II *in* Southern, central coastal, and offshore California: California Department of Conservation, Division of Oil, Gas and Geothermal Resources, TR11, v. 2, 645 p. [Also available at ftp://ftp.consrv.ca.gov/pub/oil/publications/Datasheets/Dtasheet_vol_2.pdf.]

California Department of Conservation, 2010, 2009 Annual report of the State oil and gas supervisor: California Department of Conservation, Division of Oil, Gas, and Geothermal Resources, PR06, 267 p., accessed September 2018, at ftp://ftp.consrv.ca.gov/pub/oil/annual_reports/2009/.

Campion, K.M., Morgan, S.R., and Berger, Z., 1988, Recognition of a middle Eocene unconformity in transverse ranges utilizing satellite imagery and high-altitude photography [abs.], American Association of Petroleum Geologists (AAPG)/Society of Economics, Paleontologists, and Mineralogists (SEPM)/Society of Exploration Geophysicists (SEG)/Society of Professional Well Log Analysts (SPWLA) Pacific Section annual convention, Santa Barbara Calif., April 17–19, 1988: The American Association of Petroleum Geologists Bulletin, v. 72, 376 p. [abs.]. [Also available at https://www.searchanddiscovery.com/abstracts/html/1988/sepm/abstracts/0376c.htm.]

Campion, K.M., Sullivan, M.D., May, J.A., and Warme, J.A., 1996, Sequence stratigraphy along a tectonically active margin, Paleogene of southern California, *in* Abbott, P.L., and Cooper, J.D., eds., Field Conference Guidebook and volume for the annual convention, San Diego, Calif, 1996: American Association of Petroleum Geologists and Pacific Section, Society for Sedimentary Geology, v. 80, p. 125–188. [Also available at https://archives.datapages.com/data/pac_sepm/097/097001/pdfs/125.pdf.]

Canfield, C.R., 1939, Subsurface stratigraphy of Santa Maria Valley oil field and adjacent parts of Santa Maria Valley, California: The American Association of Petroleum Geologists Bulletin, v. 23, p. 45–81. [Also available at https://archives.datapages.com/data/bulletns/1938-43/images/pg/00230001/0000/00450.pdf.]

Cannon, M.P., 2012, Cenozoic deformation along the Little Pine fault zone, and implications for the tectonic history of the Santa Maria basin, California, Long Beach, Calif., April 22–25, 2012: Annual convention and exhibition of the American Association of Petroleum Geologists, Search and Discovery Article #90142. [Also available at https://www.searchanddiscovery.com/abstracts/html/2012/90142ace/abstracts/cann.htm.]

Cannon, M.P., 2013, Cenozoic kinematics of the Little Pine fault zone, Santa Maria basin, California: Long Beach, Calif., California State University, M.S. thesis, 94 p. [Also available through the University of California Long Beach Library, OCLC number 1020289479.]

Carson, C.M., 1965, The Rincon Formation, *in* Weaver, D.W., and Dibblee, T.W., Jr., (field trip leaders), Western Santa Ynez Mountains, Santa Barbara County, California—Field trip Guidebook October 16, 1965: Ventura, Calif., Coast Geological Society, Pacific Section, American Association of Petroleum Geologists and Society of Economic Paleontologists and Mineralogists, p. 38–41. [Also available at https://archives.datapages.com/data/pacific/data/013/013001/1_ps0130001.htm.]

Cisowski, S.M., and Fuller, M., 1987, The generation of magnetic anomalies by combustion metamorphism of sedimentary rock, and its significance to hydrocarbon exploration: Geological Society of America Bulletin, v. 99, p. 21–29. [Also available at https://doi.org/10.1130/0016-7606(1987)99%3C21:TGOMAB%3E2.0.CO;2.]

Clark, D.G., 1990, Late Quaternary tectonic deformation in the Casmalia range, coastal south-central California, *in* Lettis, W.R., Hanson, K.L., Kelson, K.I., and Wesling, J.R., eds., Neotectonics of south-central coastal California, Sept. 21–23, 1990: Friends of the Pleistocene, Pacific Cell 1990 Fall Field Trip Guidebook, p. 349–383. [Also available at http://www.fop.cascadiageo.org/?page_id=550.]

Cole, R.B., and Stanley, R.G., 1994, Sedimentology of subaqueous volcaniclastic sediment gravity flows in the Neogene Santa Maria basin, California: Sedimentology, v. 41, p. 37–54. [Also available at https://doi.org/10.1111/j.1365-3091.1994.tb01391.x.]

Cole, R.B., and Stanley, R.G., 1998, Volcanic rocks of the Santa Maria province, California, chap. *R of* Evolution of sedimentary basins/onshore oil and gas investigations: U.S. Geological Survey Bulletin 1995–R, p. R1–R35. [Also available at https://doi.org/10.3133/b1995RS.]

Cooper, W.S., 1967, Coastal Dunes of California—Boulder, Colo: Geological Society of America Memoir 104, 131 p.

Cordell, L., and Grauch, V.J.S., 1985, Mapping basement magnetization zones from aeromagnetic data in the San Juan basin, New Mexico, *in* Hinze, W.J., ed., The utility of regional gravity and magnetic anomaly maps: Tulsa, Okla., Society of Exploration Geophysicists, p. 181–192. [Also available at https://doi.org/10.1190/1.0931830346.ch16.]

Crain, W.E., Mero, W.E., and Patterson, D., 1985, Geology of the Point Arguello discovery: The American Association of Petroleum Geologists Bulletin, v. 69, no. 4, p. 537–545. [Also available at https://archives.datapages.com/data/bulletns/1984-85/data/pg/0069/0004/0500/0537.htm.]

Crandall, B.G., 1961, The stratigraphy of the Buckhorn Sandstone, Santa Barbara and San Luis Obispo Counties, California: Los Angeles, Calif., University of California, M.A. thesis, 111 p. [Also available through the UCLA Library at https://catalog.library.ucla.edu/vwebv/holdingsInfo?bibId=4031188.]

Crawford, F.D., 1971, Petroleum potential of Santa Maria Province, California—Region 2, *in* Cram, I.H., ed., Future petroleum provinces of the United States—Their geology and potential—Memoir 15: American Association of Petroleum Geologists, v. 1, p. 316–328. [Also available at https://archives.datapages.com/data/specpubs/basinar1/data/a128/a128/0001/0300/0316.htm.]

Crouch, J.K., Bachman, S.B., and Shay, J.T., 1984, Post-Miocene compressional tectonics along the central California margin, *in* Crouch, J.K., and Bachman, S.B., eds., Tectonics and sedimentation along the California margin: Los Angeles, Calif., Pacific Section, Society of Economic Paleontologists and Mineralogists, p. 37–54. [Also available at https://archives.datapages.com/data/pac_sepm/054/054001/pdfs/37.htm.]

Dailey, D.H., and Popenoe, W.P., 1966, Mollusca from the Upper Cretaceous Jalama Formation, Santa Barbara County v. 65: California, Berkeley, Calif., University of California Press, Publications in Geological Sciences, 41 p.

Dibblee, T.W., Jr., 1950, Geology of southwestern Santa Barbara County, California—Point Arguello, Lompoc, Point Conception, Los Olivos, and Gaviota quadrangles: California Division of Mines and Geology Bulletin 150, 95 p., 17 pls., scale 1:62,500. [Also available from https://ngmdb.usgs.gov/Prodesc/proddesc_87.htm.]

Dibblee, T.W., Jr., 1966, Geology of central Santa Ynez Mountains, Santa Barbara County, California: California Division of Mines and Geology Bulletin 186, 99 p, 4 pls. [Also available at http://pubs.geothermal-library.org/lib/grc/1021056.pdf.]

Dibblee, T.W., Jr., 1981a, Geologic map of the Tajiguas quadrangle, California: U.S. Geological Survey Open-File Report 81–371, scale 1:24,000. [Also available at https://doi.org/10.3133/ofr81371.]

Dibblee, T.W., Jr., 1981b, Geologic map of the Solvang quadrangle, California: U.S. Geological Survey Open-File Report 81–372, scale 1:24,000. [Also available at https://doi.org/10.3133/ofr81372.]

Dibblee, T.W., Jr., 1981c, Geologic map of the Santa Ynez quadrangle, California: U.S. Geological Survey Open-File Report 81–373, scale 1:24,000. [Also available at https://doi.org/10.3133/ofr81373.]

Dibblee, T.W., Jr., 1981d, Geologic map of the Gaviota quadrangle, California: U.S. Geological Survey Open-File Report 81–374, scale 1:24,000. [Also available at https://doi.org/10.3133/ofr81374.]

Dibblee, T.W., Jr., 1982, Geology of the Santa Ynez-Topatopa Mountains, southern California, *in* Fife, D.L., and Minch, J.A., eds., Geology and mineral wealth of the California Transverse Ranges: Santa Ana, Calif., South Coast Geological Society Annual Symposium and Guidebook no. 10, p. 41–56. [Also available at http://www.southcoastgeo.org.unixweb-8.nethere.net/Guidebooks.html.]

Dibblee, T.W., Jr., 1991, Geology of the San Rafael Mountains, Santa Barbara Country (sic), in Lewis, L., and others, eds., Southern Coast Ranges: Santa Ana, Calif., South Coast Geological Society, Inc., Annual Field Trip Guidebook, v. 19, p. 3–31. [Also available at http://www.southcoastgeo.org.unixweb-8.nethere.net/Guidebooks.html.]

Dibblee, T.W., Jr., 1995, Tectonic and depositional environment of the middle and upper Cenozoic sequences of the coastal southern California region, *in* Fritsche, A.E., ed., Cenozoic paleogeography of the western United States—II: Tulsa, Okla., Pacific Section, Society for Sedimentary Geology, v. 75, p. 212–245. [Also available at https://archives.datapages.com/data/pac_sepm/092/092001/pdfs/212.htm.]

Dibblee, T.W., Jr., (Ehrenspeck, H.E., ed.), 1988a, Geologic map of the Lompoc and Surf quadrangles, Santa Barbara County, California: Dibblee Geological Foundation, Map DF–20, scale 1:24000. [Also available at https://ngmdb.usgs.gov/Prodesc/proddesc_202.htm.]

Dibblee, T.W., Jr., (Ehrenspeck, H.E., ed.), 1988b, Geologic map of the Lompoc Hills and Point Conception quadrangles, Santa Barbara County, California: Dibblee Geological Foundation, Map DF2–18, scale 1:24000. [Also available at https://ngmdb.usgs.gov/Prodesc/proddesc_201.htm.]

Dibblee, T.W., Jr., (Ehrenspeck, H.E., ed.), 1988c, Geologic map of the Santa Rosa Hills and Sacate quadrangles, Santa Barbara County, California: Dibblee Geological Foundation, Map DF–17, scale 1:24000. [Also available at https://ngmdb.usgs.gov/Prodesc/proddesc_203.htm.]

Dibblee, T.W., Jr., (Ehrenspeck, H.E., ed.), 1988d, Geologic map of the Santa Ynez and Tajiguas quadrangles, Santa Barbara County, California: Dibblee Geological Foundation, Map DF–15, scale 1:24000. [Also available at https://ngmdb.usgs.gov/Prodesc/proddesc_204.htm.]

Dibblee, T.W., Jr., (Ehrenspeck, H.E., ed.), 1988e, Geologic map of the Solvang and Gaviota quadrangles, Santa Barbara County, California: Dibblee Geological Foundation, Map DF–16, scale 1:24000. [Also available at https://ngmdb.usgs.gov/Prodesc/proddesc_205.htm.]

Dibblee, T.W., Jr., (Ehrenspeck, H.E., ed.), 1988f, Geologic map of the Point Arguello and Tranquillon Mountain quadrangles, Santa Barbara County, California: Dibblee Geological Foundation, Map DF–19, scale 1:24000. [Also available at https://ngmdb.usgs.gov/Prodesc/proddesc_206.htm.]

Dibblee, T.W., Jr., (Ehrenspeck, H.E., ed.), 1989a, Geologic map of the Casmalia and Orcutt quadrangles, Santa Barbara County, California: Dibblee Geological Foundation, Map DF–24, scale 1:24000. [Also available at https://ngmdb.usgs.gov/Prodesc/proddesc_208.htm.]

Dibblee, T.W., Jr., (Ehrenspeck, H.E., ed.), 1989b, Geologic map of the Point Sal and Guadalupe quadrangles, Santa Barbara County, California: Dibblee Geological Foundation, Map DF–25, scale 1:24000. [Also available at https://ngmdb.usgs.gov/Prodesc/proddesc_211.htm.]

Dibblee, T.W., Jr., (Ehrenspeck, H.E., ed.), 1993a, Geologic map of the Los Alamos quadrangle, Santa Barbara County, California: Dibblee Geological Foundation, Map DF–46, scale 1:24000. [Also available at https://ngmdb.usgs.gov/Prodesc/proddesc_228.htm.]

Dibblee, T.W., Jr., (Ehrenspeck, H.E., ed.), 1993b, Geologic map of the Los Olivos quadrangle, Santa Barbara County, California: Dibblee Geological Foundation, Map DF–44, scale 1:24000. [Also available at https://ngmdb.usgs.gov/Prodesc/proddesc_229.htm.]

Dibblee, T.W., Jr., (Ehrenspeck, H.E., ed.), 1993c, Geologic map of the Zaca Creek quadrangle, Santa Barbara County, California: Dibblee Geological Foundation, Map DF–45, scale 1:24000. [Also available at https://ngmdb.usgs.gov/Prodesc/proddesc_230.htm.]

Dibblee, T.W., Jr., (Ehrenspeck, H.E., ed.), 1994a, Geologic map of the Santa Maria and Twitchell Dam quadrangles, Santa Barbara and San Luis Obispo Counties, California: Dibblee Geological Foundation, Map DF–51, scale 1:24000. [Also available at https://ngmdb.usgs.gov/Prodesc/proddesc_71688.htm.]

Dibblee, T.W., Jr., (Ehrenspeck, H.E., ed.), 1994b, Geologic map of the Sisquoc quadrangle, Santa Barbara County, California: Dibblee Geological Foundation, Map DF–53, scale 1:24000. [Also available at https://ngmdb.usgs.gov/Prodesc/proddesc_71685.htm.]

Dibblee, T.W., Jr., (Ehrenspeck, H.E., ed.), 1994c, Geologic map of the Zaca Lake quadrangle, Santa Barbara County, California: Dibblee Geological Foundation, Map DF–55, scale 1:24000. [Also available at https://ngmdb.usgs.gov/Prodesc/proddesc_71689.htm.]

Dibblee, T.W., Jr., (Ehrenspeck, H.E., and Bartlett, W.L. eds.), 1994a, Geologic map of the Foxen Canyon quadrangle, Santa Barbara County, California: Dibblee Geological Foundation, Map DF–54, scale 1:24000. [Also available at https://ngmdb.usgs.gov/Prodesc/proddesc_71687.htm.]

Dibblee, T.W., Jr., (Ehrenspeck, H.E., and Bartlett, W.L. eds.), 1994b, Geologic map of the Tepusquet Canyon quadrangle, Santa Barbara County, California: Dibblee Geological Foundation, Map DF–52, scale 1:24000. [Also available at https://ngmdb.usgs.gov/Prodesc/proddesc_71686.htm.]

Dickinson, W.R., 1979, Dislocation of Paleogene depositional systems by Neogene strike slip in western Transverse Ranges of southern California: Geological Society of America Abstracts with Programs, v. 11, no. 7, 413 p. [abs.].

Dickinson, W.R., 1983, Cretaceous sinistral strike slip along Nacimiento fault in coastal California: The American Association of Petroleum Geologists Bulletin, v. 67, p. 624–645. [Also available at https://archives.datapages.com/data/bulletns/1982-83/data/pg/0067/0004/0600/0624.htm.]

Dickinson, W.R., 1995, Paleogene depositional systems of the western Transverse Ranges and adjacent southernmost Coast Ranges, *in* Fritsche, A.E., ed., Cenozoic paleogeography of the western United States—II: Tulsa, Okla., Pacific Section, Society for Sedimentary Geology, v. 75, p. 53–83. [Also available at https://archives.datapages.com/data/pac_sepm/092/092001/pdfs/53.htm.]

Dickinson, W.R., Ducea, M., Rosenberg, L.I., Greene, H.G., Graham, S.A., Clark, J.C., Weber, G.E., Kidder, S., Ernst, W.G., and Brabb, E.E., 2005, Net dextral slip, Neogene San Gregorio–Hosgri fault zone, coastal California—Geologic evidence and tectonic implications—Boulder, Colo: Geological Society of America Special Paper 391, 43 p. [Also available at https://doi.org/10.1130/0-8137-2391-4.]

Ducea, M.N., Kidder, S., Chesley, J.T., and Saleeby, J.B., 2009, Tectonic underplating of trench sediments beneath magmatic arcs—The central California example: International Geology Review, v. 51, no. 1, p. 1–26. [Also available at https://doi:10.1080/00206810802602767.]

Dumont, M.P., and Barron, J.A., 1995, Diatom biochronology of the Sisquoc Formation in the Santa Maria basin, California, and its paleoceanographic and tectonic implications, chap. K *of* Keller, M., ed., Evolution of sedimentary basins/onshore oil and gas investigations—Santa Maria province: U.S. Geological Survey Bulletin 1995–K, 17 p. [Also available at https://doi.org/10.3133/b1995JK.]

Dunham, J.B., and Blake, G.H., 1987, Guide to coastal outcrops of the Monterey Formation of western Santa Barbara County, California: Los Angeles, Calif., Pacific Section, Society of Economic Paleontologists and Mineralogists, v. 53, 39 p. [Also available at https://archives.datapages.com/data/pac_sepm/072/072001/pdfs/i.htm.]

Dunkel, C.A., 2001, Oil and gas resources in the Pacific outer continental shelf as of January 1, 1999—An expanded update to the 1995 National assessment of United States oil and gas resources: U.S. Department of the Interior, Minerals Management Service, OCS Report MMS 2001–014, 21 p. [Also available at https://www.boem.gov/sites/default/files/uploadedFiles/BOEM/Oil_and_Gas_Energy_Program/Resource_Evaluation/Resource_Assessment/1999OilandGasResourcesinthePOCShelfReport2001-014.pdf.]

Dunkel, C.A., Mayerson, D., and Piper, K.A., 1997, Central California Province, *in* Dunkel, C.A., and Piper, K.A. eds., 1995 National assessment of United States oil and gas resources—Assessment of the Pacific outer continental shelf region: U.S. Department of the Interior, Minerals Management Service, OCS Report MMS 97–0019, p. 51–95. [Also available at https://www.boem.gov/sites/default/files/uploadedFiles/BOEM/Oil_and_Gas_Energy_Program/Resource_Evaluation/Resource_Assessment/1995%20POCS%20Assessment%20MMS97-0019.pdf.]

Edwards, L.N., 1972, Notes on the Vaqueros and Rincon Formations, west-central Santa Ynez Mountains, *in* Weaver, D.W., ed., Central Santa Ynez Mountains, Santa Barbara County, California: American Association of Petroleum Geologists and Pacific Section, Society for Sedimentary Geology, p. 46–84. [Also available at https://archives.datapages.com/data/pac_sepm/013/013001/pdfs/46.htm.]

Finger, K.L., 1983, Ostracoda from the lower Rincon Formation (Oligo-Miocene) of southern California: Micropaleontology, v. 29, p. 78–109. [Also available at https://doi.org/10.2307/1485653.]

Finger, K.L., 1995, Recognition of middle Miocene foraminifers in highly indurated rocks of the Monterey Formation, coastal Santa Maria Province, central California, chap. L *of* Keller, M.A., ed., Evolution of sedimentary basins/onshore oil and gas investigations—Santa Maria Province: U.S. Geological Survey Bulletin 1995–L, 30 p., 46 pls. [Also available at https://doi.org/10.3133/b1995L.]

Frizzell, V.A., Jr., and Vedder, J.G., 1986, Geologic map of roadless areas and the Santa Lucia Wilderness in the Los Padres National Forest, southwestern California: U.S. Geological Survey Miscellaneous Field Studies Map MF–1655–A, scale 1:250,000, 16 p. [Also available at https://doi.org/10.3133/mf1655A.]

Gibson, J.M., 1972, The Anita Formation and "Sierra Blanca Limestone" (Paleocene-early Eocene), western Santa Ynez Mountains, Santa Barbara County, California, *in* Weaver, D.W. (field trip leader), Central Santa Ynez Mountains, Santa Barbara County: California, American Association of Petroleum Geologists and Pacific Section, Society of Economic Paleontologists and Mineralogists, Spring Field Trip Guidebook, p. 16–19. [Also available at https://archives.datapages.com/data/pac_sepm/013/013001/pdfs/16.htm.]

Gradstein, F.M., Ogg, J.G., Schmitz, M.D., and Ogg, G.M., eds., 2012, The geologic time scale 2012: Oxford, U.K., Elsevier, 1,144 p.

Graham, S.A., and Dickinson, W.R., 1978, Evidence for 115 kilometers of right slip on the San Gregorio–Hosgri fault trend: Science, v. 199, no. 4325, p. 179–181. [Also available at https://doi.org/10.1126/science.199.4325.179.]

Grauch, V.J.S., and Cordell, L., 1987, Limitations of determining density or magnetic boundaries from the horizontal gradient of gravity or pseudogravity data: Geophysics, v. 52, no. 1, p. 118–121. [Also available at https://doi.org/10.1190/1.1442236.]

Gray, L.D., 1980, Geology of Mesozoic basement rocks in the Santa Maria basin, Santa Barbara and San Luis Obispo Counties, California: San Diego, Calif., San Diego State University, M.S. thesis, 78 p. [Also available from the San Diego State University Library, OCLC number 941981513.]

Guptill, P.D., Heath, E.G., and Brogan, G.E., 1981, Surface fault traces and historical earthquake effects near Los Alamos Valley, Santa Barbara County, California: U.S. Geological Survey Open-File Report 81–271, 56 p., 14 pls. [Also available at https://doi.org/10.3133/ofr81271.]

Hall, C.A., Jr., 1975, San Simeon-Hosgri fault system, coastal California—Economic and environmental implications: Science, v. 190, no. 4221, p. 1291–1294. [Also available at https://doi.org/10.1126/science.190.4221.1291.]

Hall, C.A., Jr., 1978, Geologic map of Twitchell Dam, parts of Santa Maria and Tepusquet Canyon quadrangles, Santa Barbara, County, California: U.S. Geological Survey Miscellaneous Field Studies MF–933, scale 1:24,000. [Also available at https://doi.org/10.3133/mf933.]

Hall, C.A., Jr., 1981a, Map of geology along the Little Pine fault, parts of the Sisquoc, Foxen Canyon, Zaca Lake, Bald Mountain, Los Olivos, and Figueroa Mountain quadrangles, Santa Barbara County, California: U.S. Geological Survey Miscellaneous Field Studies Map MF–1285, scale 1:24,000. [Also available at https://doi.org/10.3133/mf1285.]

Hall, C.A., Jr., 1981b, San Luis Obispo transform fault and middle Miocene rotation of the western Transverse Ranges, California: Journal of Geophysical Research. Solid Earth, v. 86, no. B2, p. 1015–1031. [Also available at https://doi.org/10.1029/JB086iB02p01015.]

Hall, C.A., Jr., 1982, Pre-Monterey subcrop and structure contour maps, western San Luis Obispo and Santa Barbara Counties, south-central California: U.S. Geological Survey Miscellaneous Field Studies Map MF–1384, 28 p., 6 sheets, scale 1:62,500. [Also available at https://doi.org/10.3133/mf1384.]

Hall, C.A., Jr., 1991, Geology of the Point Sur–Lopez Point region, Coast Ranges, California—A part of the southern California allochthon: Geological Society of America Special Paper 266, 40 p. [Also available at https://doi.org/10.1130/SPE266-p1.]

Hall, C.A., and Corbató, C.E., 1967, Stratigraphy and structure of Mesozoic and Cenozoic rocks, Nipomo quadrangle, Southern Coast Ranges, California: Geological Society of America Bulletin, v. 78, p. 559–582. [Also available at https://doi.org/10.1130/0016-7606(1967)78[559:SASOMA]2.0.CO;2.]

Hall, C.A., Jr., Sutherland, M.J., and Ingersoll, R.V., 1995, Miocene paleogeography of the west-central California—Offset along the San Gregorio-Hosgri fault zone, *in* Fritsche, A.E., ed., Cenozoic Paleography of the Western United States—II—Pacific Section, Society for Sedimentary Geology, v. 75, p. 85–112. [Also available at https://archives.datapages.com/data/pac_sepm/092/092001/pdfs/85.htm.]

Hall, C.A., and Saleeby, J.B., 2013, Salinia revisited—A crystalline nappe sequence lying above the Nacimiento fault and dispersed along the San Andreas fault system, central California: International Geology Review, v. 55, no. 13, p. 1575–1615. [Also available at https://doi.org/10.1080/00206814.2013.825141.]

Henderson, N.C., Jr., and Ramirez, P.C., 1990, Control exerted by lithologic variations and pebbly units on petroleum occurrences in the Pliocene upper Sisquoc Formation, Casmalia Hills, Santa Maria basin, California, *in* Keller, M.A., and McGowen, M.K., eds., Miocene and Oligocene petroleum reservoirs of the Santa Maria and Santa Barbara basins: California, Pacific Section, Society of Economic Paleontologists and Mineralogists, Core Workshop Notes, p. 339–400. [Also available at https://doi.org/10.2110/cor.90.14.0339.]

Heiskanen, W.A., and Vening-Meinesz, F.A., 1958, The Earth and its gravity field: New York, McGraw-Hill Book Company, Inc., 470 p.

Hopson, C.A., and Frano, C.J., 1977, Igneous history of the Point Sal ophiolite, southern California, *in* Coleman, R.G., and Irwin, W.P., eds., North American ophiolites—Oregon Department of Geology and Mineral Industries Bulletin 95 p. 161–183. [Also available at https://www.oregongeology.org/pubs/B/B-095.pdf.]

Hopson, C.A., Frano, C.J., Pessagno, E.A., Jr., and Mattinson, J.M., 1975, Preliminary report and geologic guide to the Jurassic ophiolite near Point Sal, southern California coast: Geological Society of America, Cordilleran Section Field Trip Guidebook, v. 5, 36 p.

Hopson, C.A., Mattinson, J.M., Pessagno, E.A., Jr., and Luyendyk, B.P., 2008, California Coast Range ophiolite—Composite Middle and Late Jurassic oceanic lithosphere, *in* Wright, J.E., and Shervais, J.W., eds., Ophiolites, arcs, and batholiths—A Tribute to Cliff Hopson: Geological Society of America Special Paper 438, p. 1–101. [Also available at https://doi.org/10.1130/2008.2438(01).]

Hornaday, G.R., 1961, Foraminifera from the Sacate Formation south of Refugio Pass, Santa Barbara County, California—Berkeley, Calif., University of California Press: University of California Publications in Geological Sciences, v. 37, p. 165–232.

Hornaday, G.R., 1965, An Eocene foraminiferal faunule from the northwestern Santa Ynez Mountains, California—Lawrence, Kan: Cushman Foundation for Foraminiferal Research Inc., v. 16, no. 1, p. 29–39.

Hornaday, G.R., and Phillips, F.J., 1972, Paleogene correlations, Santa Barbara area, California—An alternative view, *in* Weaver, D.W., ed., Central Santa Ynez Mountains, Santa Barbara County, California, spring field trip, June 2, 1972: American Association of Petroleum Geologists and Pacific Section, Society for Sedimentary Geology Guidebook, p. 59–71. [Also available at https://archives.datapages.com/data/pac_sepm/013/013001/pdfs/59.htm.]

Hornafius, J.S., 1985, Neogene tectonic rotation of the Santa Ynez Range, western Transverse Ranges, California, suggested by paleomagnetic investigation of the Monterey Formation: Journal of Geophysical Research, v. 90, p. 12503–12522. [Also available at https://doi.org/10.1029/JB090iB14p12503.]

Hornafius, J.S., Grivetti, M.C., and Lagle, C.W., 1982, Structure and stratigraphy of the Monterey Formation near Point Pedernales, Santa Barbara County, California, *in* Fife, D.L., and Minch, J.A., eds., Geology and Mineral Wealth of the California Transverse Ranges—Mason Hill volume: Santa Ana, Calif., South Coast Geological Society, p. 331–336.

Hornafius, J.S., Luyendyk, B.P., Terres, R.R., and Kamerling, M.J., 1986, Timing and extent of Neogene tectonic rotation in the western Transverse Ranges, California: Geological Society of America Bulletin, v. 97, p. 1476–1487. [Also available at https://doi.org/10.1130/0016-7606(1986)97%3C1476:TAEONT%3E2.0.CO;2.]

Hoskins, E.G., and Griffiths, J.R., 1971, Hydrocarbon potential of northern and central California offshore, *in* Cram, I.H., ed., Future petroleum provinces of the United States—Their geology and potential, American Association of Petroleum, v. 1, no. 15, p. 212–228. [Also available at https://archives.datapages.com/data/specpubs/basinar1/data/a128/a128/0001/0200/0212.htm.]

Howard, J.L., 1988, Sedimentation of the Sespe Formation in southern California, *in* Sylvester, A.G., and Brown, G.C., eds., Santa Barbara and Ventura basins; Tectonics, structure, sedimentation, and oilfields along an east-west transect: Ventura, Calif., Coast Geological Society, v. 64, p. 53–70. [Also available at https://archives.datapages.com/data/pacific/data/078/078001/53_ps0780053.htm.]

Howard, J.L., 1995, Upper Paleogene conglomerates of the Sespe Formation along the Santa Ynez fault—Implications for the geologic history of the eastern Santa Maria basin area, California, chap. H *of* Keller, M.A., ed., Evolution of sedimentary basins/onshore oil and gas investigations Santa Maria province: U.S. Geological Survey Bulletin 1995–H, 37 p. [Also available at https://doi.org/10.3133/b1995HI.]

Howell, D.G., Vedder, J.G., McLean, H., Joyce, J.M., Clarke, S.H., Jr., and Smith, G., 1977, Review of Cretaceous geology, Salinian and Nacimiento blocks, Coast Ranges of central California, *in* Howell, D.G., Vedder, J.G., and McDougall, K., eds., Cretaceous geology of the California Coast Ranges west of the San Andreas Fault—Pacific Section, Society for Sedimentary Geology, Pacific Coast Paleogeography Field Guide 2 p. 1–46. [Also available at https://archives.datapages.com/data/pac_sepm/158/158001/pdfs/1.htm.]

Ingle, J.C., Jr., 1985, Paleobathymetric, paleoceanographic, and biostratigraphic studies, *in* Garrison, R.E., Hurst, R.W., Ingle, J., and Kastner, M., eds., The geochemical and paleoenvironmental history of the Monterey Formation—Sediments and hydrocarbons—Data synthesis and text: Canoga Park, Calif., Global Geochemistry Corporation, p. 88–161. [Also available at https://archives.datapages.com/data/pacific/data/060/060001/1_ps0600001.htm.]

Isaacs, C.M., 1980, Diagenesis in the Monterey Formation examined laterally along the Santa Barbara coast, California: U.S. Geological Survey Open-File Report 80–606, 343 p. [Also available at https://doi.org/10.3133/ofr80606.]

Isaacs, C.M., 1983, Compositional variation and sequence in the Miocene Monterey Formation, Santa Barbara coastal area, California, *in* Larue, D.K., and Steel, R.J., eds., Cenozoic Marine Sedimentation, Pacific margin: U.S.A., Pacific Section, Society for Sedimentary Geology, p. 117–132. [Also available at https://archives.datapages.com/data/pac_sepm/044/044001/pdfs/117.htm.]

Jacobson, C.E., Grove, M., Pedrick, J.N., Barth, A.P., Marsaglia, K.M., Gehrels, G.E., and Nourse, J.A., 2011, Late Cretaceous-early Cenozoic tectonic evolution of the southern California margin inferred from provenance of trench and forearc sediments: Geological Society of America Bulletin, v. 123, p. 485–506. [Also available at https://doi.org/10.1130/B30238.1.]

Jachens, R.C., and Griscom, A., 1985, An isostatic residual gravity map of California—A residual map for interpretation of anomalies from intracrustal sources, *in* Hinze, W.J., ed., The utility of regional gravity and magnetic maps: Tulsa, Okla., Society of Exploration Geophysicists, p. 347–360. [Also available at https://doi.org/10.1190/1.0931830346.ch27.]

Jenkins, D., 1982, Diatomaceous earth operations, Grefco Inc., Lompoc, California, *in* Fife, D.L., and Minch, J.A., eds., Geology and mineral wealth of the California Transverse Ranges—Mason Hill volume: Los Angeles, Calif., South Coast Geological Society, p. 513–515.

Jennings, C.W., 1959, Geologic map of California, Santa Maria sheet: California Division of Mines and Geology, scale 1:250,000. [Also available at https://ngmdb.usgs.gov/Prodesc/proddesc_329.htm.]

Jennings, C.W., Strand, R.G., Rogers, T.H., Boylan, R.T., Moar, R.R., and Switzer, R.A., 1977, Geologic map of California: California Department of Conservation, Division of Mines and Geology, no. 2, scale 1:750,000. [Also available at https://ngmdb.usgs.gov/Prodesc/proddesc_16320.htm.]

Johnson, S.Y., and Stanley, R.G., 1994, Sedimentology of the conglomeratic lower member of the Lospe Formation (lower Miocene), Santa Maria basin, California, chap. D *of* Keller, M.A., ed., Evolution of sedimentary basins/onshore oil and gas investigations—Santa Maria Province: U.S. Geological Survey Bulletin 1995–D, 28 p. [Also available at https://doi.org/10.3133/b1995DE.]

Johnson, S.Y., and Watt, J.T., 2012, Influence of fault trend, bends, and convergence on shallow structure and geomorphology of the Hosgri strike-slip fault, offshore central California: Geosphere, v. 8, p. 1632–1656. [Also available at https://doi.org/10.1130/GES00830.1.]

Johnson, S.Y., Dartnell, P., Cochrane, G.R., Golden, N.E., Phillips, E.L., Ritchie, A.C., Krigsman, L.M., Dieter, B.E., Conrad, J.E., Greene, H.G., Seitz, G.G., Endris, C.A., Sliter, R.W., Wong, F.L., Erdey, M.D., Gutierrez, C.I., Yoklavich, M.M., East, A.E., and Hart, P.E., (S.Y. Johnson and S.A. Cochran, eds.), 2015, California State Waters Map Series—Offshore of Refugio Beach, California: U.S. Geological Survey Scientific Investigations Map 3319, 11 sheets, scale 1:24,000, 42-p. pamphlet, accessed August 2016, at https://doi.org/10.3133/sim3319.

Johnson, S.Y., Dartnell, P., Cochrane, G.R., Hartwell, S.R., Golden, N.E., Kvitek, R.G., and Davenport, C.W., (S.Y. Johnson and S.A. Cochran, eds.), 2018, California State waters map series—Offshore of Point Conception, California: U.S. Geological Survey Open-File Report 2018–1024, 36 p., 9 sheets, scale 1:24,000, accessed September 2019, at https://doi.org/10.3133/ofr20181024.

Keenan, M.F., 1932, The Eocene Sierra Blanca Limestone at the type locality in Santa Barbara County, California—Transactions: San Diego Society of Natural History, v. 7, no. 8, p. 53–84. [Also available at https://brccapi.sdnhm.org/files/2613/6547/7947/Trans78_1932_Keenan.pdf.]

Kelley, F.R., 1943, Eocene stratigraphy in western Santa Ynez Mountains, Santa Barbara County, California: The American Association of Petroleum Geologists Bulletin, v. 27, p. 1–19. [Also available at https://archives.datapages.com/data/bulletns/1938-43/images/pg/00270001/0000/00010.pdf.]

Keller, M.A., ed., 1995, Evolution of sedimentary basins/onshore oil and gas investigations—Santa Maria Province: U.S. Geological Survey Bulletin 1995, multiple chapters. [Also available at https://doi.org/10.3133/b1995.]

Kellogg, K.S., Minor, S.A., and Cossette, P.M., 2008, Geologic map of the eastern three-quarters of the Cuyama 30'×60' quadrangle, California: U.S. Geological Survey Scientific Investigations Map 3002, 2 pls., scale 1:100,000, 23-p. pamphlet. [Also available at https://doi.org/10.3133/sim3002.]

Kennedy, G.L., Wehmiller, J.F., and Rockwell, T.K., 1992, Paleoecology and paleozoogeography of late Pleistocene marine-terrace faunas of southwestern Santa Barbara County, *in* Fletcher, C.H., III, and Wehmiller, J.F., eds., Quaternary coasts of the United States, marine and lacustrine systems—Broken Arrow, Okla., Society for Sedimentary Geology Special Publication 48: California, p. 343–361. [Also available at https://doi.org/10.2110/pec.92.48.0343.]

Kieniewicz, P.M., and Luyendyk, B.P., 1986, A gravity model of the basement structure in the Santa Maria basin, California: Geophysics, v. 51, p. 1127–1140. [Also available at https://doi.org/10.1190/1.1442167.]

Kitao, E.B., 2018, Determining the relative age and correlation of emergent marine terraces, Vandenberg Air Force Base, Santa Barbara County, California: Northridge Calif., California State University, M.S. thesis, 132 p. [Also available from the California State University Libraries at https://scholarworks.calstate.edu/concern/theses/6h440w79r.]

Kleinpell, R.M., 1938, Miocene stratigraphy of California: Tulsa, Okla., American Association of Petroleum Geologists, 349 p.

Kleinpell, R.M., and Haller, C.R., ed., 1980, The Miocene stratigraphy of California revisited: Tulsa, Okla., American Association of Petroleum Geology Studies, no. 11, 349 p.

Kleinpell, R.M., and Weaver, D.W., 1963, Oligocene biostratigraphy of the Santa Barbara embayment, California: Berkeley, Calif., University of California Publications Geological Sciences, v. 43, p. 1–45, 16 pls.

Knott, J.R., and Eley, D.S., 2006, Early to middle Holocene coastal dune and estuarine deposition, Santa Maria Valley, California: Physical Geography, v. 27, p. 127–136. [Also available at https://doi.org/10.2747/0272-3646.27.2.127.]

Lagoe, M.B., 1987, Middle Cenozoic basin development, Cuyama basin, California, *in* Ingersoll, R.V., and Ernst, W.G., eds., Cenozoic basin development of coastal California, Rubey v. 6: Englewood Cliffs, N.J., Prentice-Hall, p. 172–206.

Laiming, B., 1939, Some foraminiferal correlations in the Eocene of San Joaquin Valley, California: Sixth Pacific Science Conference Proceedings, v. 23, p. 535–638. [Also available at http://archives.datapages.com/data/bulletns/1938-43/data/pg/0023/0012/1850/1880.htm.]

Langenheim, V.E., 2014, Gravity, aeromagnetic and rock-property data of the central California coast ranges: U.S. Geological Survey Open-File Report 2013–1282, 12 p., accessed August 1, 2017, at https://doi.org/10.3133/ofr20131282.

Langenheim, V.E., Halvorsen, P.F., Castellanos, E.L., and Jachens, R.C., 1993, Aeromagnetic map of the southern California borderland east of the Patton Escarpment: U.S. Geological Survey Open-File Report 93–520, 1 pl., scale 1:500,000. [Also available at https://doi.org/10.3133/ofr93520.]

Langenheim, V.E., Hildenbrand, T.G., Jachens, R.C., Campbell, R.H., and Yerkes, R.F., 2006, Aeromagnetic map with geology of the Los Angeles 30′×′60 minute quadrangle, southern California: U.S. Geological Survey Scientific Investigations Map 2950, scale 1:100,000. [Also available at https://doi.org/10.3133/sim2950.]

Langenheim, V.E., Jachens, R.C., Graymer, R.W., Colgan, J.P., Wentworth, C.M., and Stanley, R.G., 2013a, Fault geometry and cumulative offsets in the central Coast Ranges, California—Evidence for northward increasing slip along the San Gregorio-San Simeon-Hosgri fault: Lithosphere, v. 5, p. 29–48. [Also available at https://doi.org/10.1130/L233.1.]

Langenheim, V.E., Jachens, R.C., and Moussaoui, K., 2009, Aeromagnetic survey map of the central California Coast Ranges: U.S. Geological Survey Open-File Report 2009–1044, scale 1:250,000. [Also available at https://pubs.usgs.gov/of/2009/1044.]

Langenheim, V.E., Sweetkind, D.S., Schmidt, K.M., and Matson, G., 2013b, Fault evolution in the onshore Santa Maria basin, California, as inferred from gravity and magnetic anomalies [abs.], *in* 125th anniversary annual meeting Oct. 27–30, 2013, Denver: Geological Society of America Abstracts with Programs, v. 45, no. 7, 375 p., accessed September 30, 2016, at https://gsa.confex.com/gsa/2013AM/webprogram/Paper225922.html.

Lettis, W.R., Hanson, K.L., Unruh, J.R., McLaren, M.K., and Savage, W.U., 2004, Quaternary tectonic setting of south-central coastal California, chap. AA *of* Keller, M.A., ed., Evolution of sedimentary basins/onshore oil and gas investigations—Santa Maria Province: U.S. Geological Survey Bulletin 1995–AA, 21 p., 1 pl., scale 1:250,000. [Also available at https://doi.org/10.3133/b1995AA.]

Levish, D., Ostenaa, D., and O'Connell, D., 1996, Paleohydrologic bounds and the frequency of extreme floods on the Santa Ynez River, California, *in* California Weather Symposium, Theme for 1996, A prehistoric look at California rainfall and floods: Rocklin, Calif., Sierra College Science Center, California Extreme Precipitation Symposium. [Also available at https://cepsym.org/Sympro1996/levish.pdf.]

Link, M.H., 1975, Matilija Sandstone; a transition from deep-water turbidite to shallow-marine deposition in the Eocene of California: Journal of Sedimentary Petrology, v. 45, no. 1, p. 63–78. [Also available at https://doi.org/10.1306/212F6CC6-2B24-11D7-8648000102C1865D.]

Link, M.H., and Welton, J.E., 1982, Sedimentology and reservoir potential of Matilija Sandstone—An Eocene sand-rich deep-sea fan and shallow marine complex, California: The American Association of Petroleum Geologists Bulletin, v. 66, no. 10, p. 1514–1534. [Also available at https://archives.datapages.com/data/bulletns/1982-83/images/pg/00660010/1500/15140.pdf.]

Luyendyk, B.P., 1991, A model for Neogene crustal rotations, transtension, and transpression in southern California: Geological Society of America Bulletin, v. 103, no. 11, p. 1528–1536. [Also available at https://doi.org/10.1130/0016-7606(1991)103<1528:AMFNCR>2.3.CO;2.]

MacKinnon, T.C., 1978, The Great Valley sequence near Santa Barbara, California, *in* Howell, D.G., and McDougall, K.A., eds., Mesozoic paleogeography of the western United States: Society of Economic Paleontologists and Mineralogists, Pacific Section, Pacific Coast Paleogeography Symposium 2, p. 483–491.

Mallory, V.S., 1959, Lower Tertiary biostratigraphy of the California Coast Ranges: Tulsa, Okla., American Association of Petroleum Geologists Bulletin, 416 p. [Also available at https://doi.org/10.1306/SV20351.]

Mallory, V.S., Herlyn, H.T., Jr., Kleinpell, R.M., and Hornaday, G.R., 1998, The Anita Shale and the type Paleocene foraminiferal stages, Santa Barbara County, California, *in* Martin, J.E., ed., Contributions to the paleontology and geology of the West Coast—In honor of V. Standish Mallory: Seattle, Wash., University of Washington Press, no. 6, p. 245–266.

Mattinson, J.M., and Hopson, C.A., 2008, New high-precision CA-TIMS U-Pb zircon plateau ages for the Point Sal and San Simeon ophiolite remnants, California Coast Ranges, *in* Wright, J.E., and Shervais, J.W., eds., Ophiolites, arcs, and batholiths—A tribute to Cliff Hopson—Boulder, Colo: Geological Society of America Special Paper 438, p. 103–112. [Also available at https://doi.org/10.1130/2008.2438(02).]

Mayerson, D., 1997, Santa Maria–Partington basin, *in* Dunkel, C.A., and Piper, K.A., eds., 1995 National assessment of United States oil and gas resources—Assessment of the Pacific outer continental shelf region: U.S. Department of the Interior, Minerals Management Service, Pacific Outer Continental Shelf Region, OCS Report 97–0019, p. 84–95. [Also available at https://www.boem.gov/uploadedFiles/BOEM/Oil_and_Gas_Energy_Program/Resource_Evaluation/Resource_Assessment/1995%20POCS%20Assessment%20MMS97-0019.pdf.]

McCrory, P.A., Wilson, D.S., Ingle, J.C., Jr., and Stanley, R.G., 1995, Neogene geohistory analysis of Santa Maria basin, California, and its relationship to transfer of central California to the Pacific Plate, chap. J *of* Keller, M.A., ed., Evolution of sedimentary basins/onshore oil and gas investigations—Santa Maria Province: U.S. Geological Survey Bulletin 1995–J, 41 p. [Also available at https://doi.org/10.3133/b1995JK.]

McCulloch, D.S., 1989, Geologic map of the south-central California continental margin, map no. 4A (geology), sheet 1 of 4, *in* Greene, H.G. and Kennedy, M.P., eds., California, continental margin geologic map series south-central California continental margin area 4 of 7: California Division of Mines and Geology, California Continental Margin Map CMM4, scale 1:250,000. [Also available at https://www.conservation.ca.gov/cgs/Pages/Publications/Counties/sba.aspx.]

McCulloch, D.S., Beyer, L.A., and Childs, J.R., 1989, Free-air gravity anomaly map of offshore Santa Maria basin, California and adjacent areas: U.S. Geological Survey Open-File Report 89–322, scale 1:250,000. [Also available at https://doi.org/10.3133/sim2950.]

McCulloch, D.S., and Chapman, R.H., 1977, Map showing residual magnetic intensity along the California coast, latitude 37 degrees 30 minutes N. to latitude 34 degrees 30 minutes N.: U.S. Geological Survey Open-File Report 77–079, 14 pls., scale 1:125,000. [Also available at https://doi.org/10.3133/ofr7779.]

McDougall, K., 2008, California Cenozoic Biostratigraphy—Paleogene, chap. 4, *of* Scheirer, A.H., ed., Petroleum systems and geologic assessment of oil and gas in the San Joaquin basin Province, California: U.S. Geological Survey Professional Paper 1713–4, 56 p. [Also available at https://doi.org/10.3133/pp17134.]

McLean, H., 1991, Distribution and juxtaposition of Mesozoic lithotectonic elements in the basement of the Santa Maria basin, California, *in* Keller, M.A., ed., Evolution of sedimentary basins/onshore oil and gas investigations—Santa Maria Province: U.S. Geological Survey Bulletin 1995–B, 12 p. [Also available at https://doi.org/10.3133/b1995B.]

McLean, H., 1993, Miocene lavas constrain right slip movement on the West Huasna fault in San Luis Obispo County to less than 8 km [abs.], Pacific Section Meeting, May 5–7, 1993, Long Beach, Calif.: American Association of Petroleum Geologists, Search and Discovery article #90992, p. 708–709. [Available at https://www.seahanddiscvery.com/abstracts/html/1993/pacific/abstracts/0708c.htm.]

McLean, H., Howell, D.G., and Vedder, J.G., 1977, An unusual Upper Cretaceous conglomerate in the central San Rafael Mountains, Santa Barbara County, California, *in* Howell, D.G., Vedder, J.G., and McDougall, K., eds., Cretaceous geology of the California Coast Ranges west of the San Andreas Fault: Pacific Section, Society for Sedimentary Geology Pacific Coast Paleogeography, v. 2, p. 79–83. [Also available at http://archives.datapages.com/data/pac_sepm/158/158001/pdfs/79.htm.]

McLean, H., and Stanley, R.G., 1994, Provenance of sandstone clasts in the lower Miocene Lospe Formation near Point Sal, California, chap. E *of* Keller, M.A., ed., Evolution of sedimentary basins/onshore oil and gas investigations—Santa Maria Province: U.S. Geological Survey Bulletin 1995–E, 7 p. [Also available at https://doi.org/10.3133/b1995DE.]

Miles, G.A., and Rigsby, C.A., 1990, Geology of the Vaqueros Formation at Hondo Field, Santa Barbara, County, California, *in* Keller, M.A. and McGowen, M.K., eds., Miocene and Oligocene petroleum reservoirs of the Santa Maria and Santa Barbara-Ventura basins, California: Broken Arrow, Okla., Society for Sedimentary Geology Core Workshop, v. 14, p. 39–87.

Minor, S.A., Kellogg, K.S., Stanley, R.G., Gurrola, L.D., Keller, E.A., and Brandt, T.R., 2009, Geologic map of the Santa Barbara coastal plain area, Santa Barbara County, California: U.S. Geological Survey Scientific Investigations Map 3001, 1 sheet, scale 1:25,000, 38-p. pamphlet. [Also available at https://doi.org/10.3133/sim3001.]

Muhs, D.R., Rockwell, T.K., and Kennedy, G.L., 1992, Late Quaternary uplift rates of marine terraces on the Pacific coast of North America, southern Oregon to Baja California Sur: Quaternary International, v. 15–16, p. 121–133. [Also available at https://doi.org/10.1016/1040-6182(92)90041-Y.]

Muir, K.S., 1964, Geology and ground water of San Antonio Creek Valley, Santa Barbara County, California: U.S. Geological Survey Water-Supply Paper 1664, 53 p., 4 pls. [Also available at https://doi.org/10.3133/wsp1664.]

Namson, J.S., and Davis, T.L., 1990, Late Cenozoic fold and thrust belt of the southern Coast Ranges and Santa Maria basin, California: The American Association of Petroleum Geologists Bulletin, v. 74, no. 4, p. 467–492. [Also available at https://archives.datapages.com/data/bulletns/1990-91/images/pg/00740004/0000/04670.pdf.]

Nelson, R.N., 1925, Geology of the hydrographic basin of the upper Santa Ynez River California: Berkeley, Calif., University of California Press, Department of Geology Science Bulletin, v. 15, no. 10, p. 327–396.

O'Brien, J.M., 1972, Narizian-Refugian (Eocene-Oligocene) marine and marginal-marine sedimentation, western Santa Ynez Mountains, Santa Barbara County, California, A progress report, *in* Weaver, D.W., ed., Central Santa Ynez Mountains, Santa Barbara County, California, Guidebook, Spring field trip, June 2, 1972: American Association of Petroleum Geologists and Pacific Section, Society for Sedimentary Geology, p. 37–43. [Also available at http://archives.datapages.com/data/pac_sepm/013/013001/pdfs/37.htm.]

O'Brien, J., 1973, Narizian-Refugian (Eocene-Oligocene) sedimentation, western Santa Ynez Mountains northwest of Santa Barbara, California: Santa Barbara, Calif., University of California Santa Barbara, Ph.D. dissertation, 304 p. [Also available from the University of California Santa Barbara Library, Primo Record ID 01UCSB_ALMA21266235080003776.]

Ogle, B.A., Wallis, W.S., Heck, R.G., and Edwards, E.B., 1987, Petroleum geology of the Monterey Formation in the offshore Santa Maria/Santa Barbara areas, *in* Ingersoll, R.V., and Ernst, W.G., eds., Cenozoic basin development of coastal California: Englewood Cliffs, N.J., Prentice-Hall, p. 382–406.

Onderdonk, N.W., 2005, Structures that accommodated differential vertical axis rotation of the western Transverse Ranges, California: Tectonics, v. 24, no. 4, 15 p. [Also available at https://doi.org/10.1029/2004TC001769.]

Orme, A.R., 1992, Late Quaternary deposits near Point Sal, south-central California—A time frame for coastal dune emplacement, *in* Fletcher, C.H., III, and Wehmiller, J.F., eds., Quaternary coasts of the United States—Marine and lacustrine systems: Tulsa, Okla., Society for Sedimentary Geology Special Publication, no. 48, p. 309–315. [Also available at https://doi.org/10.2110/pec.92.48.]

Pacific Gas and Electric Company, 1988, Final report of the Diablo Canyon long term seismic program: U.S. Nuclear Regulatory Commission, docket nos. 50–275 and 50–323, NRC–2016–0151. [Also available at https://www.pge.com/includes/docs/pdfs/shared/edusafety/systemworks/dcpp/SSHAC/legacy_documents/Long_Term_Seismic_Project_Final_Report_1988.pdf.]

Page, B.M., 1970, Sur-Nacimiento fault zone of California-continental margin tectonics: Geological Society of America Bulletin, v. 81, p. 667–690. [Also available at https://doi.org/10.1130/0016-7606(1970)81[667:SFZOCC]2.0.CO;2.]

Page, B.M., Marks, J.G., and Walker, G.W., 1951, Stratigraphy and structure of mountains northeast of Santa Barbara v. 35: California, American Association of Petroleum Geologists, p. 1727–1780. [Also available at http://archives.datapages.com/data/bulletns/1949-52/data/pg/0035/0008/1700/1727.htm.]

Payne, C.M., Swanson, O.E., and Schell, B.A., 1979, Investigation of the Hosgri fault offshore southern California, Point Sal to Point Conception: U.S. Geological Survey Open-File Report 79–1199, 17 p., 4 pls. [Also available at https://doi.org/10.3133/ofr791199.]

Pessagno, E.A., Jr., 1977, Upper Jurassic radiolaria and radiolarian biostratigraphy of the California Coast Ranges: Micropaleontology, v. 23, no. 1, p. 56–113. [Also available at https://doi.org/10.2307/1485310.]

Phillips, J.D., 2001, Designing matched bandpass and azimuthal filters for the separation of potential-field anomalies by source region and source type, 15th Geophysical Conference and Exhibition, expanded abstracts: Australian Society of Exploration Geophysicists, 4 p. [Also available as a CD-ROM and at https://doi.org/10.1071/ASEG2001ab110.]

Pisciotto, K.A., 1981, Notes on Monterey rocks near Santa Maria, California, *in* Isaacs, C.M., ed., Guide to the Monterey Formation in the California coastal area, Ventura to San Luis Obispo: Los Angeles, Calif., Pacific Section, American Association of Petroleum Geologists, v. 52, p. 73–81.

Pisciotto, K.A., and Garrison, R.E., 1981, Lithofacies and depositional environments of the Monterey Formation, California, *in* Garrison, R.E., and Douglas, R.G., eds., The Monterey Formation and related siliceous rocks of California: Pacific Section, Society of Economic Paleontologists and Mineralogists, p. 97–122. [Also available at http://archives.datapages.com/data/pac_sepm/030/030001/pdfs/97.htm.]

Plouff, D., 1977, Preliminary documentation for a FORTRAN program to compute gravity terrain corrections based on topography digitized on a geographic grid: U.S. Geological Survey Open-File Report 77–535, 45 p. [Also available at https://doi.org/10.3133/ofr77535.]

Powell, R.E., 1993, Balanced palinspastic reconstruction of pre-late Cenozoic paleogeography, southern California, *in* Powell, R.E., Weldon, R.J., II, and Matti, J.C., eds., The San Andreas Fault system—Displacement, palinspastic reconstruction, and geologic evolution—Boulder, Colo: Geological Society of America Memoir 178, p. 1–106. [Also available at https://doi.org/10.1130/MEM178-p1.]

Prothero, D.R., 2001, Magnetostratigraphic tests of sequence stratigraphic correlations from the southern California Paleogene: Journal of Sedimentary Research, v. 71, p. 526–536. [Also available at https://doi.org/10.1306/051500710526.]

Prothero, D.R., and Britt, J., 1998, Magnetic stratigraphy and tectonic rotation of the middle Eocene Matilija Sandstone and Cozy Dell Shale, Ventura County, California—Implications for sequence stratigraphic correlations: Earth and Planetary Science Letters, v. 163, no. 1–4, p. 261–273. [Also available at https://doi.org/10.1016/S0012-821X(98)00192-7.]

Prothero, D.R., and Rapp, S.G., 2001, Magnetic stratigraphy and tectonic rotation of the lower Miocene (type Saucesian) Rincon Formation, Ventura and Santa Barbara counties, California, *in* Prothero, D.R., ed., Magnetic stratigraphy of the Pacific coast Cenozoic: Pacific Section, Society for Sedimentary Geology, v. 91, p. 263–271. [Also available at http://archives.datapages.com/data/pac_sepm/109/109001/pdfs/263.htm.]

Ramirez, P.C., 1990, Stratigraphy, sedimentology, and paleoceanographic implications of the late Miocene to early Pliocene Sisquoc Formation, Santa Maria area, California: Santa Cruz, Calif., University of California, Ph.D. dissertation, 384 p. [Also available at the University of California Santa Cruz Library, MMS ID 991015109019704876.]

Ramirez, P.C., and Garrison, R.E., 1998, Stratigraphy of the fine-grained facies of the Sisquoc Formation, Santa Maria basin, California—Paleoceanographic and tectonic implications, chap. U *of* Keller, M.A., ed., Evolution of sedimentary basins/onshore oil and gas investigations—Santa Maria Province: U.S. Geological Survey Bulletin 1995–U, 15 p. [Also available at https://doi.org/10.3133/b1995TUV.]

Redwine, L.E., Ryall, P., and Whaley, H., 1975, General stratigraphy of eastern Santa Maria, *in* Oltz, D., and Suchsland, R., eds., Geologic field guide of the eastern Santa Maria area, Annual fall field trip, Oct. 4, 1975: Pacific Section, Society of Economic Paleontologists and Mineralogists, Annual Fall Field Trip, 24 p. [Also available at http://archives.datapages.com/data/pac_sepm/151/151001/pdfs/i.htm.]

Reed, R.D., and Hollister, J.S., 1936, Structural evolution of southern California: Tulsa, Okla., American Association of Petroleum Geologists, v. 20, no. 12, p. 1529–1704.

Richmond, G.M., and Fullerton, D.S., 1986, Introduction to Quaternary glaciations in the United States of America, *in* Richmond, G.M., and Fullerton, D.S., eds., Quaternary glaciations in the United States of America: Quaternary Science Reviews, v. 5, p. 3–10. [Also available at https://doi.org/10.1016/S0277-3791(86)80003-8.]

Rietman, J.D., and Beyer, L.A., 1982, Bouguer gravity map of California—Santa Maria sheet, *in* Bouguer gravity map of California: California Division of Mines and Geology, scale 1:250,000.

Rigsby, C.A., 1998, Paleogeography of the western Transverse Range Province, California; new evidence from the late Oligocene and early Miocene Vaqueros Formation, chap. T *of* Keller, M.A., ed., Evolution of sedimentary basins/onshore oil and gas investigations—Santa Maria Province: U.S. Geological Survey Bulletin 1995–T, 18 p. [Also available at https://doi.org/10.3133/b1995TUV.]

Rigsby, C.A., and Schwartz, D.E., 1990, Lithostratigraphy and depositional environments of the Vaqueros Formation, Capitan field, *in* Keller, M.A., and McGowen, M.K., eds., Miocene and Oligocene petroleum reservoirs of the Santa Maria and Santa Barbara-Ventura basins, California—Society of Economic Paleontologists and Mineralogists, Core Workshop no. 14: California, p. 88–136. [Also available at https://doi.org/10.2110/cor.90.14.0088.]

Roberts, C.W., Jachens, R.C., and Oliver, H.W., 1990, Isostatic residual gravity map of California and offshore southern California: California Division of Mines and Geology, no. 7, scale 1:750,000. [Now the California Department of Conservation, California Geological Survey].

Robyn, E.S., 1980, A description of the Miocene Tranquillon Volcanics and a comparison with the Miocene Obispo tuff: Santa Barbara, Calif., University of California, M.A. thesis, 110 p. [Also available at the University of California Santa Barbara Library, Primo Record ID 01UCSB_ALMA21167866530003776.]

Rockwell, T.K., Nolan, J., Johnson, D.L., and Patterson, R., 1992, Ages and deformation of marine terraces between Point Conception and Gaviota, western Transverse Ranges, *in* Fletcher, C.H., III, and Wehmiller, J.F., eds., Quaternary coasts of the United States—Marine and lacustrine systems—Broken Arrow, Okla., Society for Sedimentary Geology Special Publication 48: California, p. 333–341. [Also available at https://doi.org/10.2110/pec.92.48.0333.]

Saenz, J.A., 2002, Geological controls of hydrocarbon seeps in Santa Maria basin, offshore California: Northridge, Calif., California State University, M.S. thesis, 307 p., 7 pls. [Also available through California State University Northridge Oviatt Library at http://scholarworks.csun.edu/handle/10211.3/165464.]

Saucedo, G.J., Bedford, D.R., Raines, G.L., Miller, R.J., and Wentworth, C.M., 2000, GIS data for the geologic map of California: Sacramento, Calif., California Department of Conservation, CD 2000–07.

Sauer, P.E., and Mariano, J., 1990, Isostatic residual gravity and aeromagnetic maps of the Santa Maria province including portions of the Santa Maria, San Luis Obispo, Los Angeles, and Bakersfield quadrangles and adjacent offshore areas, California: U.S. Geological Survey Open-File Report 90–308, 2 pls., scale 1:250,000. [Also available at https://doi.org/10.3133/ofr90308.]

Schmitka, R.O., 1973, Evidence for major right-lateral separation of Eocene rocks along the Santa Ynez fault, Santa Barbara County, California: Geological Society of America Abstracts with Programs, v. 5, no. 1, p. 104.

Schneider, J.-L., and Fisher, R.V., 1996, Obispo Formation, California; remobilized pyroclastic material, chap. O *of* Keller, M.A., ed., Evolution of sedimentary basins/onshore oil and gas investigations—Santa Maria Province: U.S. Geological Survey Bulletin 1995–O, 21 p. [Also available at https://pubs.er.usgs.gov/publication/b1995MNO.]

Schroeter, C.E., 1972, Local paleogeography of the Sierra Blanca Limestone (Eocene), *in* Weaver, D.W. (field trip leader), Central Santa Ynez Mountains, Santa Barbara County, California—Guidebook, Pacific sections, American Association of Petroleum Geologists and Society of Economic Paleontologists and Mineralogists, Spring Field trip, p. 20–29. [Also available at http://archives.datapages.com/data/pac_sepm/013/013001/pdfs/20.htm.]

Sedlock, R.L., and Hamilton, D.H., 1991, Late Cenozoic tectonic evolution of southwestern California: Journal of Geophysical Research, v. 96, B2, p. 2325–2351. [Also available at https://doi.org/10.1029/90JB02018.]

Seeber, L., and Sorlien, C.C., 2000, Listric thrusts in the western Transverse Ranges, California: Geological Society of America Bulletin, v. 112, p. 1067–1079. [Also available at https://doi.org/10.1130/0016-7606(2000)112%3C1067:LTITWT%3E2.0.CO;2.]

Sorlien, C.C., Kamerling, M.J., and Mayerson, D., 1999a, Rotation and termination of the Hosgri strike-slip fault, California, from three-dimensional map restoration: Geology, v. 27, no. 11, p. 1039–1042. [Also available at https://doi.org/10.1130/0091-7613(1999)027%3C1039:BRATOT%3E2.3.CO;2.]

Sorlien, C.C., Nicholson, C., Behl, R.J., Marshall, C.J., and Kennett, J., 2014, The Quaternary North Channel-Pitas Point fault system in northwest Santa Barbara Channel, California [abs.]: American Geophysical Union, 2014 Fall Meeting, abstract T34A–07, accessed May 7, 2021, at http://adsabs.harvard.edu/abs/2014AGUFM.T34A.07S.

Sorlien, C.C., Nicholson, C., and Luyendyk, B.P., 1999b, Miocene extension and post-Miocene transpression offshore of south-central California, chap. Y *of* Keller, M.A., ed., Evolution of sedimentary basins/onshore oil and gas investigations—Santa Maria Province: U.S. Geological Survey Bulletin 1995–Y, 38 p., 1 pl. [Also available at https://doi.org/10.3133/b1995YZ.]

Stanley, R.G., Cotton, M.L., Bukry, D., Filewicz, M.V., Valin, Z.C., and York, D.R., 1994, Stratigraphic revelations regarding the Rincon Shale (lower Miocene) in the Santa Barbara coastal area, California [abs.], Pacific Section Meeting, April 27–29, 1994, Ventura, Calif.: American Association of Petroleum Geologists Bulletin, v. 78, no. 4, Search and Discovery Article #90981, p. 675–676. [Also available at https://www.searchanddiscovery.com/abstracts/html/1994/pacific/abstracts/0675c.htm.]

Stanley, R.G., Johnson, S.Y., Swisher, C.C., III, Mason, M.A., Obradovich, J.D., Cotton, M.L., Filewicz, M.V., and Vork, D.R., 1996, Age of the Lospe Formation (early Miocene) and origin of the Santa Maria basin, California, chap. M *of* Keller, M.A., ed., Evolution of sedimentary basins/onshore oil and gas investigations—Santa Maria Province: U.S. Geological Survey Bulletin 1995–M, 37 p. [Also available at https://doi.org/10.3133/b1995MNO.]

Stanley, R.G., Johnson, S.Y., Tuttle, M.L., Mason, M.A., Swisher, C.C., Cotton Thornton, M.L., Vork, D.R., Filewicz, M.V., Cole, R.B., and Obradovich, J.D., 1991, Age, correlation, and origin of the type Lospe Formation (lower Miocene), Santa Maria basin, central California [abs.], *in* American Association of Petroleum Geologists (AAPG)/Society of Economics, Paleontologists, and Mineralogists (SEPM)/Society of Exploration Geophysicists (SEG)/Society of Professional Well Log Analysts (SPWLA) Pacific Section annual meeting, Bakersfield, Calif., March 6–8, 1991: The American Association of Petroleum Geologists Bulletin, v. 75, no. 2, p. 382. [Also available at https://www.osti.gov/biblio/5199568.]

Stanley, R.G., Valin, Z.C., and Pawlewicz, M.J., 1992, Rock-eval pyrolysis and vitrinite reflectance results from outcrop samples of the Rincon Shale (lower Miocene) collected at the Tajiguas landfill, Santa Barbara County, California: U.S. Geological Survey Open-File Report 92–0571, 27 p. [Also available at https://doi.org/10.3133/ofr92571.]

Stauffer, P.H., 1967, Sedimentologic evidence on Eocene correlations, Santa Ynez Mountains, California: American Association of Petroleum Geologists, v. 51, no. 4, p. 607–611. [Also available at http://archives.datapages.com/data/bulletns/1965-67/data/pg/0051/0004/0600/0607.htm.]

Surpless, K.D., Ward, R.B., and Graham, S.A., 2009, Evolution and stratigraphic architecture of marine slope gully complexes—Monterey Formation (Miocene), Gaviota Beach, California: Marine and Petroleum Geology, v. 26, p. 269–288. [Also available at https://doi.org/10.1016/j.marpetgeo.2007.10.005.]

Sweetkind, D.S., Langenheim, V.E., and McDougall-Reid, K., 2021, Data release—Geologic and geophysical maps of the onshore parts of the Santa Maria and Point Conception 30'x60' quadrangles, California: U.S. Geological Survey data release, https://doi.org/10.5066/P9FU7SJL.

Sweetkind, D.S., Tennyson, M.E., Langenheim, V.E., and Shumaker, L.E., 2010, Digital tabulation of stratigraphic data from oil and gas wells in the Santa Maria basin, central California coast: U.S. Geological Survey Open-File Report 2010–1129, 11 p., 3 tables. [Also available at https://doi.org/10.3133/ofr20101129.]

Sylvester, A.G., and Darrow, A.C., 1979, Structure and neotectonics of the western Santa Ynez fault system in southern California: Tectonophysics 52, p. 389–405. [Also available at https://doi.org/10.1016/B978-0-444-41783-1.50065-9.]

Tan, S.S., Jones, T.A., and Clahan, K.B., 2003, Geologic map of the Pitas Point 7.5-minute quadrangle Ventura County, California—A digital database: California Geological Survey Preliminary Geologic Map, scale 1:24,000. [Also available at https://www.conservation.ca.gov/cgs/maps-data/rgm/preliminary.]

Telford, W.M., Geldart, L.O., and Sheriff, R.E., 1990, Applied geophysics 2nd ed.: New York, Cambridge University Press, 770 p. [Also available at https://doi.org/10.1017/CBO9781139167932.]

Tennyson, M.E., 1992, Preliminary geologic map of Santa Maria 30'×60' quadrangle, California: U.S. Geological Survey Open-File Report 92–189, 9 p., 2 pls., scale 1:100,000. [Also available at https://doi.org/10.3133/ofr92189.]

Tennyson, M.E., 1995a, Tables of subsurface formation depths for exploration wells in Santa Maria basin, Santa Barbara and San Luis Obispo Counties, California, compiled from publications of the California Division of Oil and Gas: U.S. Geological Survey Open-File Report 95–14, 22 p. [Also available at https://doi.org/10.3133/ofr9514.]

Tennyson, M.E., 1995b, Santa Maria basin province (012), *in* Gautier, D.L., Dolton, G.L., Takahashi, K.I., and Varnes, K.L., eds., 1995 National assessment of United States oil and gas resources—Results, methodology, and supporting data: U.S. Geological Survey Digital Data Series DDS–30, 1 CD–ROM. [Also available at https://doi.org/10.3133/ds30.]

Tennyson, M.E., Beeman, W.R., and Urban, S.B., 1995, Preliminary digital geologic map of the Santa Maria 30'×60' quadrangle, California, in ARC/INFO, with exploration well locations and subsurface formation depths: U.S. Geological Survey Open-File Report 95–25, 2 p. [Also available at https://doi.org/10.3133/ofr9525.]

Tennyson, M.E., and Isaacs, C.M., 2001, Geologic setting and petroleum geology of Santa Maria and Santa Barbara basins, *in* Isaacs, C.M., and Rullkötter, J., eds., The Monterey Formation—From rocks to molecules: New York, Columbia University Press, p. 206–229.

Tennyson, M.E., Keller, M.A., Filewicz, M.V., and Cotton Thornton, M.L., 1991, Contrasts in early Miocene subsidence history across Oceanic-West Huasna fault system, northern Santa Maria province, California [abs.], *in* American Association of Petroleum Geologists (AAPG)/Society of Economics, Paleontologists, and Mineralogists (SEPM)/Society of Exploration Geophysicists (SEG)/Society of Professional Well Log Analysts (SPWLA) Pacific Section annual meeting, Bakersfield, Calif., March 6–8, 1991: American Association of Petroleum Geologists Bulletin, v. 75, no. 2, article #91009, p. 383. [Also available at https://www.searchanddiscovery.com/abstracts/html/1991/pacific/abstracts/0383b.htm.]

Tennyson, M.E., and Kropp, A.P., 1998, Regional cross section across Santa Barbara Channel from northwestern Santa Rosa Island to Canada de Molino, *in* Kunitomi, D.S., Hopps, T.E., and Galloway, J.M., eds., Structure and petroleum geology, Santa Barbara Channel, California: American Association of Petroleum Geologists, Pacific Section, p. 185–193, 3 pl. [Also available at https://doi.org/10.32375/1998-MP46.16.]

Tipton, A., 1980, Foraminiferal zonation of the Refugian Stage, latest Eocene of California, *in* Sliter, W.V., ed., Studies in marine micropaleontology and paleoecology—A memorial volume to Orville L. Bandy: Lawrence, Kan., Cushman Foundation for foraminiferal research, no. 19, p. 258–277. [Also available at https://cushmanfoundation.allenpress.com/Portals/_default/SpecialPublications/sp19.pdf.]

Turner, D.L., 1970, Potassium-argon dating of Pacific coast Miocene foraminiferal stages, in Bandy, O.L., ed., Radiometric dating and paleontologic zonation—Boulder, Colo: Geological Society of America Special Paper 124, p. 91–130. [Also available at https://doi.org/10.1130/SPE124-p91.]

Up de Graff, J., 1984, Gravity study of the northern boundary of the western Transverse Ranges, California: Santa Barbara, University of California, M.A. thesis, 171 p. [Also available at the University of California Santa Barbara Library, Primo Record ID 01UCSB_ALMA21176239700003776.]

Up de Graff, J.E., and Luyendyk, B.P., 1989, Gravity study of the boundary between the western Transverse Ranges and Santa Maria basin, California: Journal of Geophysical Research, v. 94, no. B2, p. 1817–1825. [Also available at https://doi.org/10.1029/JB094iB02p01817.]

Upson, J.E., 1951, Former marine shore lines of the Gaviota quadrangle, Santa Barbara County, California: The Journal of Geology, v. 59, no. 5, p. 415–446. [Also available at https://doi.org/10.1086/625888.]

Upson, J.E., and Thomasson, H.G., Jr., 1951, Geology and water resources of the Santa Ynez River basin, Santa Barbara County, California: U.S. Geological Survey Water Supply Paper 1107, 194 p., 7 pls., scale 1:48,000. [Also available at https://doi.org/10.3133/wsp1107.]

U.S. Geological Survey Geologic Names Committee, 2018, Divisions of geologic time—Major chronostratigraphic and geochronologic units: U.S. Geological Survey Fact Sheet 2018–3054, 2 p., http://pubs.usgs.gov/fs/2010/3059/.]

Van de Kamp, P.C., Harper, J.D., Gonniff, J.J., and Morris, D.A., 1974, Facies relations in the Eocene-Oligocene in the Santa Ynez Mountains, California: Geological Society of London Journal, v. 130, p. 545–565. [Also available at https://doi.org/10.1144/gsjgs.130.6.0545.]

Vedder, J.G., 1972, Revision of stratigraphic names for some Eocene formations in Santa Barbara and Ventura counties, California: U.S. Geological Survey Bulletin 1354–D, 12 p. [Also available at https://doi.org/10.3133/b1354D.]

Vedder, J.G., Beyer, L.A., Moore, G.W., Roberts, A.E., Taylor, J.C., and Wagner, H.C., 1974, Preliminary report on the geology of the continental borderland of southern California: U.S. Geological Survey Miscellaneous Field Investigations Map 624, 9 pls., scale 1:500,000, 14-p. pamphlet. [Also available at https://doi.org/10.3133/mf624.]

Vedder, J.G., and Brown, R.D., Jr., 1968, Structural and stratigraphic relations along the Nacimiento fault in the southern Santa Lucia Range and San Rafael Mountains, California, *in* Dickinson, W.R., and Grantz, A., eds., Proceedings of conference on geologic problems of San Andreas fault system: Stanford, Calif., Stanford University Publications in Geological Sciences, v. 11, p. 242–259.

Vedder, J.G., and Dibblee, T.W., Jr., 1991, Southern Coast Ranges field trip road log, *in* Lewis, L., Hubbard, P., Heath, E., and Pace, A., eds., Southern Coast Ranges—Santa Ana, Calif., South Coast Geological Society Field Trip Guidebook 19, p. 3–31. [Also available at http://southcoastgeology.org/?p=433.]

Vedder, J.G., Gower, H.D., Clifton, H.E., and Durham, D.L., 1967, Reconnaissance geologic map of the central San Rafael Mountains and vicinity, Santa Barbara County, California: U.S. Geological Survey Map I-487, 1 pl., scale 1:48,000. [Also available at https://doi.org/10.3133/i487.]

Vedder, J.G., Greene, H.G., Clarke, S.H., and Kennedy, M.P., 1986, Geologic map of the mid-central California continental margin—Map no. 2A (Geology), *in* Greene, H.G. and Kennedy, M.P., eds., California continental margin geologic map series: California Division of Mines and Geology, 1 pl., scale 1:250 000.

Vedder, J.G., Howell, D.G., and McLean, H., 1977, Upper Cretaceous redbeds in the Sierra Madre-San Rafael Mountains, *in* Howell, D.G., Vedder, J.G., and McDougall, K., eds., Cretaceous geology of the California Coast Ranges, west of the San Andreas Fault: Tulsa, Okla., Pacific Section, Society of Economic Paleontologists and Mineralogists, no. 2, p. 71–78. [Also available at http://archives.datapages.com/data/pac_sepm/158/158001/pdfs/71.htm.]

Vedder, J.G., Howell, D.G., and McLean, H., 1982, Stratigraphy, sedimentation, and tectonic accretion of exotic terranes, southern Coast Ranges, California, *in* Watkins, J.S., and Drake, C.L., eds., Studies in continental margin geology: American Association of Petroleum Geologists Memoir 34, p. 471–496. [Also available at https://doi.org/10.1306/M34430C25.]

Vedder, J.G., Howell, D.G., and McLean, H., 1989a, Geologic map of Miranda Pine Mtn. quadrangle and part of Taylor Canyon quadrangle, California: U.S. Geological Survey Open-File Report 89–469, 1 pl., scale 1:24,000. [Also available at https://doi.org/10.3133/ofr89161.]

Vedder, J.G., Howell, D.G., and McLean, H., 1989b, Geologic map of Chimney Canyon quadrangle and part of Huasna Peak quadrangle, California: U.S. Geological Survey Open-File Report 89–161, 1 pl., scale 1:24,000. [Also available at https://doi.org/10.3133/ofr89161.]

Vedder, J.G., Howell, D.G., and McLean, H., 1994, Preliminary geologic map of Bates Canyon quadrangle and part of Peak Mountain quadrangle, California: U.S. Geological Survey Open-File Report 94–128, 1 pl., scale 1:24,000. [Also available at https://doi.org/10.3133/ofr94128.]

Vedder, J.G., Howell, D.G., McLean, H., Stanley, R.G., and Wiley, T.J., 1991, Preliminary geologic map of the Tepusquet Canyon and Manzanita Mtn. quadrangles, California: U.S. Geological Survey Open-File Report 91–109, 1 pl., scale 1:24,000. [Also available at https://doi.org/10.3133/ofr91109.]

Vedder, J.G., Howell, D.G., McLean, H., and Wiley, T.J., 1988, Geologic map of Los Machos Hills and Caldwell Mesa quadrangles and part of the Tar Spring Ridge quadrangle, California: U.S. Geological Survey Open-File Report 88–253, 1 pl., scale 1:24,000. [Also available at https://doi.org/10.3133/ofr88253.]

Vedder, J.G., and Stanley, R.G., 2001, Geological map and digital database of the San Rafael Mtn. 7.5-minute quadrangle, Santa Barbara County, California: U.S. Geological Survey Open-File Report 02–290, 22 p., 1 pl., scale 1:24,000. [Also available at https://doi.org/10.3133/ofr01290.]

Vedder, J.G., Stanley, R.G., McLean, H., Cotton, M.L., Filewicz, M.V., and Vork, D.R., 1998, Age and tectonic inferences from a condensed(?) succession of Upper Cretaceous and Paleogene strata, Big Pine Mountain, Santa Barbara County, California, chap S *of* Evolution of sedimentary basins/onshore oil and gas investigations—Santa Maria Province: U.S. Geological Survey Bulletin 1995–S, p. S1–S33. [Also available at https://doi.org/10.3133/b1995RS.]

Wahl, A.D., 1998, Cenozoic deformation of the Franciscan Complex, eastern Santa Maria basin, *in* Keller, M.A., ed., Evolution of sedimentary basins/onshore oil and gas investigations—Santa Maria Province: U.S. Geological Survey Bulletin 1995–W, 20 p., 1 pl., scale 1:10,000. [Also available at https://doi.org/10.3133/b1995WX.]

Walker, G.W., 1950, Sierra Blanca Limestone in Santa Barbara County, California: Sacramento, Calif., California Department of Natural Resources, Division of Mines and Geology Special Report 1–A, 5 p.

Weaver, D.W., 1962, Eocene foraminifera from west of Refugio Pass, Calif: University of California Publications in Geological Sciences, v. 37, p. 353–420.

Weaver, D.W., 1965, Summary of Tertiary stratigraphy, western Santa Ynez Mountains, *in* Weaver, D.W., and Dibblee, T.W., Jr., eds., Western Santa Ynez Mountains, Santa Barbara County, California, Gaviota, Calif., Oct. 16, 1965: Pacific Section, American Association of Petroleum Geologists and Society of Economic Paleontologists and Mineralogists, Field trip Guidebook, p. 16–30. [Also available at http://archives.datapages.com/data/pacific/data/013/013001/1_ps0130001.htm.]

Weaver, D.W., and Molander, G.E., 1964, The Eocene faunal sequence in the eastern Santa Rosa Hills, Santa Barbara County, California: Berkeley, Calif., University of California Publications in Geological Sciences, v. 41, p. 161–248, 18 pls.

Weaver, W.R., and Weaver, D.W., 1962, Upper Eocene foraminifera from the southwestern Santa Ynez Mountains, California: Berkeley, Calif., University of California Publications in Geological Sciences, v. 41, p. 1–96.

Whidden, K.J., Bottjer, D.J., Lund, S.P., and Sliter, W.V., 1995, Paleogeographic implications of Paleogene shallow water limestones in southern San Rafael Mountains, *in* Fritsche, A.E., ed., Cenozoic paleogeography of the western United States II: Society of Economic Paleontologists and Mineralogists, Pacific Section, Book 75: California, p. 193–211.

Willingham, C.R., Rietman, J.D., Heck, R.G., and Lettis, W.R., 2013, Characterization of the Hosgri fault zone and adjacent structures in the offshore Santa Maria basin, south-central California, chap. CC *of* Keller, M.A., ed., Evolution of sedimentary basins/onshore oil and gas investigations—Santa Maria Province: U.S. Geological Survey Bulletin 1995–CC, 105 p., 7 pls., scale 1:200,000. [Also available at https://doi.org/10.3133/b1995CC.]

Wilson, D.S., McCrory, P.A., and Stanley, R.G., 2005, Implications of volcanism in coastal California for the Neogene deformation history of western North America: Tectonics, v. 24, no. 3, 22 p. [Also available at https://doi.org/10.1029/2003TC001621.]

Woodring, W.P., and Bramlette, M.N., 1950, Geology and paleontology of the Santa Maria district, California: U.S. Geological Survey Professional Paper 222, 185 p., 5 pls., scale 1:24,000. [Also available at https://doi.org/10.3133/pp222.]

Woodring, W.P., Bramlette, M.N., and Lohman, K.E., 1943, Stratigraphy and paleontology of the Santa Maria district, California: American Association of Petroleum Geologists, v. 27, no. 10, p. 1335–1360. [Also available at http://archives.datapages.com/data/bulletns/1938-43/data/pg/0027/0010/1300/1335.htm.]

Worts, G.F., Jr., 1951, Geology and ground-water resources of the Santa Maria Valley area, California, with a section on surface-water resources: U.S. Geological Survey Water-Supply Paper 1000, 169 p., 6 pls. [Also available at https://doi.org/10.3133/wsp1000.]

Yaldezian, J.G., II, Popelar, S.J., and Fritsche, A.E., 1983, Movement on the Nacimiento fault in northern Santa Barbara County, California, *in* Anderson, D.W., and Rymer, M. J., eds., Tectonics and sedimentation along faults of the San Andreas system: Tulsa, Okla., Pacific Section, Society of Economic Paleontologists and Mineralogists, v. 30, p. 11–15. [Also available at http://archives.datapages.com/data/pac_sepm/045/045001/pdfs/11.htm.]

Yerkes, R.F., Greene, H.G., Tinsley, J.C., and Lajoie, K.R., 1981, Maps showing seismotectonic setting of the Santa Barbara Channel area, California: U.S. Geological Survey Miscellaneous Field Investigations Map MF–1169, 2 plates, scale 1:250,000, 25-p. pamphlet. [Also available at https://doi.org/10.3133/mf1169.]

Appendix 1. Tables of Locations for Paleontological Samples

Tables of locations and interpreted fossil ages for paleontological samples collected in the Santa Maria and part of the Point Conception 30'×60' quadrangles, California. Table 1.1 describes samples originally collected from outcrop by Chevron Oil Company. Table 1.2 describes samples collected from outcrops and boreholes by the U.S. Geological Survey. Table 1.3 describes samples collected in exposures at the Tajiguas landfill (Stanley and others, 1992). Table 1.4 describes samples collected from outcrops in the Arroyo el Bulito section (McDougall, 2008).

Table 1.1. Fossils collected from outcrops by Chevron Oil Company in Sweetkind and others, 2021.
This table is available in a Microsoft Excel file at https://doi.org/10.5066/P9FU7SJL.

Table 1.2. Fossils collected from outcrops and boreholes by the U.S. Geological Survey in Sweetkind and others, 2021.
This table is available in a Microsoft Excel file at https://doi.org/10.5066/P9FU7SJL.

Table 1.3. Sample traverse of Stanley (1992) from the Tajiguas landfill in the western Santa Ynez Mountains, California in Sweetkind and others, 2021.
This table is available in a Microsoft Excel file at https://doi.org/10.5066/P9FU7SJL.

Table 1.4. Sample traverse of Tipton (1980) in the western Santa Ynez Mountains in Sweetkind and others, 2021.
This table is available in a Microsoft Excel file at https://doi.org/10.5066/P9FU7SJL.

References Cited

McDougall, K., 2008, California Cenozoic biostratigraphy—Paleogene, chap. 4 *of* Scheirer, A.H., ed., Petroleum systems and geologic assessment of oil and gas in the San Joaquin basin Province, California: U.S. Geological Survey Professional Paper 1713–4, 56 p. [Also available at https://doi.org/10.3133/pp17134.]

Stanley, R.G., Valin, Z.C., and Pawlewicz, M.J., 1992, Rock-Eval pyrolysis and vitrinite reflectance results from outcrop samples of the Rincon Shale (lower Miocene) collected at the Tajiguas landfill, Santa Barbara County, California: U.S. Geological Survey Open-File Report 92–571, 28 p. [Also available at https://doi.org/10.3133/ofr92571.]

Sweetkind, D.S., Langenheim, V.E., and McDougall-Reid, K., 2021, Data release—Geologic and geophysical maps of the onshore parts of the Santa Maria and Point Conception 30'x60' quadrangles, California: U.S. Geological Survey data release, https://doi.org/10.5066/P9FU7SJL.

Appendix 2. Foraminifer Fossil Checklist Tables

Foraminifer fossil checklist tables for paleontological samples collected in the Santa Maria and part of the Point Conception 30'×60' quadrangles, California. Tables 2.1 and 2.2 present two different checklist formats for miscellaneous U.S. Geological Survey samples. Table 2.3 is a fossil checklist table for samples collected in exposures at the Tajiguas landfill (Stanley and others, 1992). Table 2.4 is a fossil checklist table for samples collected from outcrops in the Arroyo el Bulito section (McDougall, 2008).

Table 2.1. Fossil checklist from miscellaneous U.S. Geological Survey samples in Sweetkind and others, 2021.
This table is available in a Microsoft Excel file at https://doi.org/10.5066/P9FU7SJL.

Table 2.2. U.S. Geological Survey (USGS) miscellaneous foraminifer samples in Sweetkind and others, 2021.
This table is available in a Microsoft Excel file at https://doi.org/10.5066/P9FU7SJL.

Table 2.3. Foraminifer fossil samples for the Tajiguas landfill section, Santa Maria and part of Point Conception 30'×60' quadrangles, California in Sweetkind and others, 2021.
This table is available in a Microsoft Excel file at https://doi.org/10.5066/P9FU7SJL.

Table 2.4. Foraminifer fossil samples for the Arroyo el Bulito section, Santa Maria and part of Point Conception 30'×60' quadrangles, California in Sweetkind and others, 2021.
This table is available in a Microsoft Excel file at https://doi.org/10.5066/P9FU7SJL.

References Cited

Beck, R.S., 1943, Eocene foraminifera from Cowlitz River, Lewis County, Washington: Journal of Paleontology, v. 17, no. 6, p. 584–614, pls. 98–109.

Blow, W.H., 1979, The Cainozoic Globigerinida—A study of the morphology, taxonomy, evolutionary relationships and the stratigraphic distribution of some Globigerinida (mainly Globigerinacea) v. 1–3: Leiden, Netherlands, E.J. Brill, 1413 p.

Bukry, D., 1973, Low-latitude coccolith biostratigraphic zonation, *in* Edgar, N.T., Kaneps, A.G., and Herring, J.R., eds., Initial reports of the Deep Sea Drilling Project v. 15: Washington, D.C., U.S. Government Printing Office, p. 685–703. [Also available at https://doi.org/10.2973/dsdp.proc.15.116.1973.]

Cushman, J.A., 1936, New genera and species of the families Verneuilinidae and Valvulinidae and of the subfamily Virgulininae: Cushman Foundation for Foraminiferal Research, Special Publication 6, 71 p.

Cushman, J.A., and Hanna, M.A., 1927, Foraminifera from the Eocene near San Diego, California: Transactions of the San Diego Society of Natural History, v. 5, no. 4, p. 45–64, pls. 4–6.

Cushman, J.A., and Laiming, B., 1931, Miocene foraminifera from Las Sauces Creek, Ventura County, California: Journal of Paleontology, v. 5, no. 2, p. 79–120, pls. 9–14.

Cushman, J.A., and Schenck, H.G., 1928, Two foraminiferal faunules from the Oregon Tertiary: University of California Publications, Bulletin of the Department of Geological Sciences, v. 17, no. 9, p. 305–324, pls. 42–45.

Cushman, J.A., and Siegfus, S.S., 1942, Foraminifera from the type area of the Kreyenhagen shale of California: San Diego Society of Natural History, Transactions, v. 9, no. 34, p. 385–426, pls. 14–19.

Cushman, J.A., Stewart, R.E., and Stewart, K.C., 1949, Upper Eocene foraminifera from the Toledo Formation, Toledo, Lincoln County, Oregon: Oregon Department of Geology and Mineral Industries, Bulletin 36, no. 6, p. 126–147, pls. 14–16.

Dibblee, T.W., Jr., 1966, Geology of central Santa Ynez Mountains, Santa Barbara County, California: California Division of Mines and Geology, Bulletin 186, 99 p., 4 pls. [Also available at http://pubs.geothermal-library.org/lib/grc/1021056.pdf.]

Hall, C.A., Jr., 1981, Map of geology along the Little Pine fault, parts of the Sisquoc, Foxen Canyon, Zaca Lake, Bald Mountain, Los Olivos, and Figueroa Mountain quadrangles, Santa Barbara County, California: U.S. Geological Survey Miscellaneous Field Studies Map MF–1285, scale 1:24,000.

Kleinpell, R.M., 1938, Miocene stratigraphy of California: Tulsa, Okla., American Association of Petroleum Geologists, 450 p.

Mallory, V.S., 1959, Lower Tertiary biostratigraphy of the California Coast Ranges: Tulsa, Okla., American Association of Petroleum Geologists, 416 p., 42 pls.

McDougall, K., 2008, California Cenozoic biostratigraphy—Paleogene, chap. 4, *of* Scheirer, A.H., ed., Petroleum systems and geologic assessment of oil and gas in the San Joaquin basin Province, California: U.S. Geological Survey Professional Paper 1713–4, 56 p. [Also available at https://doi.org/10.3133/pp17134.]

Schrader, H.-J., 1973, Cenozoic diatoms from the Northeast Pacific, Leg 18, *in* Kulm, L.D., von Huene, R., and others, Initial reports of the Deep Sea Drilling Program, 18: Washington, U.S. Govt. Printing Office, p. 673–797. [Also available at https://doi.org/10.2973/dsdp.proc.18.117.1973.]

Stanley, R.G., Valin, Z.C., and Pawlewicz, M.J., 1992, Rock-Eval pyrolysis and vitrinite reflectance results from outcrop samples of the Rincon Shale (lower Miocene) collected at the Tajiguas Landfill, Santa Barbara County, California: U.S. Geological Survey Open-File Report 92–571, 28 p. [Also available at https://doi.org/10.3133/ofr92571.]

Sweetkind, D.S., Langenheim, V.E., and McDougall-Reid, K., 2021, Data release—Geologic and geophysical maps of the onshore parts of the Santa Maria and Point Conception 30′x60′ quadrangles, California: U.S. Geological Survey data release, https://doi.org/10.5066/P9FU7SJL.

Geosciences and Environmental Change Science Center
Publishing support provided by the Science Publishing Network,
Denver Publishing Service Center
For more information concerning the research in this report, contact the Center Director, USGS Geosciences and Environmental Change Science Center
Box 25046, Mail Stop 980
Denver, CO 80225
(303) 236-5344
Or visit the Geosciences and Environmental Change Science Center website at https://www.usgs.gov/centers/gecsc

ISSN 2329-132X (online)
https://doi.org/10.3133/sim3472